1-1-2015

Assessment Of Temporal And Spatial Alterations In Spinal Glial Reactivityand The Extent Of Cervical Spinal Axonal Injury In The Rat After Blast Overpressure

Heena S. Purkait
Wayne State University,

ASSESSMENT OF TEMPORAL AND SPATIAL ALTERATIONS IN SPINAL GLIAL REACTIVITY AND THE EXTENT OF CERVICAL SPINAL AXONAL INJURY IN THE RAT AFTER BLAST OVERPRESSURE EXPOSURE.

by

HEENA S. PURKAIT

THESIS

Submitted to the Graduate School

of Wayne State University,

Detroit, Michigan

in partial fulfillment of the requirements

for the degree of

MASTER OF SCIENCE

2015

MAJOR: BIOMEDICAL ENGINEERING

Approved By:

_____

Advisor Date

DEDICATION

Rabbana rabbir hamhuma kama rabbayani saghira

-A Dua from Holy Quran

TRANSLATION:

My Lord! Bestow on them (parents)

thy Mercy even as they

cherished me in childhood.

To my incredible parents, my ambitious father, Mr. Sultan Purkait who inspired me to live my dream and never to give up; and my brave mother, Mrs. Ansura Purkait; who bestowed knowledge in me for so many years and made me the person I am today. Nothing of what I have achieved would have been possible without their blessings.

ACKNOWLEDGMENTS

I would like to take this opportunity to thank all those who have assisted me in the successful completion of my thesis at Wayne State University.

I am greatly thankful to my advisor Dr. Srinivasu Kallakuri, co-advisor Dr. John M. Cavanaugh, committee members Dr. Weiping Ren and Dr. Chaoyang Chen for being a part of my thesis committee.

I would like to sincerely thank Dr. Srinivasu Kallakuri for giving me an opportunity to work under him. He has been a great mentor and supported me throughout the completion of my thesis. I thoroughly appreciate his dedication, effort and patience. I would also like to thank Dr. John Cavanaugh for being my co-advisor. He was always there for me in times of need and his valuable support and encouragement helped me to keep up my work.

My heartfelt gratitude to Mr. Alok Desai for his guidance throughout the duration of the project. Even a page of acknowledgement would not be enough to appreciate his help. He introduced me to the technical aspects of the study and helped me develop an analytical mind. I would also like to thank Mr. Karthik Somasundaran, Mr. Satya Dalvayi & Ms. Karthika Andrew for their timely assistance and supporting me in the completion of my thesis. Additionally I am extremely thankful to all my other lab mates who kept me company and a cheerful environment in the lab.

I am extremely thankful to the North American Spine Society (NASS) for funding the research.

I am deeply grateful to my brother Mr. Asif Purkait and my best friend Ms. Bhakti Lonkar who have inspired me to attain knowledge and excellence in my life. It would be remiss not to mention my friends Mr. Sreeshanth Pillai, Ms. Leena Kadam and Ms. Neeraja Purandare for their constant encouragement and support. Also, I would like to thank my family and friends, who stood by me and believed in me. Without their love and support, I would not be able to make it here. Lastly, to the little joys of my life, my nieces and nephew; Khushi, Aisha, Aamir, and Humaira. I hope this inspires you to achieve greater things in life.

TABLE OF CONTENTS

LIST OF TABLES

LIST OF FIGURES:

CHAPTER 1 - INTRODUCTION

1.1 Motivation:

Blast induced neurotrauma (BINT) is a signature wound of veterans returning from various military operations. The increasing use of explosive devices as a tool of terrorism is not only a threat to the military personnel, but also risks the lives of the civilians considering the indiscriminate nature of these devices. With the help of improvised body armor and advanced medical care, the survival rates of the veterans exposed to blast explosion have increased. However, these returning veterans suffer from many unexplained symptoms such as fatigue, headaches, indigestion, insomnia, dizziness, respiratory disorder and memory problems. One of the most common challenge faced by these veterans is the new or ongoing pain following their military service. Pain was reported as the most common symptom in the Persian Gulf War, Operations Enduring Freedom (OEF), Operation Iraqi Freedom (OIF) and Operation New Dawn (OND) veterans (Cifu et al., 2013; Gironda et al., 2006; Kroenke et al., 1998).

In a study, Lew. et. al. identified 81.5% out of the 340 OEF/OIF veterans matched the criteria for chronic pain as shown in figure 1. The high prevailing pain locations identified in these returning OIF and OEF veterans were the head (58%) and back (55%) (Lew et al., 2009). Ruff et. al reported that the OEF/OIF veterans experienced severe headaches, severe pain and impaired sleep from blast exposure (Ruff et al., 2008). In fact, pain management was considered as a national priority by the Veterans Affairs (VA) pain management strategy (Kerns et al., 2011). Pain can significantly affect the quality of life and thereby decreases the person's life satisfaction (Wollaars et al., 2007). Unfortunately, to date, the mechanism of the pain and the cellular changes caused due to the blast exposure in these veterans continues to remain an enigma, giving rise to a new field of

research. However, even before we understand the pain mechanisms after blast, we need to understand the underlying cellular changes especially in the spinal cord that may contribute to the sensory changes.

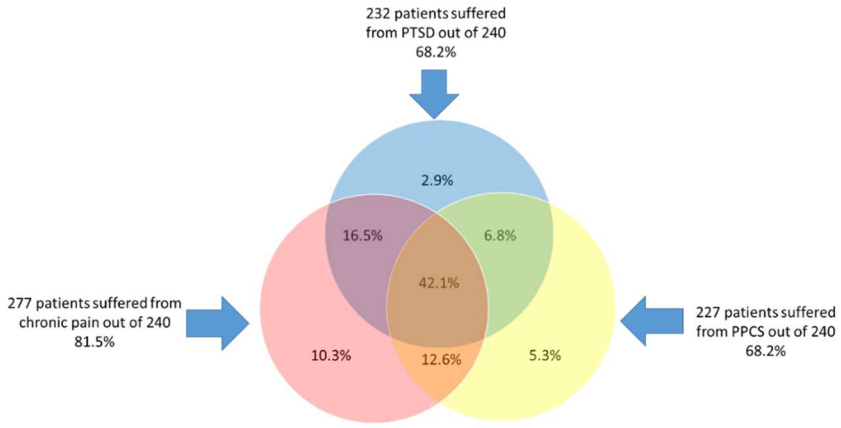

Figure 1: The 'polytrauma clinical triad' in OEF/OIF veterans: incidence of post-traumatic stress disorder (PTSD), persistent post-concussive systems (PPCS), and chronic pain in 340 veterans of Operation Enduring Freedom and Operation Iraqi Freedom

1.2 Blast Injury

A blast or explosion releases a high pressure wave which initiates from the center of the blast. Blast wave is a type of propagating disturbance that causes a discontinuous increase in pressure, density, temperature and velocity. It is an instantaneous increase in pressure giving rise to a typical shock wave, also termed as Friedlander wave. A Friedlander wave is a variation of pressure over time as shown below in the Figure 2

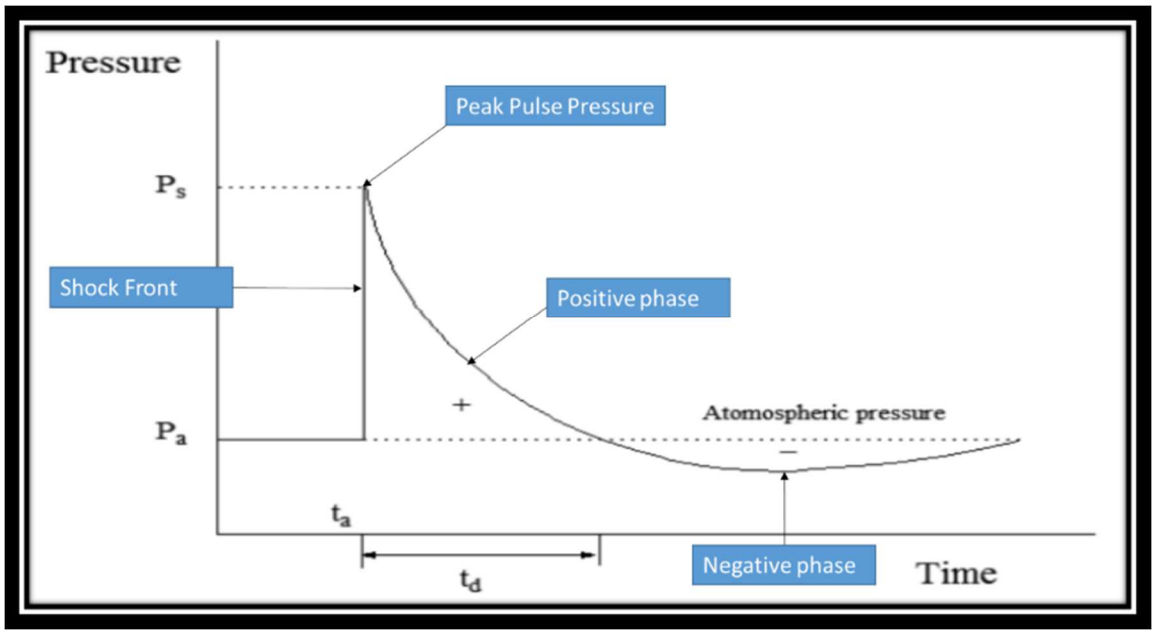

Figure 2: Friedlander wave showing peak pulse pressure, positive phase and negative phase.

The Friedlander wave is characterized by a peak pulse pressure followed by the overpressure (positive phase) and ending with an underpressure which returns to the ambient pressure (negative phase). The figure shows the instantaneous rise in pressure on the arrival of the blast wave denoted by Ps and it gradually decreases back to ambient pressure Pa. Blast overpressure is the increase in pressure above the atmospheric pressure. The strength of the blast is characterized by the ratio of overpressure to ambient pressure. The positive phase duration of the blast wave is followed by the negative phase where the pressure goes below the ambient pressure and returns back to the ambient pressure. This sudden increase in ambient pressure induces tissue injury as the overpressure travels through the body without causing any external trauma. (Pode et al., 1989).

To characterize the shock waves by positive peak overpressure, positive and negative phase duration, the Friedlander equation was developed during the Second World War as shown below:

$$P(t) = Ps\ (1-t/td)\exp(-bt/td)$$

Where P(t) is the pressure at any time t

Ps is the peak overpressure (static pressure)

td is the duration of the positive phase of the wave

b is a decay constant describing the decay rate

This high energy wave moves spherically affecting the tissues, and causes blast injuries. The severity and type of blast injuries depends upon on several factors such as the material of the explosive, method of delivery, distance between the victim and the site of blast, and the surrounding environment (Prevention., 2006). Blast injuries are classified into four categories; primary, secondary, tertiary and quaternary (Cheng et al., 1984; Mellor, 1988) as described below:

Primary blast injury: This injury is caused due to the direct effect of the transmitted wave. This injury is mostly related with air filled organs such as the lungs, ear and gastrointestinal tract.

Secondary blast injury: This injury is caused by the flying fragments of debris that get thrown by the explosion.

Tertiary blast injury: This injury is caused due to part or the whole body of the victim is blown away by the blast wind which is followed by the pressure wave.

Quaternary: This injury is a result of the chemical or heat burns due to the explosion.

The injuries caused by projectiles, shrapnel and chemicals are classified under secondary and tertiary blast injury. Secondary, tertiary and quaternary blast injuries together are known as indirect effects of blast. The field of research to mitigate these indirect effects has been the major focus of most of the researchers. However, it is recently that this seemingly simple blast wave that causes primary blast neurotrauma has gained recognition (Cernak et al., 1999; Ling et al., 2009; Martin et al., 2008; Warden and French, 2005; Warden et al., 2009). It was suggested that 47% of the injuries suffered by the surviving veterans were primary blast injuries (Mayorga, 1997).

1.3 Literature Review of Traumatic Brain Injury and Spinal Cord Injury.

TRAUMATIC BRAIN INJURY (TBI)

The Defense and Veterans Brain Injury Center (DVBIC) estimates that 313,816 service personnel were diagnosed with traumatic brain injury (TBI) between 2000 and 2014 (as of December 1, 2014), with only 1.5% suffered from penetrating injuries as shown in figure 3 (DVBIC, 2015).

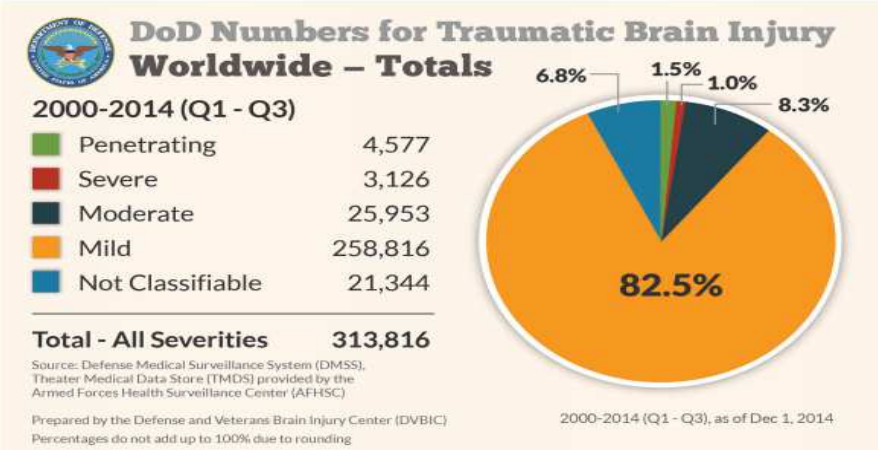

Figure 3: Department of Defense (DoD) numbers for Traumatic Brain Injury (DVBIC, 2015)

The high prevalence of mild traumatic brain injury (mTBI) (82.5%) among the veterans is a shocking finding which influenced many researchers to understand the

mechanism(s). In fact, approximately 60% mTBI injuries were primary blast injuries which is also known as blast induced traumatic brain injury (bTBI) (Warden and French, 2005). With the increasing exposure of blast conditions, it was suggested that bTBI is the signature brain injury faced by the current military personnel (Bhattacharjee, 2008).

Early in the years, studies were conducted to understand transmission of wave through the body. An interesting experiment performed on dogs showed that a simple impact on the head without any movement created concussion in the brain. The dog's head was held by the hand and stuck with a hammer, which resulted brain injury in the form of concussion. They proposed that the resultant brain injury was induced due to the transmission of pressure wave through the skull (Gurdjian et al., 1964). In another study, rabbits were exposed to blast overpressure with chest protection. Two pressure sensors were placed; one on the lumbar region in the spinal cord or above the spinal cord and other in the abdomen cavity. An increase in the spinal cord sensor (where was thus sensor placed: on the surface of the spinal cord, inserted directly into the spinal cord etc) was observed, while no pressure change was detected in the other sensor. The authors suggested the possible increase at the spinal cord sensor may be a result of the blast wave travelling down the brainstem to the spinal cord (Clemedson, 1956). However, due to technological limitations of the time, there was no histological assessment to understand the underlying cellular changes if any.

With the advancement of research and technology, various studies have shown the blast induced underlying cellular changes occur in the brain without any penetrating wounds in the head (Bauman et al., 2009; Cernak and Noble-Haeusslein, 2010; de Lanerolle et al., 2011; Warden et al., 2009). Different locations of the brain have indicated proliferation of astrocytes and microglia with significant phenotypical changes following

blast overpressure using various animal models (Cho et al., 2013; de Lanerolle et al., 2011; Goldstein et al., 2012; Kaur et al., 1995; Lu et al., 2012; Readnower et al., 2010). Another significant component of traumatic brain injury is diffuse traumatic axonal injury (DAI), random occurrence of disrupted axons. Therefore, brain was identified as a susceptible target for blast overpressure (Hicks et al., 2010). We will now review some of the studies demonstrating the cellular changes in the brain following blast overpressure.

Cernak and her team have shown evidence that exposure to blast overpressure causes ultrastructural and biochemical effects in the region of hippocampus of the rat brain which is related to the cognitive defects (Cernak et al., 2001). They also showed the presence of axonal injury in the form of swollen axons and myelin debris in a rat model following blast overpressure (Cernak et al., 2001). Saljo et al., demonstrated that activation of glial cells led to neuronal degeneration and axonal injury in the rat brain after exposure to 34psi of air overpressure. Moreover, they have also shown that the glial cells continued to remain elevated 21 days post the exposure to the blast (Saljo et al., 2001). Similar results were reported by Bauman and his team using a swine model. They studied the propagation of blast wave through the skull by implanting sensors on the forebrain, thalamus and hind brain following blast overpressure. Their pressure data showed transmission of waves elevated intracranial pressure (ICP), which resulted in blast induced traumatic injury (Bauman et al., 2009). Also, significant proliferation of astrocytes was reported in the hippocampus of the brain after a single exposure to blast overpressure. Kaur and co-workers exposed rats to blast overpressure, and found increased expression of microglia in the different areas of the brain at 14 days post exposure (Kaur et al., 1995). In another study on rat brain ischaemia model, Moriaka and co-workers observed that microglia migrated to the site of injury following activation (Morioka et al., 1991). With

respect to axonal injury, Garmen and co-workers exposed rats to 35 psi of blast overpressure (BOP) using a shock tube. They identified axonal injury as the most striking event at 24 hours post exposure in the deep cerebellar white matter of the rat brain (Garman et al., 2011).

Taken together, activation of glial cells and axonal injury were the two most significant phenomenon witnessed in the brain following blast overpressure. Wiesler-Frank et. al. postulated that glial activation could be the cause for continuous pain followed by the healing of the original injury (Wieseler-Frank et al., 2005).Therefore it can be proposed that the underlying cellular changes in the brain in the form of glial activation and axonal injury may induce pain in the body.

SPINAL CORD INJURY (SCI)

As described earlier, the changes in the brain following blast overpressure (BOP) are well documented. However, the injury to spinal cord as a consequence of BOP has never been investigated. It is well known that much of spinal cord injury in humans is a result of blunt trauma to the spinal cord. Spinal cord injury is a catastrophic event which results in inability to walk, dysfunction in bladder or bowel control and chronic pain (Persu et al., 2009; van Hedel and Dietz, 2010; Yezierski, 2000).

In a survey conducted on 348 participants, 76% suffered from chronic pain following spinal cord injury .The participants were patients who received treatment from the Veterans Spinal Cord Injury Centre with chronic pain due to spinal cord injury. The various reasons that resulted this injury were fall, motor vehicle crash, violence, sports, falling or flying objects and others being diseases, explosions, aircraft accidents and surgery(Rintala et al., 2005). These results suggest that pain is a common occurrence for the patients suffering from spinal cord injury.

To mimic the spinal cord injury, various animal models were designed to understand the cellular changes that resulted in the pain in the body. The different models used were contusion, ischeamia/perfusion, hemi section and photochemical models (Hooshmand et al., 2014; Lee et al., 2000; McIntosh et al., 1987; Noble and Wrathall, 1989; Watson et al., 1986). One of the most commonly used is the contusion model, which is known to be suitable to create inflammation in the spinal cord (David and Kroner, 2011). In this model, computer controlled devices were used to drop weight directly on the exposed spinal cord. Many studies conducted on rat spinal cord injury have shown that glial cells get activated following blunt impact to the spinal cord (Fitch et al., 1999; Kyrkanides et al., 1999; Tikka et al., 2001).

Using contusion model, Lee. et. al. showed elevated expression of astrocytes and microglia with axonal injury in rats(Lee et al., 2000). They suggested that these alterations in the glial reactivity resulted in the release cytokines which are known to cause pain like conditions in the body. Li and co-workers showed proliferation of astrocytes and microglia around the lesion area in rat model following spinal cord injury (Li et al., 1995). Based on these studies, it can be inferred that glial cells proliferate and release substances in response to spinal cord injury. Another mechanism witnessed in spinal cord injury is presence of axonal injury. In a study was conducted on 18 human spinal cords with acute cord compression with paralysis to assess the extent of axonal injury. With the help of beta amyloid precursor protein as marker, the researchers detected axonal disruptions not only the area around the lesion site, but also far from the lesion site. They concluded that the acute cord compression demonstrated extensive occurrence of axonal injury in location of the injury as well as in the other regions of the spinal cord (Cornish et al., 2000). Similar results were shown by Sjovold et. al in the rat spinal cord model, where white

matter damage was detected in the form of accumulated APP in the rostal end of the spinal cord (Sjovold et al., 2013). Taken together, these studies show evidence of glial activation and axonal injury in the spinal cord following an insult. Whether such changes also occur following exposure to blast over pressure which may suggest the injurious nature of the blast exposure has never been investigated.

1.3 Rationale for the Proposed Study

Based on the literature review, it was found that activation of glial cells and axonal injury were the common events following TBI and SCI. In the context to blast induced spinal cord injury (BISCI), the question that needs to be addressed is whether blast overpressure induces any similar injury changes in the spinal cord. Since the spinal cord is the extending part of the brain, it will be interesting to study if there are similar changes in the spinal cord also. The spinal cord is the pathway between the peripheral nervous system and the brain, and therefore it is essential to investigate the cascade of events that occur in the spinal cord following blast overpressure. Thus, our study will be the first step to address the underlying cellular changes in the spinal cord.

RAT SPINAL CORD MODEL

We will now review the various animals used to detect in the injury in traumatic brain injury and spinal cord injury. The summary of the animal models used for TBI and SCI with different methods of injury induction are shown below:

TYPE OF INJURY	MODEL	ANIMAL
TRAUMATIC BRAIN INJURY (TBI)	Fluid Percussion Injury	Cat[1], rabbit[2], rat[3], mouse[4], dog[5], sheep[6], swine[7]
	Weight Drop	Rat[8], mouse[9]
	Blast Injury	Rat[10], mouse[11], Swine[12]

Table 1: Table showing the various animal models for traumatic brain injury (TBI).

References for Traumatic Brain Injury: 1. (Hayes et al., 1987)2. (Hartl et al., 1997) 3. (Hooshmand et al., 2014; McIntosh et al., 1987; McIntosh et al., 1989)4.(Carbonell et al., 1998)5.& 6. (Pfenninger et al., 1989) 7. (Armstead, 2001) 8. (Feeney et al., 1981; Marmarou et al., 1994; Shohami et al., 1988) 9. (Albert-Weissenberger et al., 2012; Chen et al., 1996)10. (Cernak et al., 2001; Koliatsos et al., 2011)11. (Goldstein et al., 2012)12. (Bauman et al., 2009; de Lanerolle et al., 2011)

TYPE OF INJURY	MODEL	ANIMAL
SPINAL CORD INJURY (SCI)	Contusion Model	Rat[1], dog[2], mouse[3], pig[4], guinea pig[5]
	Ischeamia/reperfusion injury	Rat[6], rabbit[7], mouse[8], swine[9]
	Photochemical Model	Rat[10]

Table 2: Table showing the various animals used for spinal cord injury (SCI).

References for Spinal Cord Injury: 1.(Noble and Wrathall, 1989) (Hooshmand et al., 2014)2. (Gerber et al., 1980)3. (Watson et al., 2014)4.(Lee et al., 2013)5.(Luo et al., 2002)6.(Celic et al., 2014)7.(Hashizume et al., 2005) 8. (Stone et al., 2009)9. (Simon et al., 2011)10. (Watson et al., 1986)

From these tables, it can be inferred that rat is the most commonly used animal model for both traumatic brain injury and spinal cord injury. The rodent models are considered ideal to mimic the injury seen in humans. (Xiong et al., 2013). We cannot study the effects of blast overpressure directly on a human spinal cord. Due to the anatomical similarities between rat and human spinal cord, it is logical to study the rat model. The brain and spinal cord are a part of the central nervous system (CNS), and any trauma to the CNS, i.e. blast induced traumatic brain injury (TBI) or spinal cord injury (SCI) could result in striking neuropathology and delayed recovery. (Donnelly and Popovich, 2008). Based on the structural analogies of the brain and spinal cord, rat model was selected to study the BISCI.

1.4 HYPOTHESIS AND SPECIFIC AIMS:

HYPOTHESIS

Studies have shown that the shock wave passes through the skull and retains its typical Friedlander waveform without any decrease in the strength of the overpressure using human, pig, rabbit and rat model (Bauman et al., 2009; Chavko et al., 2007; Clemedson, 1956; Saljo et al., 2001). We hypothesize that this shock wave moves down the brainstem and passes through the spinal cord inducing cellular changes in the spinal cord also. As a first step, we attempted to identify and describe the effects of blast exposure on the spinal cord by the studying the alterations in the glial cells and axons. This study may provide an insight about the effects of blast overpressure on the spinal cord.

SPECIFIC AIMS:

Based on our hypothesis, we proposed the following specific aims to study the effects of blast overpressure on the spinal cord as shown in the figure 4 below:

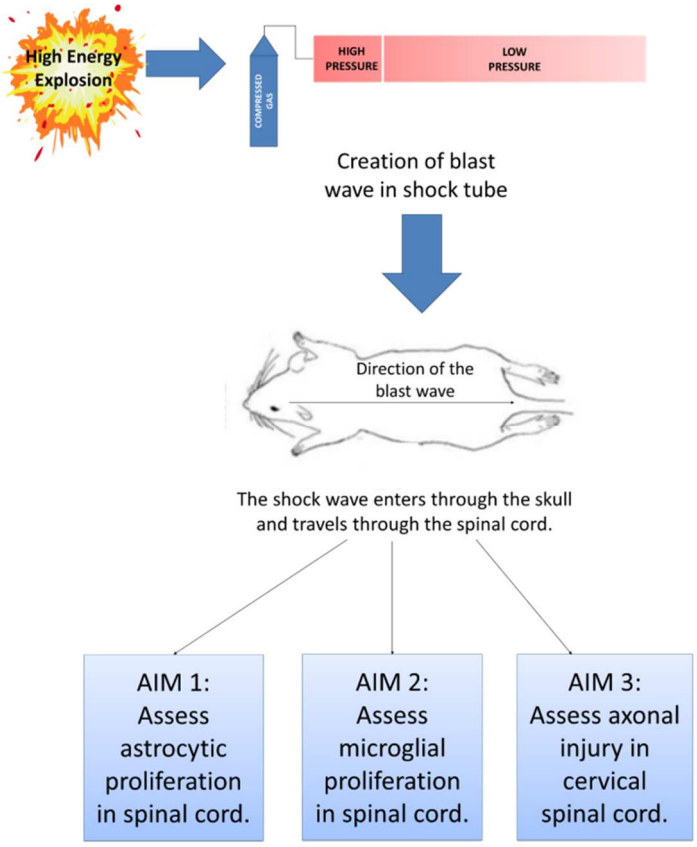

Figure 4: The diagrammatic representation of the hypothesis and specific aims of the study.

Specific Aim 1:

To assess the temporal and spatial alterations in the expression of astrocytes in different levels of the rat spinal cord following blast overpressure.

Specific Aim 2:

To assess the temporal and spatial alterations in the expression of microglia in the different levels of the rat spinal cord following blast overpressure.

Specific Aim 3:

To investigate the presence axonal injury in the cervical spinal cord following blast overpressure.

1.5 Introduction of upcoming chapters

Chapter 2 discusses the anatomy of the central nervous system. The objective of chapter 2 is to understand the structural overview and components of the central nervous system. Chapter 3 briefly describes the materials and methods used in this study. Chapter 4 and 5 summarizes the overall results and discussions. Finally, the last chapter 6 presents the conclusions and recommendations for future work.

CHAPTER 2 - NERVOUS SYSTEM

The nervous system is a highly organized system responsible for the coordination of all the voluntary and involuntary actions of the body and transmission of signals between parts of the body. The nervous system is divided into two parts namely central nervous system (CNS) and peripheral nervous system (PNS). The central nervous system acts as the receiving center of the all information from where and sends out the appropriate information to the peripheral nervous system.

2.1 Structural Overview of Central Nervous System

The two main organs of CNS are the brain and the spinal cord. The peripheral nervous system is made up of nerves that forms the connection between the CNS and the muscles and other sensory organs. The brain is enclosed in the thick bones of skull, and

spinal cord is contained within the vertebral column. Both the brain and spinal cord are enveloped in three layers of meninges namely, the Dura mater, arachnoid mater and pia mater. There is a space in between the pia and arachnoid mater known as the subarachnoid space. Another important component of the CNS, cerebrospinal fluid (CSF) is found in the subarachnoid space. It is clear, colorless liquid produced in the choroid plexus in the brain and flows around the brain and spinal cord as shown in figure 5.

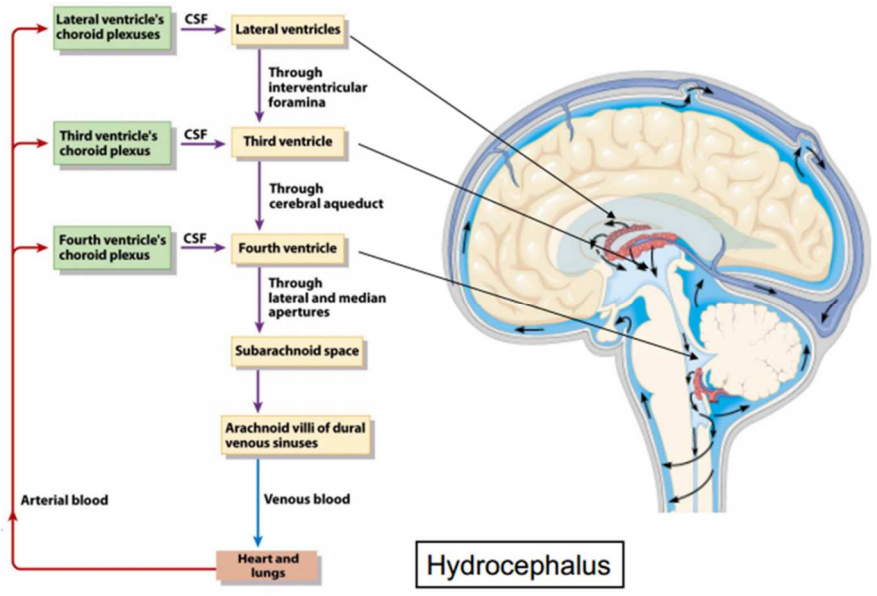

Figure 5: Pathway of cerebrospinal fluid (CSF) flow.

The main function is to provide protective layer to the brain and spinal cord while other functions include circulation of nutrients and chemicals from the blood and the removal of waste products from the CNS.

BRAIN:

The brain is the most sophisticated and complex organ of the human body. An average human brain weighs 3.3 pounds and makes up only 2% weight of the body. It is

responsible for the control of all the other organs, the secretions of glands and maintenance of homeostasis.

Anatomically, the brain is divided into three main sections i.e. forebrain, midbrain and hindbrain interconnected with fluid filled ventricles as shown in figure 6. The forebrain (pros encephalon) forms the upper part of the brain comprising the cerebrum, thalamus, hypothalamus and the pineal gland. The midbrain (mesencephalon) located in the center of the brain is composed of a portion of the brainstem, while the remaining brainstem, cerebellum and pons together form the hindbrain (rhombcenphalon).

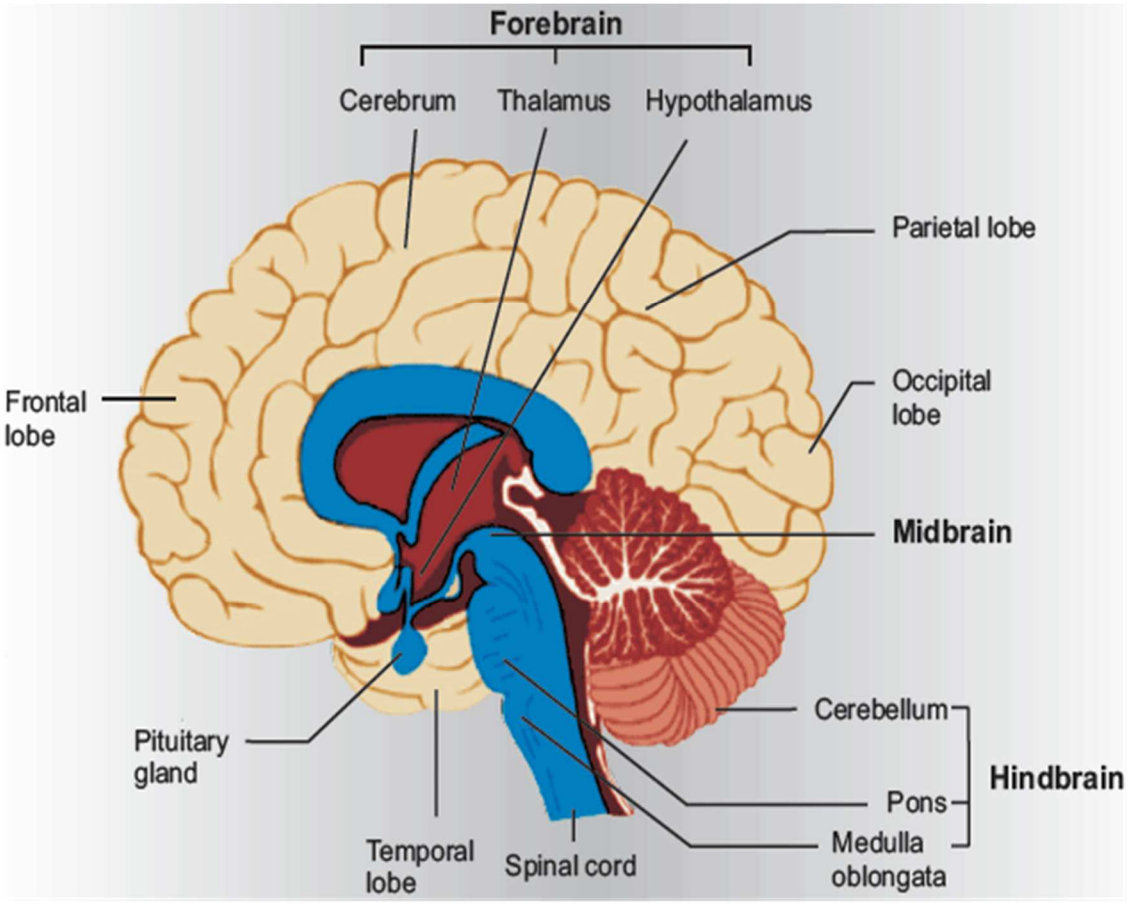

Figure 6: The three regions of the brain with the fluid filled ventricles.
Modified from http://www.aghazenau.com/brain.html

SPINAL CORD:

The spinal cord is the connecting pathway between the brain and the peripheral nervous system. It is about 40-50 cm in length and 1-1.5 cm in diameter. The functions of the spinal cord include the transmission of sensory and motor signals between the brain and other parts of the body, and also acts as a minor reflex center.

The spinal cord is surrounded and protected by the vertebral column. It is continuous with the medulla oblongata of the brainstem, to the first or second lumbar vertebra as shown fig 7. (Larry R. Squire, 2008).

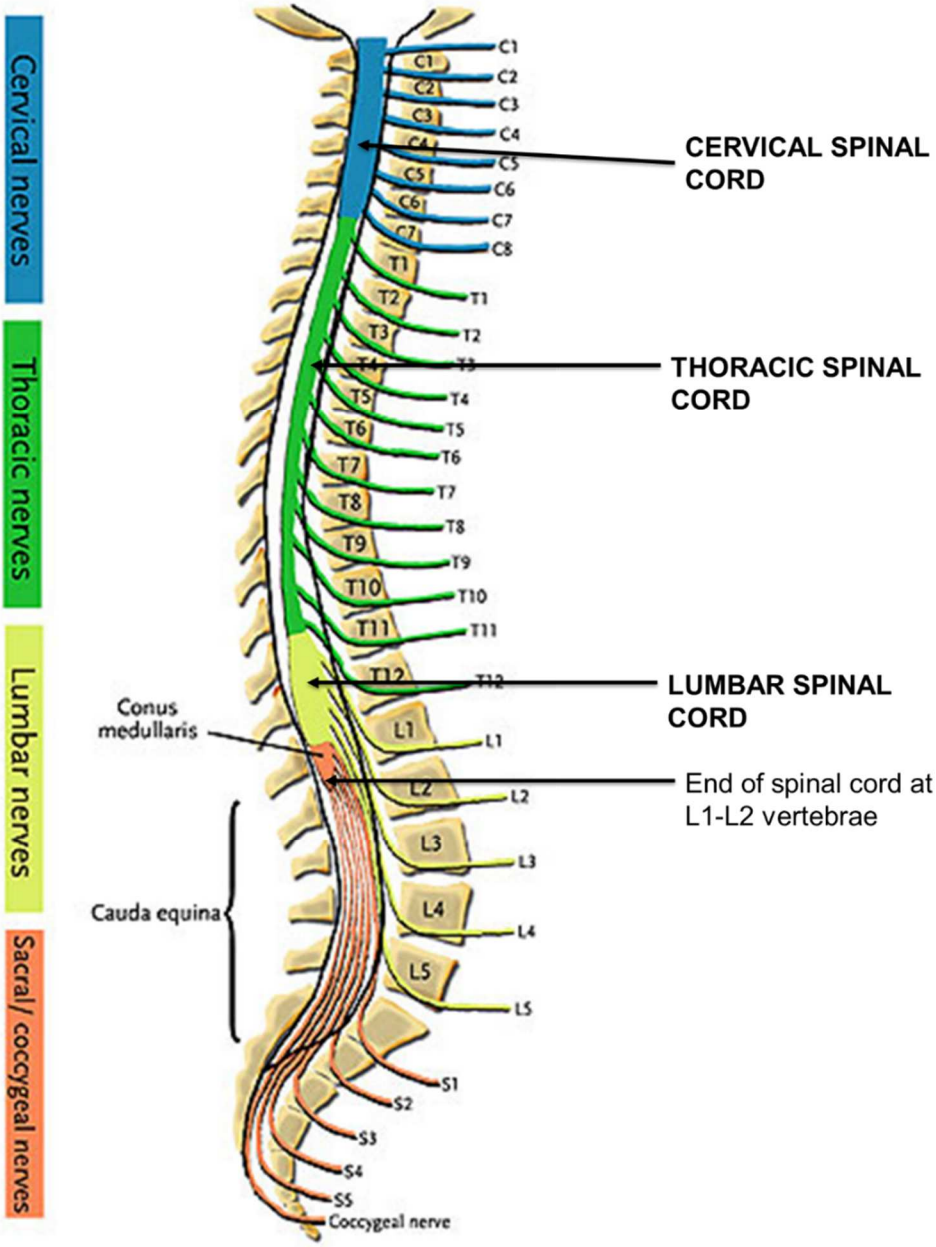

Figure 7: Spinal cord contained in the vertebral column
(Modified from http://pixshark.com/spinal-nerves.htm)

The vertebral column made up of total 33 vertebrae is arranged in five different regions: 7 cervical, 12 thoracic, 5 lumbar, 5 sacral and 4 coccygeal. The 5 sacral and 4 coccygeal vertebrae are fused in adults, which form the sacrum and coccyx respectively.

Also, the spinal cord itself is divided into 31 different segmental levels each consisting 31 pair of spinal roots coming out between of the corresponding vertebral segments(Eric P. Widmaier, 2006). Like the vertebral column, the spinal cord also has 8 cervical, 12 thoracic, 5 lumbar, 5 sacral and 1 coccygeal segments. However, these spinal segments are not situated in the same vertebral segments. The first two spinal cord segments of the cervical and thoracic match the corresponding first vertebral segments, but the remaining segments not match. The C3-C8 segments are situated between C3 and C7 vertebral levels, T3-T12 cord segments between T3 and T8 and the L1-L5 cord segments between T9-L1 as shown in figure 6 (Drake et al., 2015) .

2.2 Composition of Nervous System:

The CNS is composed of grey matter and white matter. The grey matter has a pinkish-grey color and contains the cell bodies, dendrites, unmyelinated axons and axon terminals of neurons. The white matter is composed of myelinated axons connecting different parts of grey matter to each other. It is the myelinated axons which give the white color to the white matter.

The composition of the brain and spinal cord is reversed as shown in the figure 8. The outer part of the brain is made up of grey matter, and the remaining part of the brain is made up of white matter. In the case of spinal cord, the grey matter of the spinal cord is a butterfly or H-shaped surrounded by the outer white matter. There is a hole in the center of the spinal cord known as the central canal which allows passage of the cerebrospinal fluid (CSF).

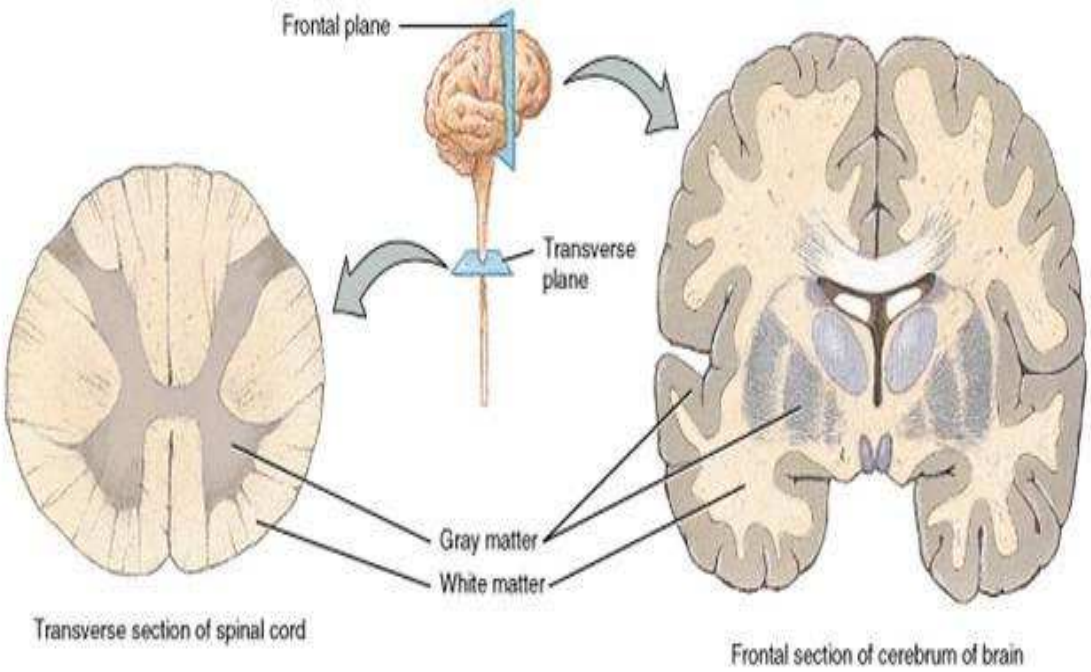

Figure 8: Reversed anatomy of the brain and spinal cord

Based on the cellular structure, the CNS is composed of two types of cells; neurons and glial cells as shown in figure 9.

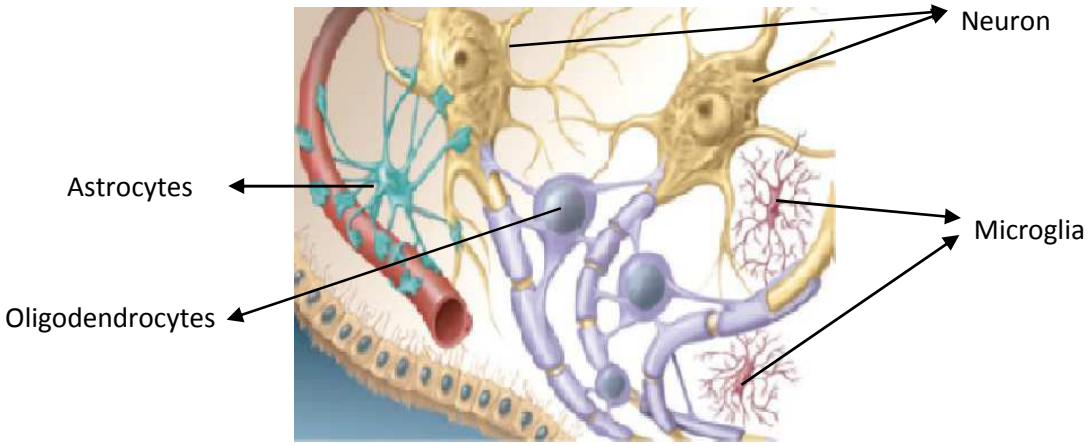

Figure 9: Neuron & Glial Cells (Eric P. Widmaier, 2006)
Modified from the types of glial cells.

NEURON:

The fundamental cellular unit of the nervous system is the nerve cell, or neuron. They use chemical synapses that can evoke electrical signals, called action potentials, to relay signals throughout the body. There are roughly 100 billion neurons with different shapes and sizes present in the central nervous system.

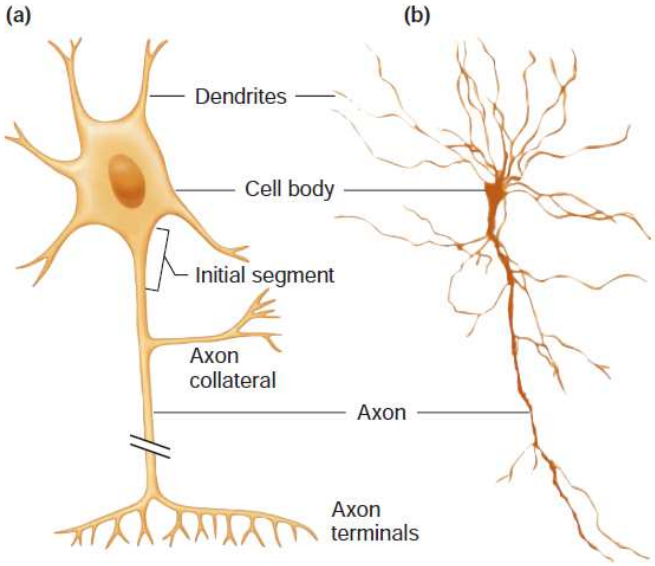

Figure 10: Diagrammatic representation of a neuron. (b) A neuron as observed through a microscope.

A typical neuron is made up of three parts, the Soma or cell body, dendrites and axon as shown in figure 10. Dendrites are numerous thin extensions with branches, where they receive signals from other neurons in the form of nerve impulses. These signals are transferred to the soma or cell body. The soma consists of a nucleus and DNA material, and it is responsible of processing the information sent by the dendrites.

Neurons are categorized in three types; afferent, efferent and interneurons as shown in figure 11. Afferent neurons, also known as sensory neurons, transfer the information from the sensory organs of body to the CNS. These neurons respond to touch, light and sound and send signals to the brain and spinal cord. Efferent neurons or motor neurons that react to the signals from the CNS and trigger muscle movements in the body. Interneurons are found in the same region, where they are interconnected with neurons.

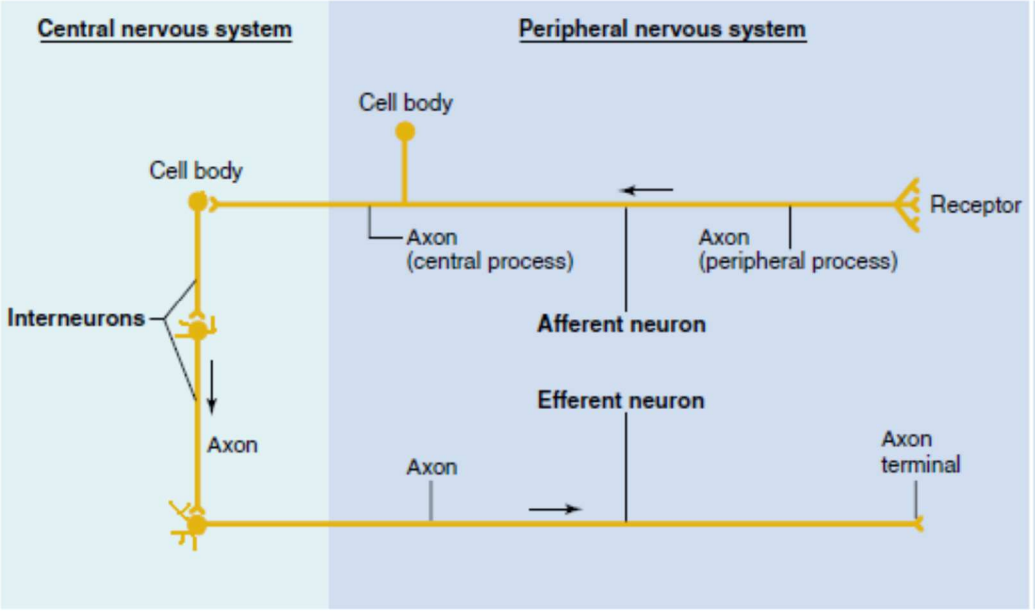

Figure 11: Types of neurons and their locations.

AXON:

Every neuron consists of a single axon which is responsible for the propagation of signals to other neurons. An axon is a long, slender projection of a nerve cell, or neuron that conducts electrical impulses away from the neuron's cell

body or soma. The average diameter of the axons in the CNS ranges from 0.2 to 17μm, while the average in spinal cord is 1 to 1.5μm.

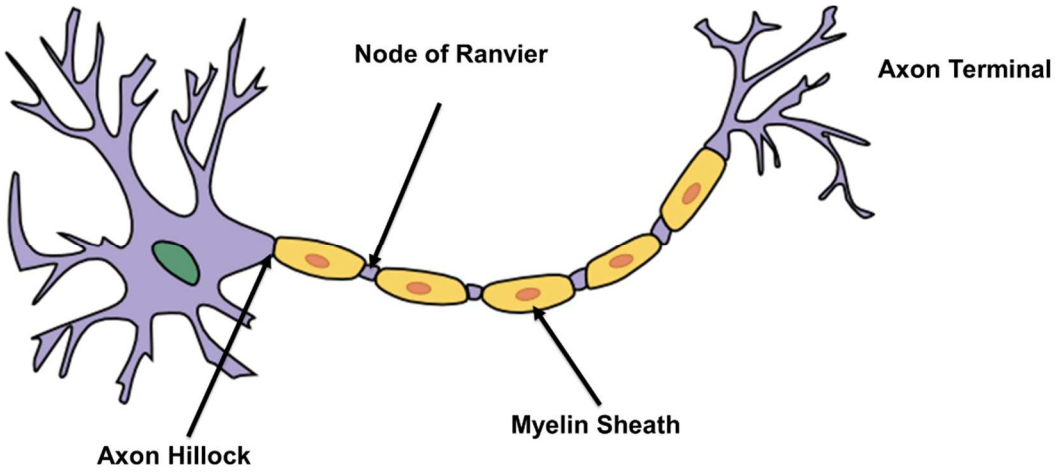

Figure 12: Different parts of the axon

The different parts of the axon is shown in the figure 12. Axon hillock, also known as initial segment, is the part connecting the axon to the cell body. It is in this location where the action potential initiates. The axon is wrapped by a protein rich bilayer of insulating material known as myelin sheath. The myelin sheath acts like an insulation allowing the effective transport of impulses. Another part of the axon known nodes of Ranvier are the spaces found between the myelin sheath, These nodes are responsible for the saltatory conduction, which is the transmission of action potential from node to node across the axon.

GLIAL CELLS:

In 1856, the famous German neuropathologist Rudolf Virchow first discovered neuroglia, and named them “nervenkitt” as shown in figure 13. He suggested that they were round shaped connective tissue and the purpose was to

fill up the extracellular space to provide structural support. (Somjen, 1988). It was believed that these cells did not play role in neurotransmission.

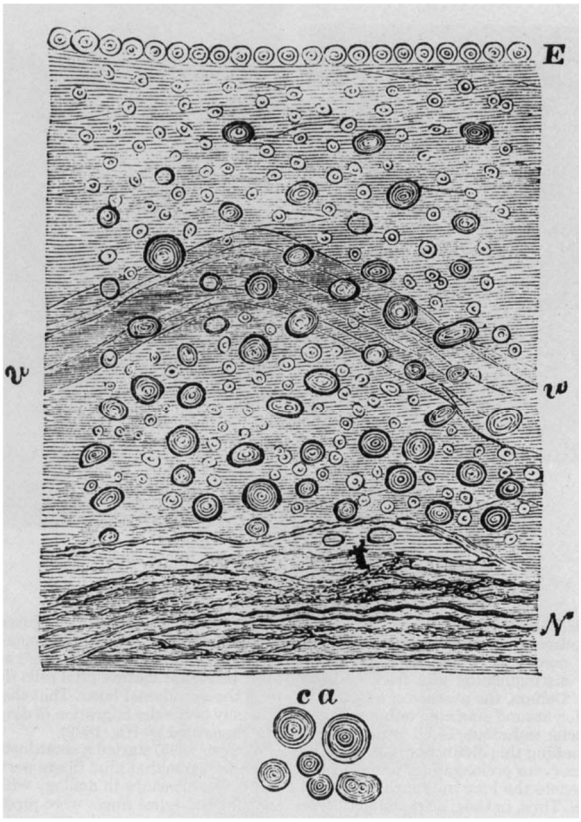

Figure 13: Sketch made by Rudolf Virchow showing neuroglia as a connective tissue of the nervous system. (Somjen, 1988)

However, post a century from the discovery of glial cells, our understanding about the diversity and functions of these cells has grown significantly enhanced. The main function of glial cells is to maintain homeostasis. The other functions are to provide support and nutrition, form myelin, and participate in signal transmission in the nervous system and to destroy and remove the carcasses of dead neurons (Somjen, 1988).

Glial cells are found in both the central nervous system as well as the peripheral nervous system. The different types of glial cells based on their location is shown in the figure 14.

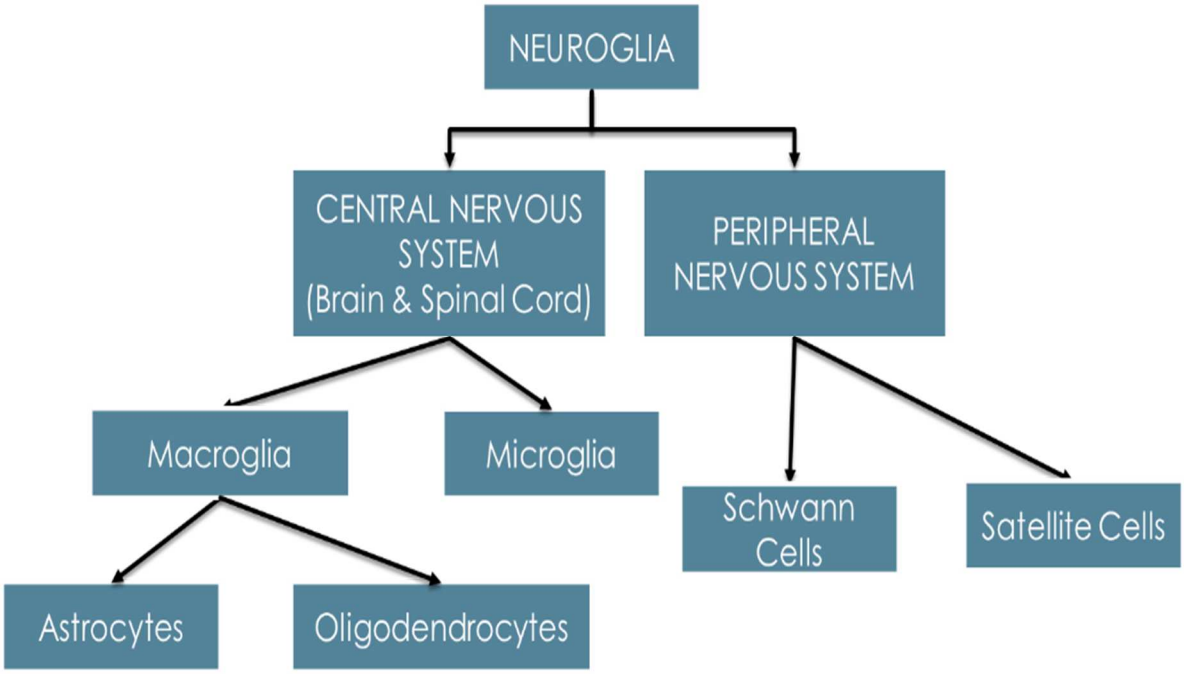

Figure 14: Figure showing the different types of neuroglia of the central and peripheral nervous system.

The PNS glial cells include the satellite cells and Schwann cells. The satellite cells are small cells and surround the neurons in the peripheral ganglia (Hanani, 2005). Schwann cells are responsible for the myelination of the axons in the PNS. They show phagocytic property and help in regrowth of PNS neurons by the clearance of debris.

The three types of CNS supporting cells are Astrocytes, Microglia and Oligodendrocytes. These cells constitute half of the total volume of the brain and

spinal cord. The next section will discuss the phenotype, function and the role of glial cells in case of injury or disease condition,

2.3 Types of Glial cells

ASTROCYTES:

Astrocytes are a type of star shaped process bearing glial cells which combine to form 30-65% of the total cells in the CNS. These cells are found close to the blood brain barrier, and prevents the entry of materials from the blood into the brain.

The two main forms are the fibrous astrocytes and protoplasmic astrocytes. Another form is the radial glial cells which give rise to the astrocytes embryonically. Fibrous astrocytes are found in the white matter in the brain and spinal cord, while the protoplasmic astrocytes are found in the grey matter. Fibrous astrocytes exhibit vascular feet which connects the cell to the outside of the capillary wall. They have few organelles and show long unbranched cellular processes. Protoplasmic astrocytes possess a larger quantity of organelles, and exhibit short and highly branched processes. (Ren, 2010)

The function of astrocytes range from response to central nervous system, information processing, and mechanical support to neurons as shown in figure 15. (Buffo et al., 2010). Astrocytes play a vital role in maintaining homeostasis of the CNS.

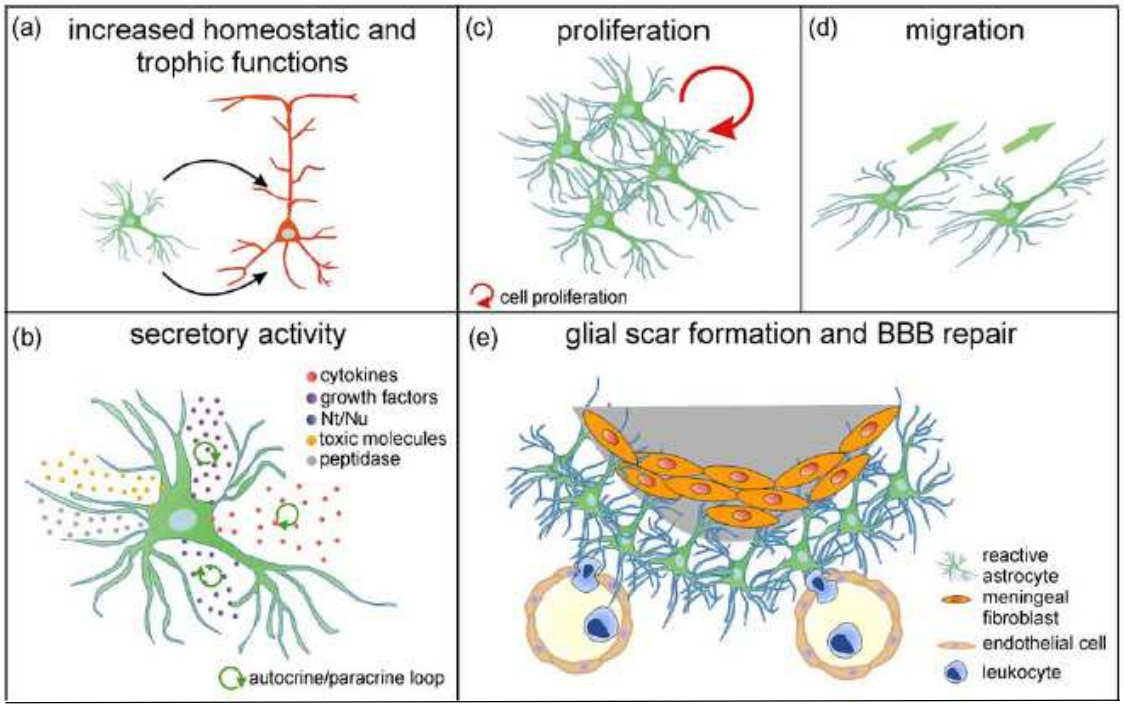

Figure 15: Functions of astrocytes. Upon CNS injury, activated astrocytes increase their homeostatic functions (a), the production of growth factors and cytokines, as well as the release of nucleotides and toxic compounds (b). Their secretion is regulated via complex autocrine and paracrine loops (b). Astrogliosis includes cell proliferation (c) and migration towards the lesion site (d). Reactive astrocytes participate in glial scar formation, and contribute to the resealing of the damaged blood–brain barrier, thus excluding infiltrating leukocytes and meningeal fibroblasts from the injured tissue (e) BBB, blood–brain barrier (Buffo et al., 2010).

In response to CNS trauma or injury, the astrocytes get activated and undergo morphological changes. Reactive astrocytes migrate to the site of injury and undergo proliferation. Also, there is increased production of intermediate filaments such Glial fibrillary acidic protein (GFAP) and vimentin and release of inflammatory mediators such as Interleukin -1 (IL-1), Tumor Necrosis Factor (TNF) and Substance P (SP).(Buffo et al., 2010). It is believed that these cytokines promote neurotoxicity (Liberto et al., 2004; Rao et al., 2012). It is suspected that astrocytes contribute to the sealing of the blood brain barrier in brain injury. (Bush

et al., 1999). Astrocytes are also a major component of the glial scar. The critical function of the glial scar is to restore the structural and chemical integrity of the CNS. The extended filaments get thicker and surround the injured area that seals the nervous/non-nervous tissue boundary. This helps in the prevention of any foreign body or infection to cause further damage to the CNS. However, the glial scar restricts the neuronal regrowth as the growth inhibitory molecules released by astrocytes abstains axonal extensions (Liuzzi and Lasek, 1987).

MICROGLIA:

First reported by Marinesco in 1986 as glial cells that get rid of dying neurons by phagocytosis.(Somjen, 1988) as shown in figure 16.

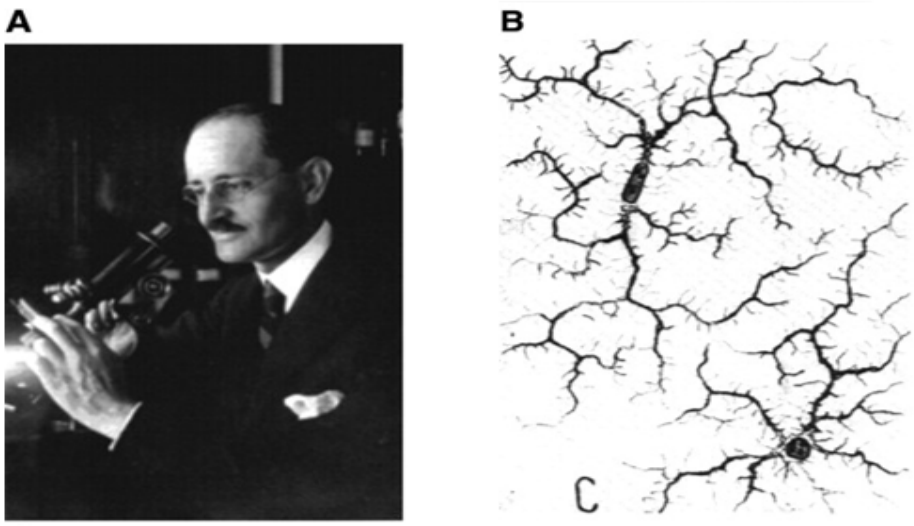

Figure 16: Image of Marinesco who first suggested phagocytosis as a function of microglia (A) and a sketch drawn by him to show the structure of microglia (B). (Somjen, 1988)

Over the years, researchers have discovered the different phenotypes and functions of the microglia. Microglia are the resident macrophages of the CNS and are known to be the scavenging cells within the parenchyma.(Aguzzi et al., 2013; Goldmann and Prinz, 2013; Ransohoff and Perry, 2009; Saijo and Glass, 2011). They compose approximately 10% of total glial cells, with a small somata and multiple processes (Nimmerjahn et al., 2005).

Microglia are classified based on their morphology and functions. There are two morphologies demonstrated by microglia, i.e. ramified and amoeboid. In normal conditions, microglia are said to be in the 'resting' state and they exhibit ramified morphology. (Wieseler-Frank et al., 2005). The microglia consist of small soma with shorter processes compared to astrocytes. The term 'resting state' is a little misleading, since microglia is continuously scavenging the environment for any type of inflammation caused to injury to the CNS or entry of a foreign body like bacteria. They also contribute to the removal and clearance of toxic substances released by damaged neurons.

Microglia are also known to remain activated due to injury to the axons (Smith, 2013). They are the first cells that arrive at the site of injury to induce the cascade of inflammatory mediators. (Parekkadan et al., 2008).

Once activated, they undergo morphological changes and retract their processes inwards demonstrating an amoeboid appearance. (Kreutzberg, 1996). The first stage of activation of microglia is the release of cytotoxic substances such as glutamate, reactive oxygen intermediates, such as hydrogen peroxide, and

reactive nitrogen intermediates, such as nitric oxide. These substances breakdown the foreign bodies into debris.

The activated microglia are characterized as classical pro-inflammatory state (M1 Microglia) and alternatively activated state (M2 microglia). (Colton, 2009; David and Kroner, 2011). M1 microglia are responsible for antigen presentation. Once the debris are surrounded by the microglia, the M1 microglia start signaling of the T-cells which in turn increases inflammation. Therefore, it can be said that microglia are activated by inflammation and also, contributes in the increased inflammation by release of inflammatory mediators. The M2 microglia perform phagocytosis of dying cells, myelin and axonal debris.(Ghasemlou et al., 2010; Tanaka et al., 2009). These types of microglia are associated with repair, healing and remodeling of the injury neurons. In a review, Cherry et. al. studied the types of microglia and suggested that increased level of M2 microglia can be helpful for therapeutic treatments as shown in figure 17.

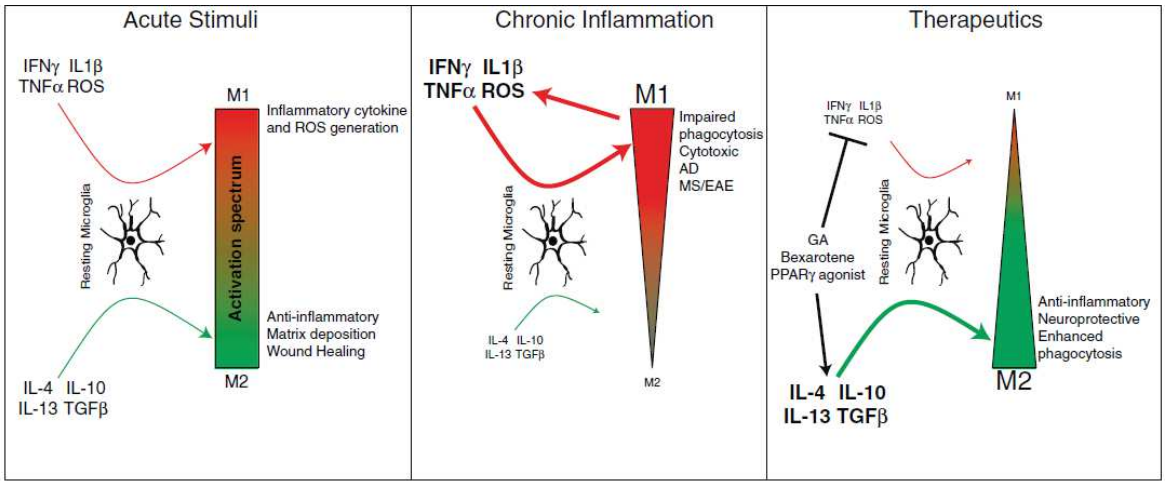

Figure 17: Types of Microglia responses. A) Microglia response to injury B) Microglia response to inflammation and C) Microglia response to therapy. (Cherry et al., 2014)

OLIGODENDROCYTES:

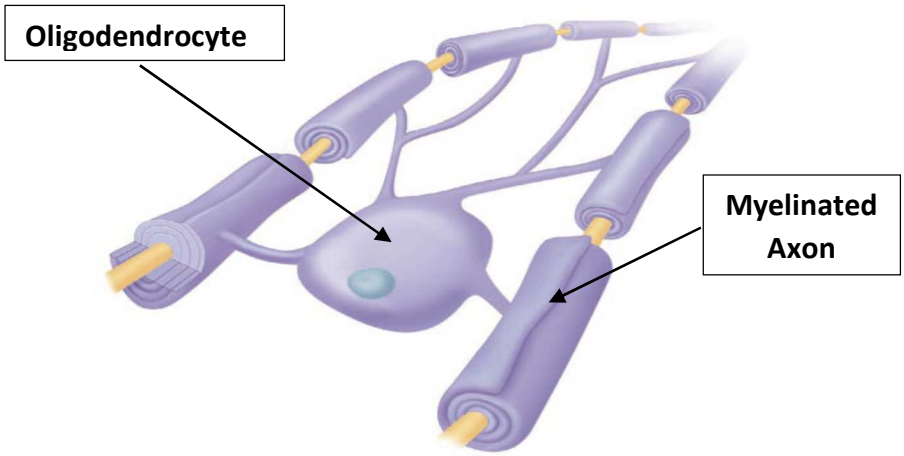

Figure 18: Figure showing the myelinated axons connected to oligodendrocytes (Eric P. Widmaier, 2006)

The glial cells also include oligodendrocytes, which are known as the myelin providing cells. As the name implies, they are small cells with shorter processes that get embedded in the myelin sheath wrapped around the axon as shown in figure 18. A single oligodendrocyte can provide up to 40 axons. The myelin sheath enables the faster transport and maintains the integrity of the axons. Since these cells are in direct contact with the axons, they contribute to the various neurodegenerative diseases associated with axonal injury such as amyotrophic lateral sclerosis (ALS), Alzheimer's disease (AD) and multiple sclerosis (MSA) (Liu and Zhou, 2013).

CHAPTER 3 - MATERIALS & METHODS

3.1 Animal Handling

All animal handling procedures were approved by the Institutional Animal Care and Use Committee (IACUC), Wayne State University, Detroit. A total of 40 adult male Sprague Daley rats (Harlan, Indianapolis, IN) weighing 300 ± 29.93 grams were utilized for this study. The weights of the animals is provided in Appendix C. The rats were randomly divided into the two main groups namely Sham (n=16) and Blast (n=24) with acute (6 hours and 24 hours) and sub-acute (3 days and 7 days) survival periods as shown in the table 3 below. All rats had free access to food and water.

	6 HOURS	24 HOURS	3 DAYS	7 DAYS
SHAM	4	4	4	4
BLAST	6	6	6	6

Table 3: Survival Period groups: Rats classified into two groups with acute and sub-acute survival periods.

3.2 Wayne State Shock Tube:

There are various techniques available to create a blast wave using a shock tube such as detonation of charges, ignition of fuel/air mixtures, or by rupture of a membrane in a compressed gas driver (Bolander, 2012). A single-driver shock tube system activated by compressed gas is considered as an ideal apparatus for the generation of blast wave in an experimental setup for blast induced neurotrauma (BINT) (Sundaramurthy and Chandra, 2014). In fact, previous studies associated with BINT have used compressed gas-driven shock tubes to produce the primary blast injuries (Bolander et al., 2011; Cernak

et al., 2011; Rafaels et al., 2012; Svetlov et al., 2010). We will now discuss the methodology of creation of shock wave using a shock tube.

The shock tube is made up of a driver chamber (pressurized) and a driven chamber (ambient). The driver chamber is the high pressure region and the driven chamber is the low pressure region shown in the figure 19. The driven chamber opens at one at one end, which is important in preventing excessive under pressure (Leonardi et al., 2011). The driver chamber and driven chamber are divided by the Mylar membrane. Usually, the length of the driven chamber is greater than the length of the driver chamber.

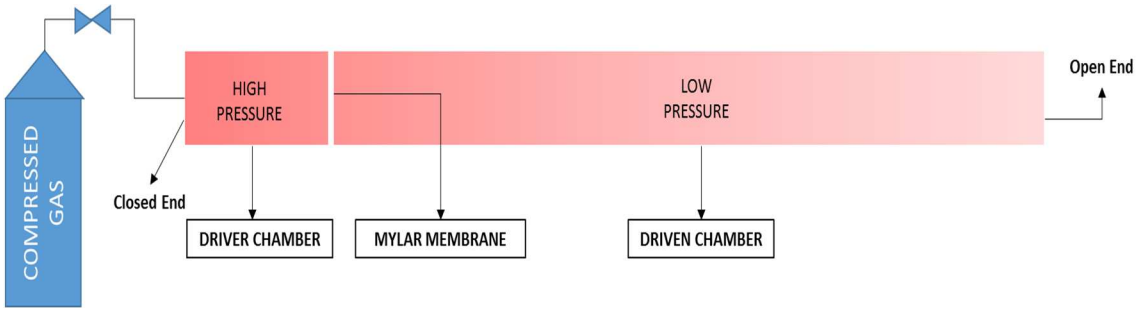

Figure 19: Figure showing the driver chamber and the driven chamber separated by the Mylar membrane

The driver chamber is pressurized by compressed gas, until the Mylar membrane ruptures to release the gas into the driven chamber. The peak blast pressure is dependent on the thickness of the Mylar membrane (Sundaramurthy and Chandra, 2014). Since compressed gas was used to produce the blast wave in place of explosive, the wave is termed as shock wave.

For this study, the custom-built shock tube (ORA Inc. Fredericksburg, VA) located at Wayne State University Bioengineering Department was used. This shock tube is capable of producing complex shock waves of different peak static overpressures up to 150 psi. The shock tube consists of a metal section and transparent Lexan section. The first 30 inches of the metal section is the driver chamber, while the remaining 192 inches

of the metal section and the 40 inches of Lexan section together form the driven chamber as shown in figure 20. The transparent Lexan section is used to view the location of the rat specimen in the shock tube.

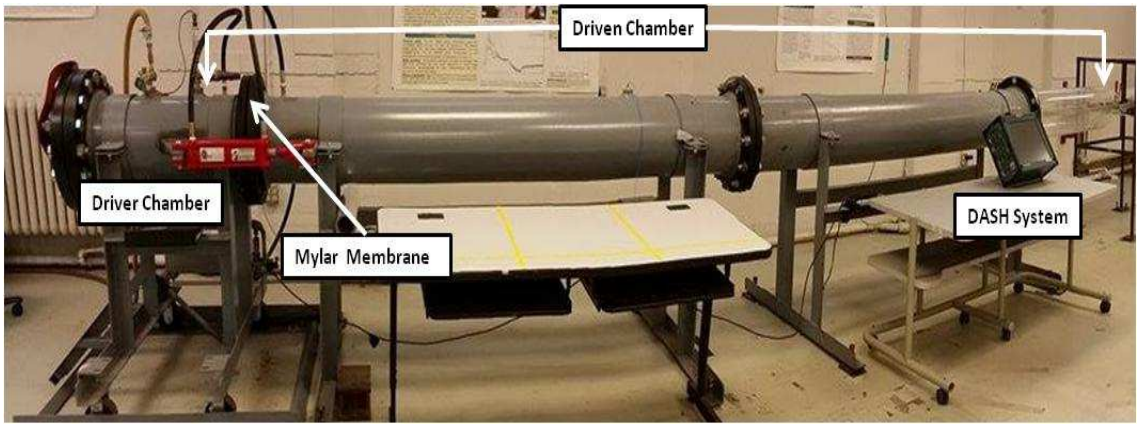

Figure 20: Wayne State Shock Tube showing the driver chamber and driven chamber with DASH system.

For the placement of the rats, a metal stand was anchored to the ground and a pole was attached to a trolley system mounted on it as shown in figure 21. This pole was

used to place the rat specimen and sensor. The rat specimen was placed 48 inches from the open end of tube.

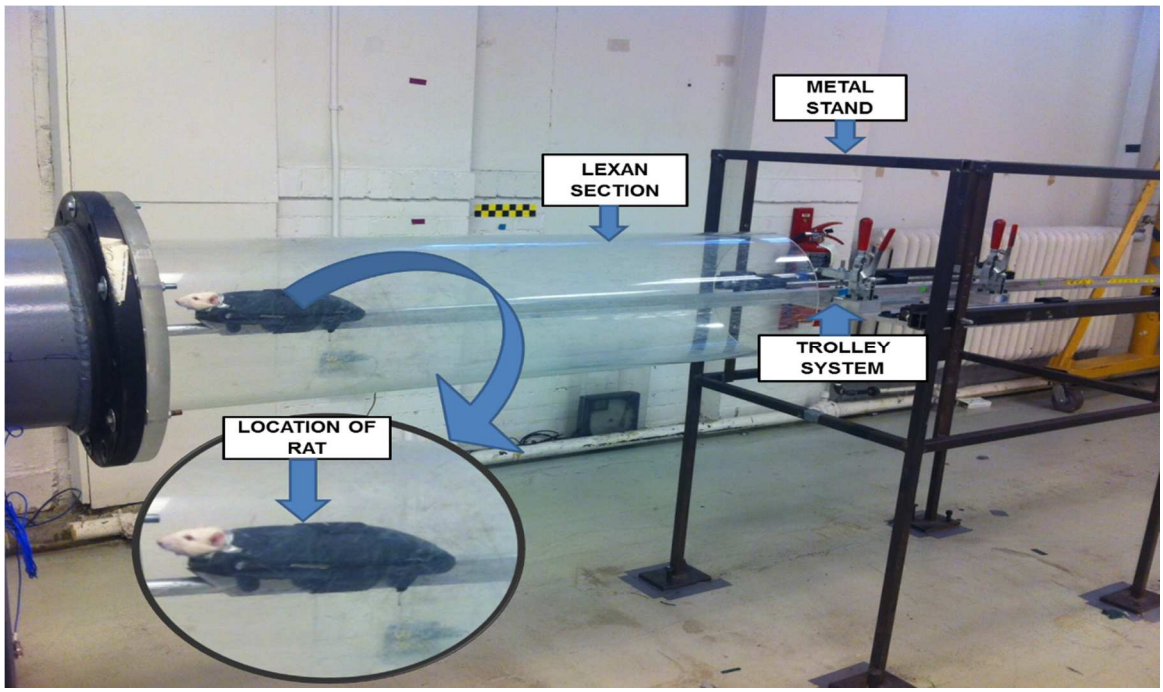

Figure 21: Wayne State Shock Tube showing the Lexan section and metal stand where the trolley system mounted to hold the rat and magnified view of the location of the rat.

Prior to the induction of blast, calibrated Mylar sheets (GE Richards Graphics Supplies Inc., Landsville, PA) were inserted between the two chambers to allow the pressurization of driver chamber with helium gas. With the help of Mylar sheets of different thickness; 10 mil and 3mil, we were able to create the required driver pressure of 22 psi. Helium gas has the capability to replicate the short time course of the initial positive pressure pulse similar to the high explosive detonations in the open field. (Huber et al., 2013). Therefore, helium is considered as an ideal gas to produce the shock wave. Upon the rupture of the Mylar sheets, a blast wave was generated which propagated through the driver chamber and developed into a Friedlander wave similar to a free-field blast wave.

The first sensor is placed in the driver section, and measures the pressure just before the rupture of the membrane. The second and third sensors are placed 2.4 meters apart in the driven chamber, and measures the static and dynamic pressure respectively. The last sensor is housed inside the pole below the animal mounted on the trolley system. This sensor is used to measure the total pressure. All the pressure measurements were collected at 250 kHz using a DASH 8HF data acquisition system (Astro-Med, Inc., West Warwick, RI) as shown in figure 22. This ensued consistent exposure pressures were maintained between the subjects.

Figure 22: Image showing the driver pressure of 22psi on the DASH system.

3.3 Preparation for Blast Induction

Initially, the rats were anesthetized by a mixture of 3% isoflurane and 0.6L/min oxygen in an anesthesia chamber for 4 minutes. At the end of 4 minutes, the rats without any chest protection were harnessed on the pole mounted on the trolley system with a rostral cephalic orientation faced towards the shock wave while still maintaining anesthesia via a nose cone for an additional 2 min resulting in a total anesthesia duration of 6 min. The moving sled consists of a metal rod that houses the pencil below the rat as

shown in the figure 23 (Model: 137A22, PCB Piezotronics Inc.). A metal based harness was designed to hold the rat in rostocephalic position which helped to prevent the movement of the entire body. The harness was fixed to the blast end of the moving sled and was wrapped over the rats exposing only the head towards the blast. After 6 min of anesthesia induction, the animals were positioned 49 inches from the open end of the shock tube for the induction of blast as explained in the earlier section. The Sham group animals were subjected to identical experimental procedures but not subjected to the blast overpressure (22psi).

3.4 Surface Righting Time

After the induction of blast, the rats were also monitored for duration to surface right (SR), which is considered as an indirect indicator of loss of consciousness (LOC) (Adams, 1986). A mesencephalic reflex that returns during recovery from unconsciousness resulting from anesthesia or brain injury prior to thalamocortical function is known as righting reflex (Alkire et al., 2007; Bignall, 1974). The duration of the righting reflex varies with the type of anesthesia and injury. For this study, the time taken for an animal to correct from a supine position to prone position as shown in the figure 23 following blast overpressure was measured.

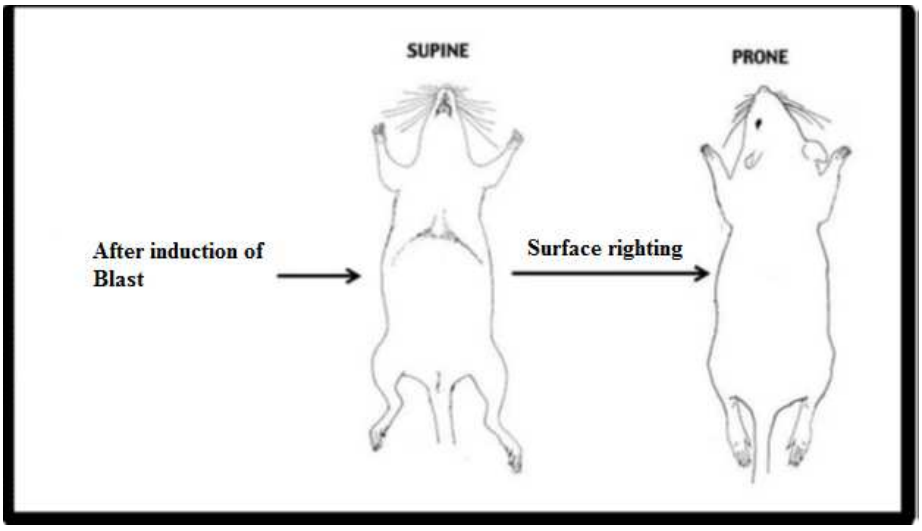

Figure 23: Diagram of a rat in supine position turning over to prone position, displaying the surface righting reflex following blast overpressure.
Modified from (Yang et al., 2002)

3.5 Termination & Perfusion

Prior to the terminal perfusion, cerebrospinal fluid (CSF) and serum samples were collected from all animals for future biomarker studies. At end of their respective survival periods, the animals were anaesthetized by 50mg/kg of sodium pentobarbital. The depth of anesthesia was assessed by response to aversive pinching of the paws. The rats were then placed in the sternal recumbency with the chest and front legs placed flat on the surgical bed. An incision was made at the atlanto-occipital region to reach the cisterna magna of the brain to collect the CSF. In a study conducted at Illinois State University, Pegg found that collection of cerebrospinal fluid (CSF) from the cisterna magna resulted in quick and reliable yields of large quantities (50–150 µl) in rats.(Pegg et al., 2010) For this study, a TB syringe with 26 x ½" gauge needle was inserted in the atlanto-occipital membrane followed by the underlying dura to collect 50-100 µl of CSF in 500µl centrifuge tube from each rat.

Following the extraction of the CSF, the rats were placed in the supine position to cut open the lateral chest wall and the overlying skin with a pair of blunt scissors on both sides of the sternum exposing the heart. Additionally, blood (1.5mL) was also collected directly in 2ml centrifuge tubes from the heart with the help of 26 x ½ “gauge needle. CSF and blood were centrifuged at 10,000 relative centrifugal force (rcf) for 5 minutes at and 10 minutes respectively. Serum was separated from the blood and both CSF and serum samples were stored in -20 degree Celsius.

22” gauge needle was introduced in the aorta via the apex of left ventricle and then 100 ml of saline was pumped into the aorta to flush out the blood. A cut was made in the right atrium to drain out the blood from the venous return as shown in figure 24. Then 400 ml of 4% cold paraformaldehyde was perfused in order to fix the animal. At the end of perfusion, the brain and spine were harvested and post fixed in 30% sucrose prepared in 4% paraformaldehyde (pH 7.4) for future histological procedures.

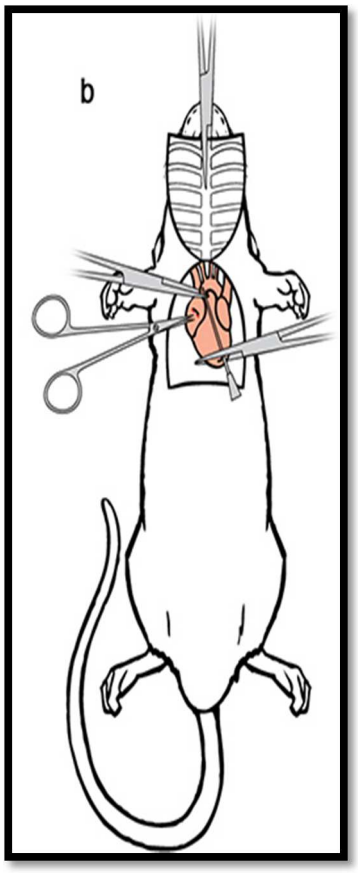

Figure 24: Transcardial perfusion of 4% paraformaldehyde

3.6 Tissue Collection and Processing

Post fixation of the spine, laminectomy was performed and the spinal cord was exposed. Once the required spinal cord level was exposed, a pair of dorsal root ganglia (DRG) from each level of spinal cord were harvested and stored for future studies. The C2-C7 spinal cord was collected below the C1-C7 vertebrae and the T1-T8 spinal cord was collected from the T1-T8 vertebrae. As mentioned in the anatomy of the spinal cord, the lumbar spinal vertebrae and lumbar spinal cord are not in the same alignment. The lumbar spinal cord L1-L5 was harvested from the T11-L4 vertebrae. The approximate length of the cervical, thoracic and lumbar spinal cord segments were 1.5cm, 3 cm and 2 cm respectively as shown in the figure 25 below:

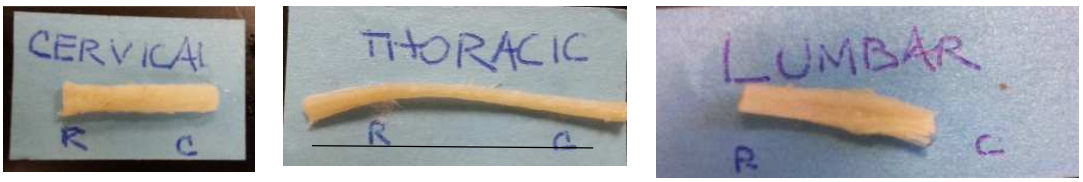

Figure 25: Spinal cord segments of a) cervical, b) thoracic and c) lumbar region harvested from the post fixed spine of rat

To prepare the horizontal sections, respective spinal cord segments were placed in an acrylic brain matrix and a 1 cm long segment was cut. This 1cm long segment was placed in a plastic cup with optimum cutting compound (OCT), and allowed to freeze (-20 degrees Celsius) to prepare a frozen block. This OCT embedded block was then affixed on to a chuck. Then 40μm thick horizontal frozen sections were cut using a cryostat (Leica CM 3020) and collected in 96 well plates filled with 0.1 M Phosphate-buffered saline (PBS). To avoid the degradation of the tissue, 3 drops of 4% paraformaldehyde were added to each well.

3.7 Immunohistochemistry

To study the expression of astrocytes and microglia, sections from all three levels of the spinal cord were stained with anti-glial fibrillary acidic protein (GFAP) and anti-ionized calcium binding adaptor molecule-1 antibodies respectively. For assessing axonal injury in cervical spinal cord, anti-beta-amyloid precursor protein also was used. Horizontal sections of the respective spinal cord from each animal were washed in 0.1 M PBS (3x2 min) and incubated in citrate buffer (pH 6.0) at 90° C for 1 hour for antigen retrieval. The sections then were immersed in 0.6% of hydrogen peroxide for one hour at room temperature to quench endogenous peroxidase activity. Next, the sections were incubated overnight at 4°Cwith the following primary antibodies: anti-Glial Fibrillary Acidic Protein (GFAP; mouse polyclonal;1:5000; Cat# NE1015, Calbiochem, San Diego, CA, USA); anti-Ionized calcium-Binding Adaptor molecule-1(IBA-1;rabbit polyclonal; 1:2000; Wako; Osaka, Japan) and anti- β-Amyloid Precursor Protein (β–APP; rabbit polyclonal; 1:250;Cat # 51-2700, Invitrogen, Camarillo, CA, USA) diluted in 1% bovine serum albumin (BSA, Sigma Aldrich, St Loius, MO, USA)with 2% normal goat serum (NGS, Vector Laboratories, Burlingame, CA, USA). The primary antibodies were omitted in the control sections. Next day, the sections were washed in 0.1 M PBS (3x2 min) and incubated in biotinylated secondary antibodies (Anti-Mouse; 1:1000; Vector; Burlingame, CA, USA or Anti-rabbit; 1:1000; Vector; Burlingame, CA, USA) on a rotating platform for 1.5 hours at room temperature. The sections were then immersed in avidin-biotin complex (Vectastain ABC-elite®, Vector). The peroxidase activity was then developed by brief incubation in 3, 3'-diaminobenzidine (DAB) diluted in distilled water for 5-10 minutes. The stained sections were washed in 0.1M PBS (3×5 minutes), mounted on glass slides and allowed to dry

overnight. The slides were then dipped in containers filled with xylene (3x2mins) and cover slipped with DPX mountant (VWR; EC) which preserves the stain and dries quickly.

3.8 Imaging and Quantification

All stained sections were observed under a light microscope (Leica DMLB, Leica Microsystems Ltd, Heerburg, Switzerland) to visualize the expression of astrocytes, microglia and beta amyloid precursor protein (βAPP) accumulation. Digital images were obtained using a digital camera system (ProgRes C7, JENOPTIK Laser Optik Systeme, GmbH) and taken at a single focal plane.

For the quantification of astrocytes and microglia, first the entire slide was scanned at 5x magnification and then 5 specific locations were selected in the grey and white matter of the spinal cord. Then individual 10x images were taken of the selected location as shown in the figure 26.

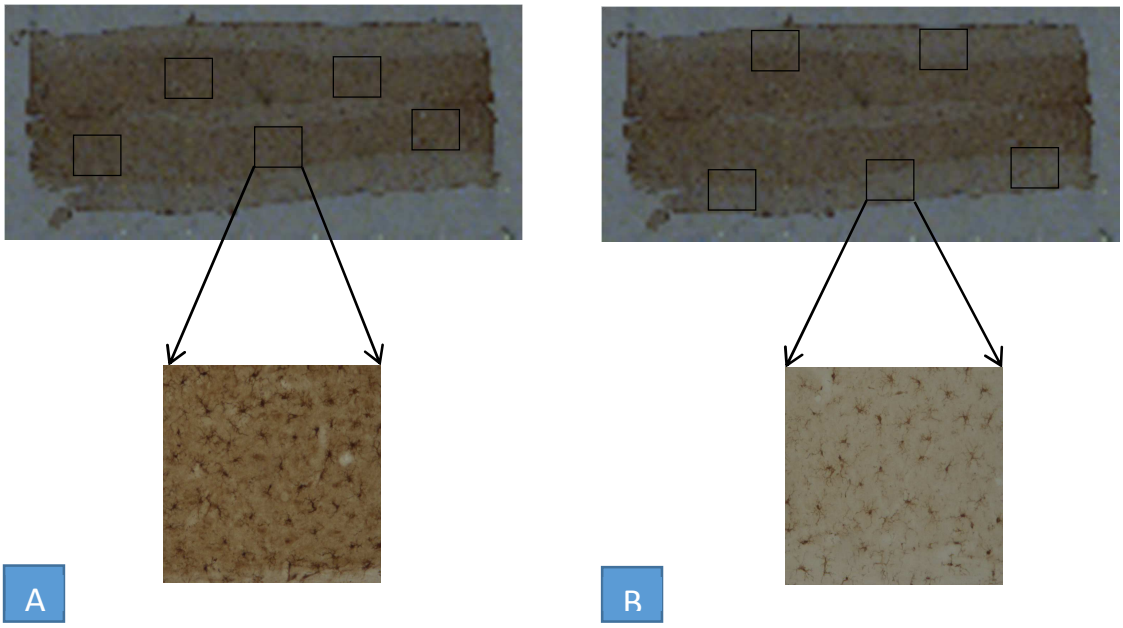

Figure 26: The 5x scanned image of the entire section with the representative locations for the 5 specific locations. (A) showing the grey matter quantification and (B) showing the white matter.

The accumulation of beta-amyloid precursor protein was measured by quantifying the number of the immunoreactive (IR) zones. The entire section was scanned and the images of the IR zones were taken. The presence of swollen axons, retraction bulbs and disruptive axons was used as the criteria to define the IR zones. The accumulation of beta-amyloid precursor protein (βAPP) is an indicator of impaired axoplasmic transport, a component of traumatic axonal injury.

To assess the proliferation of glial cells, quantitative analysis was done on the 10x digital images of the grey matter and white matter of the respective regions of the spinal cord .Each 10x digital images was opened in ImageJ, and a manual quantification was carried out. Using the cell counter tool, all the astrocytes and microglia present in a given image were manually counted and stored in an excel sheet for further statistical analysis as shown in the figure 27.

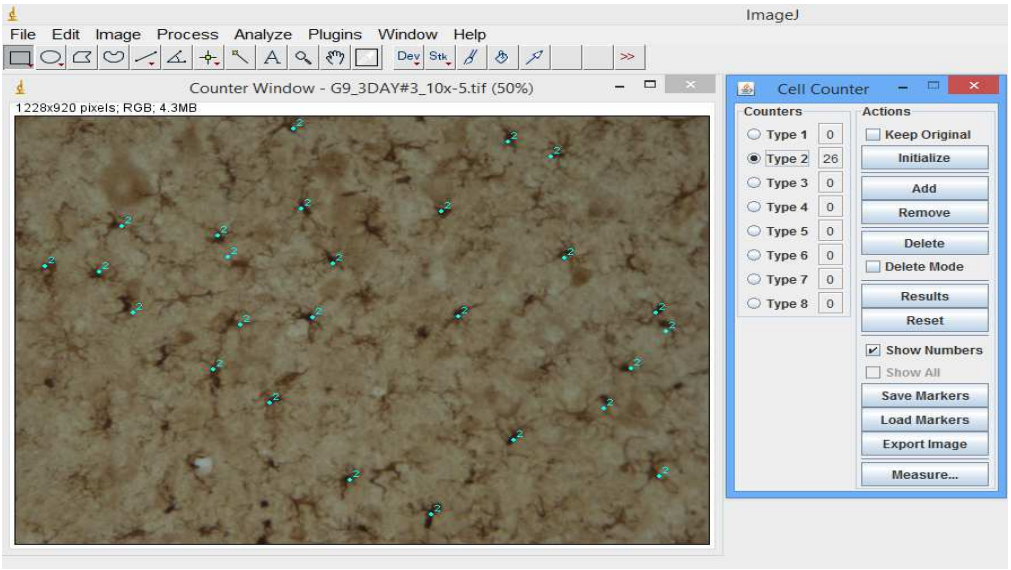

Figure 27: The 5x scanned image of the entire section with the representative locations for the 5 specific locations

3.9 Statistical Analysis

The statistical significance of all data were analyzed using SPSS (Version 22, SPSS Inc., Chicago, IL). The sham group and blast group were compared using the Mann-Whitney Wilcoxon Test. To study the temporal alterations between the acute and sub-acute survival periods (6 hours, 24 hours, 3 days and 7days) of the sham and blast group, One way Analysis of Variance (ANOVA) was performed. Post-Hoc test was done to analyze the difference within the groups using the Tukey test. Also, the presence of beta-amyloid precursor protein was analyzed using One-way Analysis of Variance (ANOVA). A p value of less than 0.05 was deemed significant.

CHAPTER 4 - RESULTS

4.1 Surface right time

It was observed that the rats in blast group (n=24) showed significantly prolonged SR duration time compared to sham group rats (n=16). Compared to the SR duration of 124.875±71.39 seconds in sham rats, the average SR duration in blast rats was a significant 187.80± 76.84 seconds ($p<0.05$) as shown in figure 28.

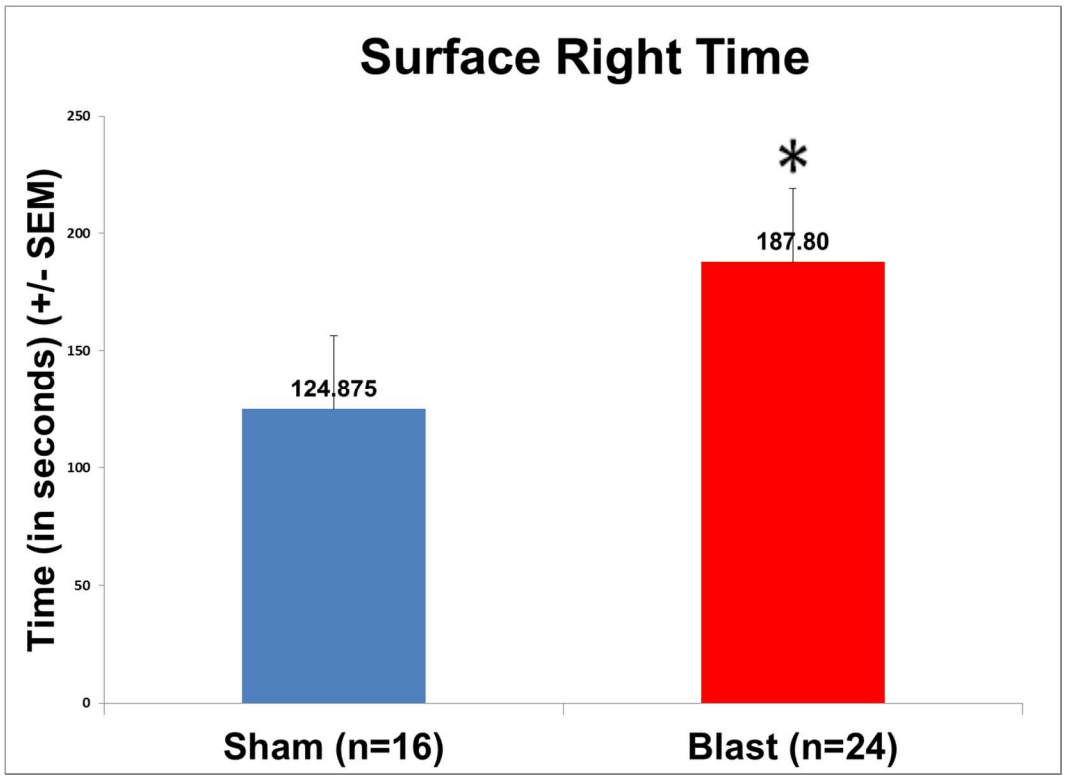

Figure 28*:* Plot showing mean SR duration of sham and blast group rats. * indicates significant difference ($p<0.05$) in SR duration of blast group rats compared to sham rats.

4.2 Alterations in the expression of astrocytes

The spinal cord sections were immunostained using antibodies against Glial Fibrillary Acidic Protein (GFAP), an intermediate filament protein expressed by astrocytes, to study the alterations in the expression of astrocytes. GFAP is considered an ideal marker to assess changes in the expression of astrocytes upon injury (Ransom, 1991).

We assessed blast induced alterations in the expression of astrocytes at different levels of the spinal cord. The blast group spinal cord showed significant proliferation of astrocytes compared to sham group ($p<0.05$) as shown in figure 29.

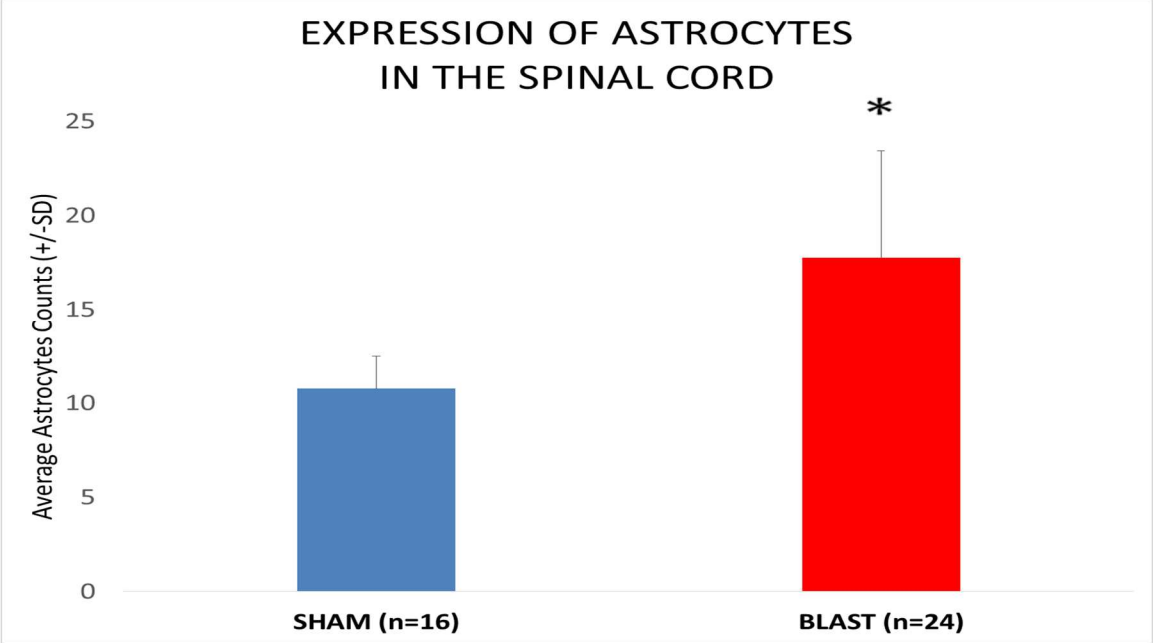

Figure 29: Histogram showing alterations in the expression of astrocytes in the sham and blast group spinal cord. * indicates significant difference ($p<0.05$) in the expression of astrocyte in the blast group compared to the sham group.

CERVICAL SPINAL CORD- ASTROCYTE CHANGES

To study the proliferation changes in the expression of astrocytes, respective digital images were taken from the sham and blast group as shown in figure 30. Increased GFAP reactive astrocytes were observed in the blast group compared to the sham group.

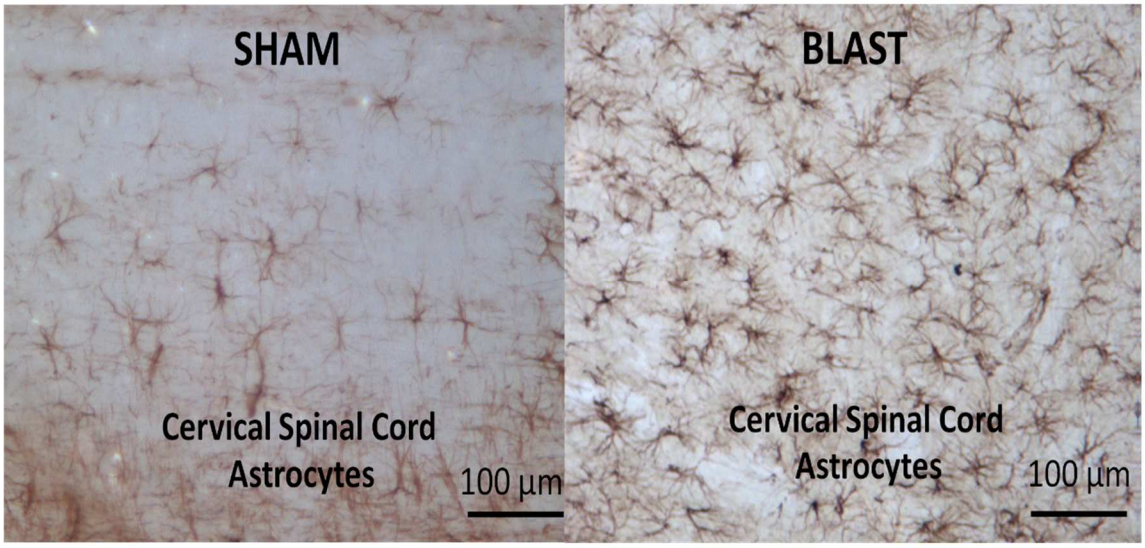

Figure 30: Images showing representative GFAP expressing astrocytes in the cervical spinal cord. A: Sham group B. Blast group. Scale Bar: 100 um= 10x magnification.

Additionally, the number of astrocytes in the grey matter and white matter regions were quantified seperately to better understand the expression of astrocytes in the cervical spinal cord. In both the regions, there was significant increase observed in the blast group in comparison to the sham group as shown in figure 31. The expression of astrocytes was higher in the grey matter compared to the white matter. All the alterations observed in the grey matter and white matter regions in the blast group were statiscally significant ($p < 0.05$) for the respective regions of the blast group.

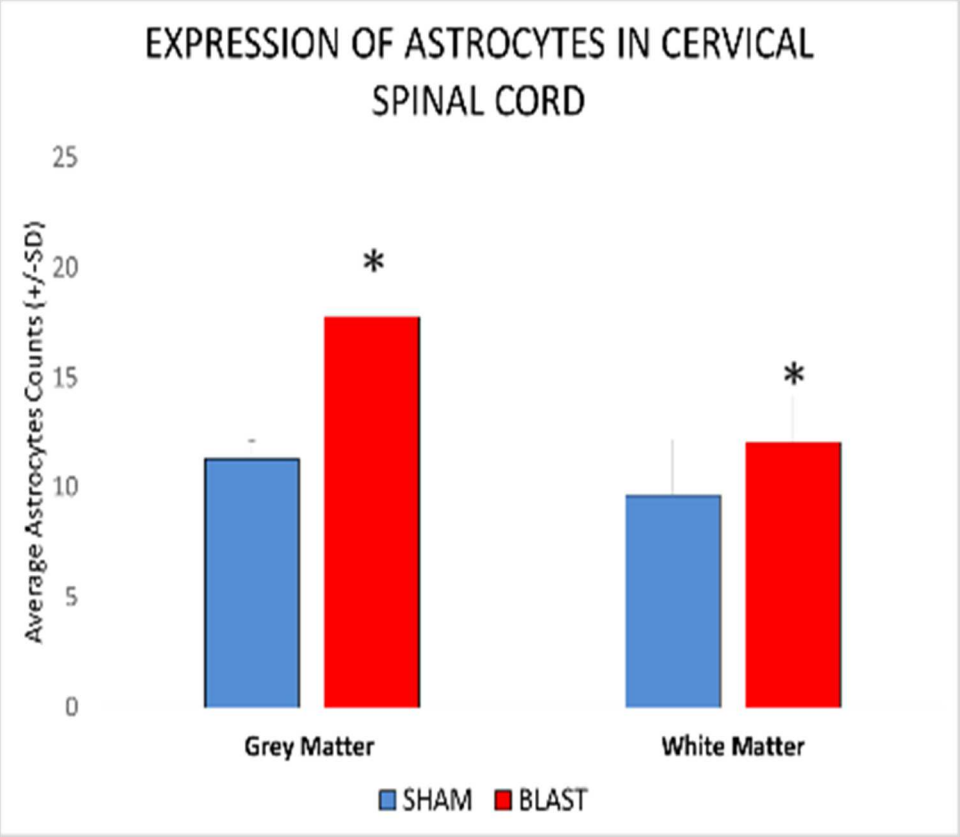

Figure 31: Histogram showing alterations in the expression of astrocytes in the grey matter and white matter of cervical spinal cord. * indicates significant difference ($p<0.05$) in the expression of astrocyte in the blast group compared to the sham group.

Astrocyte proliferation in cervical spinal cord Grey Matter at various post blast time points

In the grey matter of the cervical spinal cord, the expression of astrocytes showed significant elevation in the blast group at all survival periods compared to corresponding sham group as shown in figure 32. Also, there was no significant difference observed in the expression of astrocytes at various survival periods of the sham group. In the blast group, although the proliferation of astrocytes was reduced at 24 hours post exposure it was still significant compared to the corresponding sham counts. The astrocyte counts increased again at 3 days survival period with their expression being reduced at 7days

that remained higher than the sham group. All the alterations in the blast group were statistically significant for all survival periods compared to their corresponding sham counterparts ($p<0.05$).

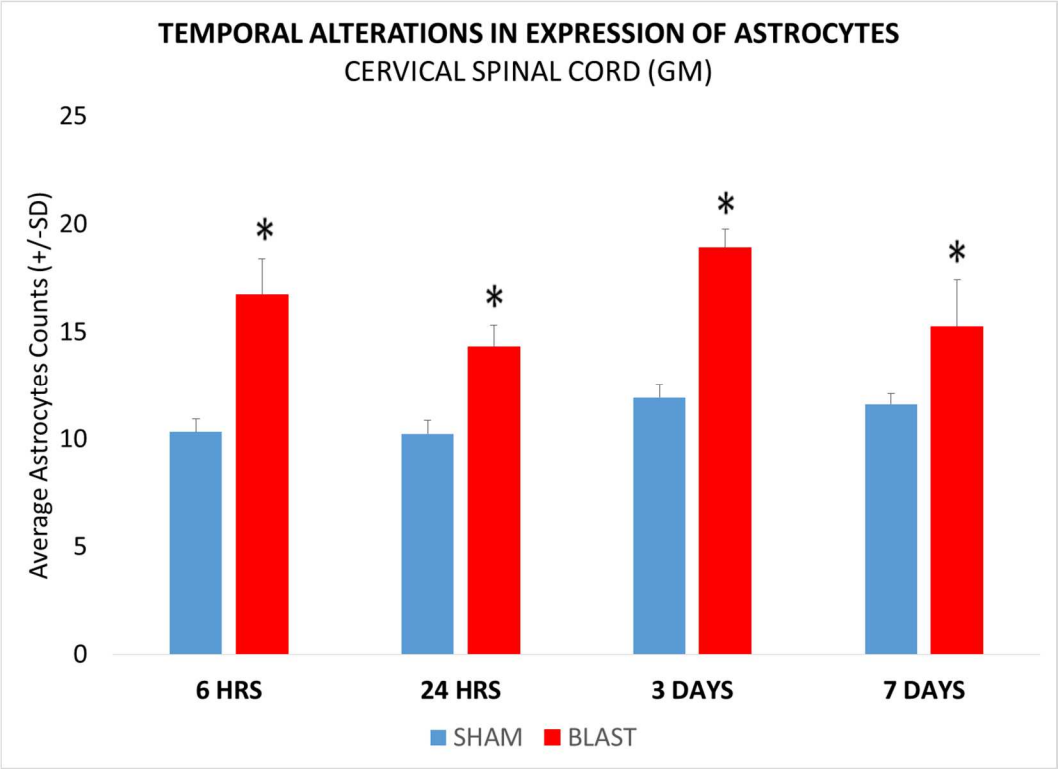

Figure 32: Histogram showing alterations in expression of astrocytes in the grey matter of the cervical spinal cord at various acute and sub-acute periods (6hours, 24 hours, 3 days and 7 days) following blast overpressure. * indicates significant difference ($p<0.05$) in expression of astrocytes in blast group compared to sham group.

Astrocyte proliferation in cervical spinal cord White Matter at various post blast time points:

In the white matter of the cervical spinal cord, the expression of astrocytes was significantly elevated at 6 hours and 24hours survival period in the blast group compared to the corresponding sham group ($p<0.05$) as shown in figure 33. There was peak elevation observed at 6 hour survival period, which reduced at the other survival periods.

Although, high white matter astrocytes counts were observed at 3 days and 7 days post blast there was no significant difference compared to those in sham.

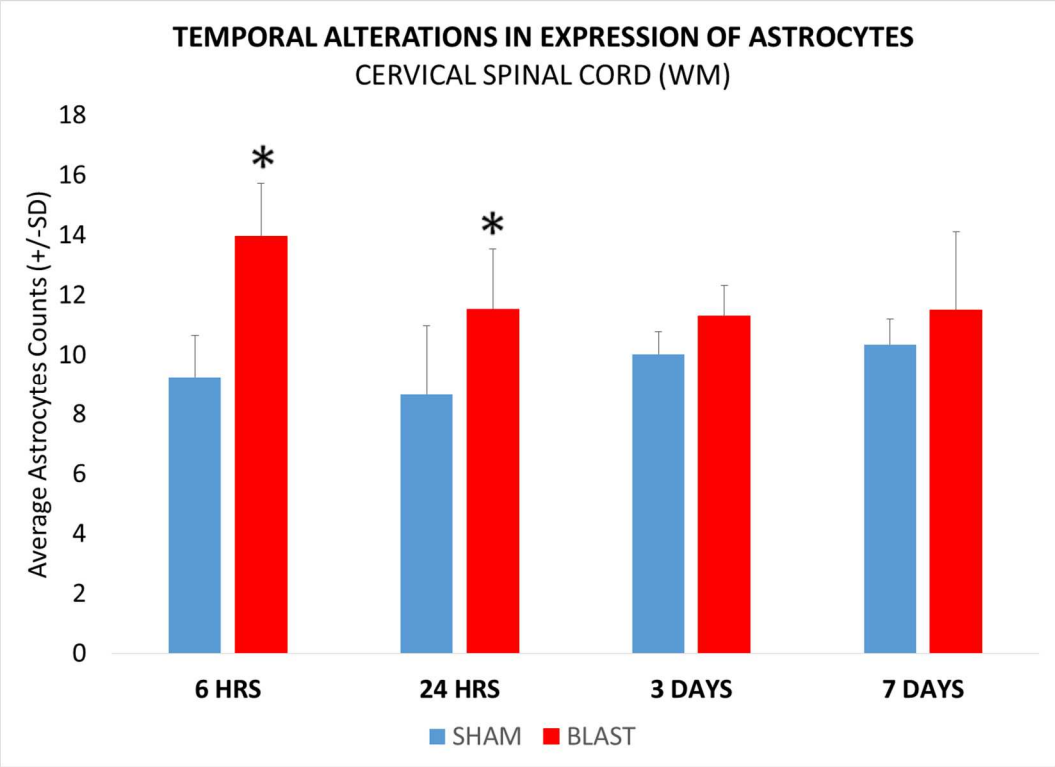

Figure 33: Histogram showing alterations in expression of astrocytes in the white matter of the cervical spinal cord at various acute and sub-acute periods (6hours, 24 hours, 3 days and 7 days) following blast overpressure. . * indicates significant difference ($p<0.05$) in the expression of astrocytes in blast group compared to sham group.

THORACIC SPINAL CORD ASTROCYTE CHANGES

Similar to the cervical region as mentioned earlier, respective images of the sham group and blast group from the thoracic spinal cord are shown in figure 34.

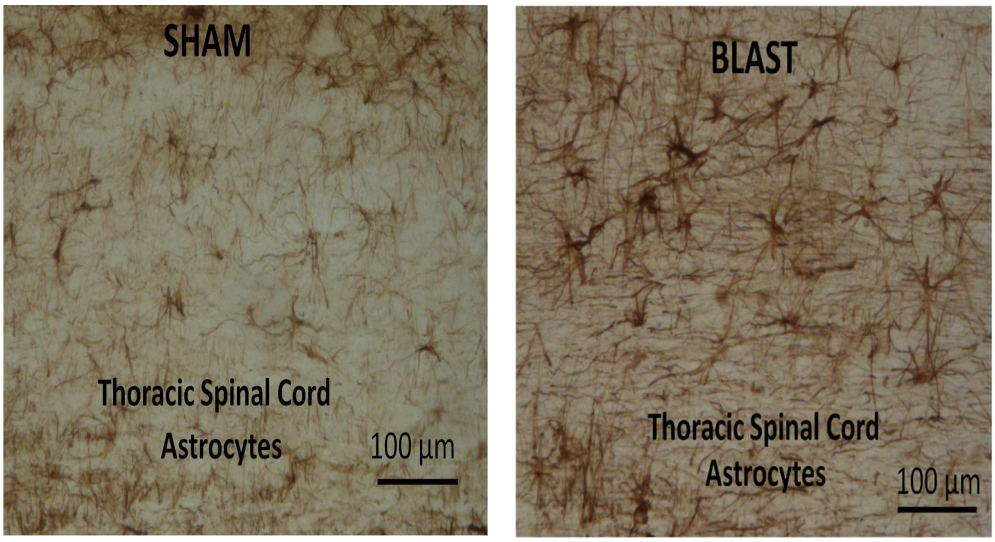

Figure 34: Image showing the expression of astrocytes in the thoracic spinal cord. A: Sham group B. Blast group. Scale Bar: 100 um= 10x magnification.

The grey matter and white matter regions were assessed to study the expression of astrocytes in the thoracic spinal cord. In both regions, there was significant increase observed in the blast group in comparison to the sham group as shown in figure 35.

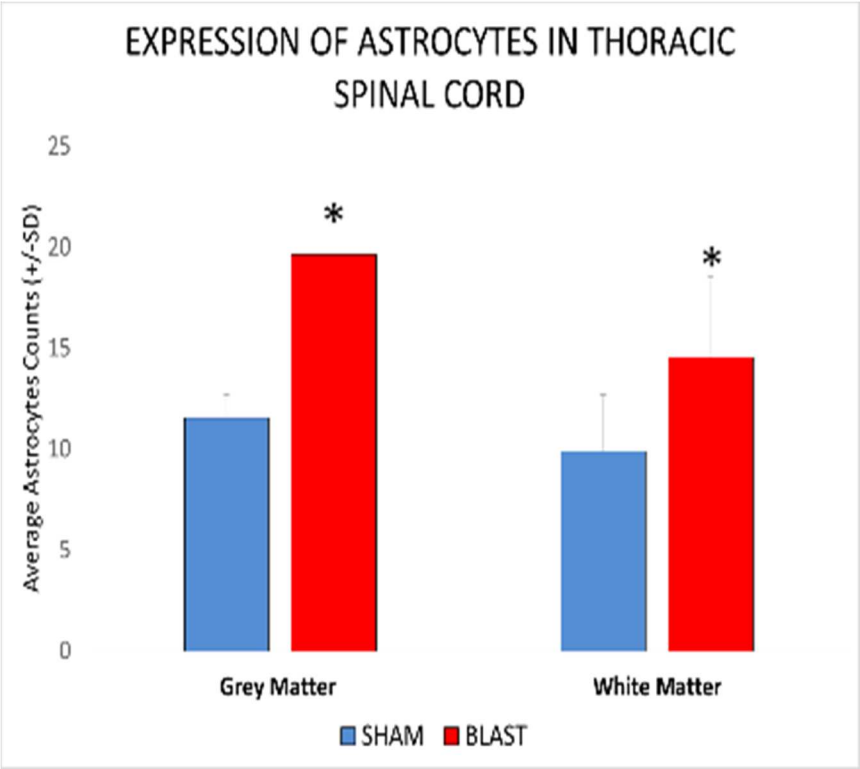

Figure 35: Histogram showing alterations in the expression of astrocytes in the grey matter and white matter of thoracic spinal cord.* indicates significant difference ($p<0.05$) in expression of astrocyte in blast group compared to sham.

The alterations in the expression of astrocytes was quantified for grey and white matter regions of the thoracic spinal cord separately to better understand their temporal distribution.

Astrocyte proliferation in thoracic spinal cord Grey Matter at various post blast time points

The expression of astrocytes in the grey matter of the thoracic spinal cord, showed significant elevation in the blast group at all survival periods compared to Sham group as shown in figure 34. There was an increased expression of astrocytes at 6hours, which reduced at 24hours post exposure. In the 3 days following exposure, the expression increased. The expression of astrocytes reduced at 7days, however it remained higher

than the Sham group. The peak elevation in the expression of astrocytes was observed at 3 days following blast exposure. All the alterations in the blast group were statistically significant for all survival periods compared to the corresponding sham counts. ($p<0.05$).

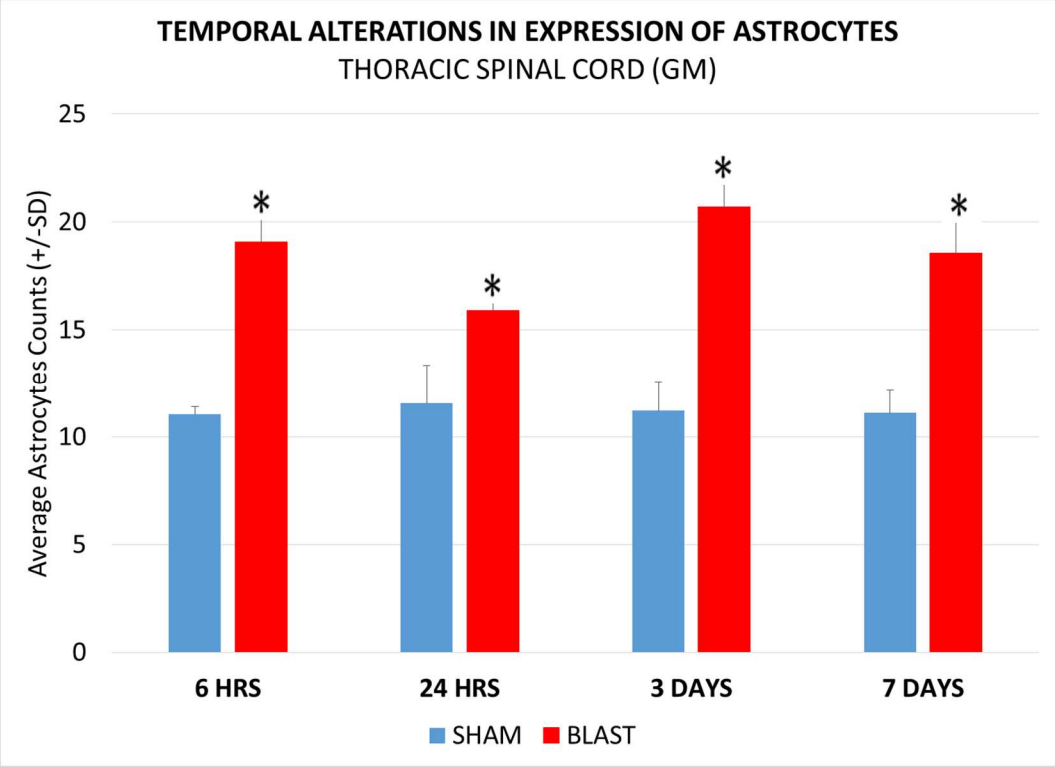

Figure 36: Histogram showing alterations in expression of astrocytes in the grey matter of the thoracic spinal cord at various acute and sub-acute periods (6hours, 24 hours, 3 days and 7 days) following blast overpressure.* indicates significant difference ($p<0.0$)) in expression of astrocyte in blast group compared to sham.

Astrocyte proliferation in cervical spinal cord White Matter at various post blast time points

In the white matter of the thoracic spinal cord, the expression of astrocytes showed significant elevation at 24 hours and 3days of the Blast group compared to Sham group as shown in figure 37 ($p<0.05$). A slight drop was observed at 24hours post exposure compared to 6hours following blast overpressure, and there was an increase again at 3

days survival period compared to the sham group. The expression of astrocytes reduced at 7days and similar to the Sham group.

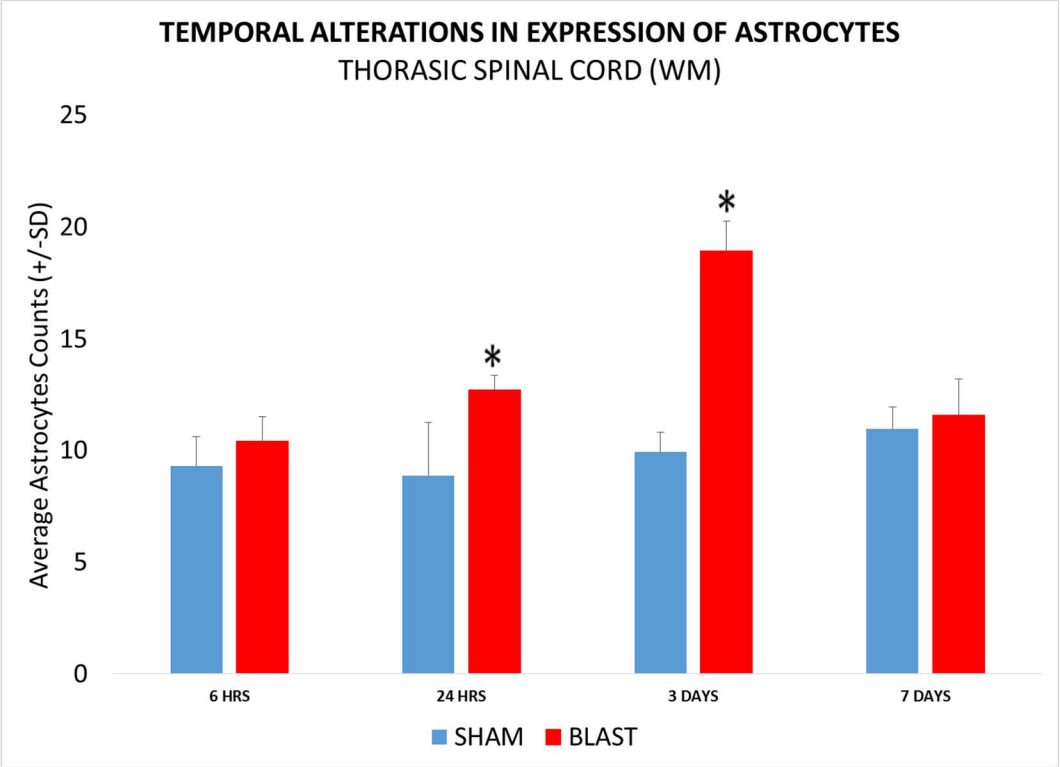

Figure 37: Histogram showing alterations in expression of astrocytes in the white matter of the thoracic spinal cord at various acute and sub-acute periods (6hours, 24 hours, 3 days and 7 days) following blast overpressure. * indicates significant difference ($p<0$) in expression of astrocytes in blast group compared to sham.

LUMBAR SPINAL CORD ASTROCYTE CHANGES

Similar to the qualitative and quantitative analysis for the cervical and thoracic regions, the lumbar region was studied for the expression of at various survival periods. The images astrocytes from the sham group and the blast group are shown in figure 38.

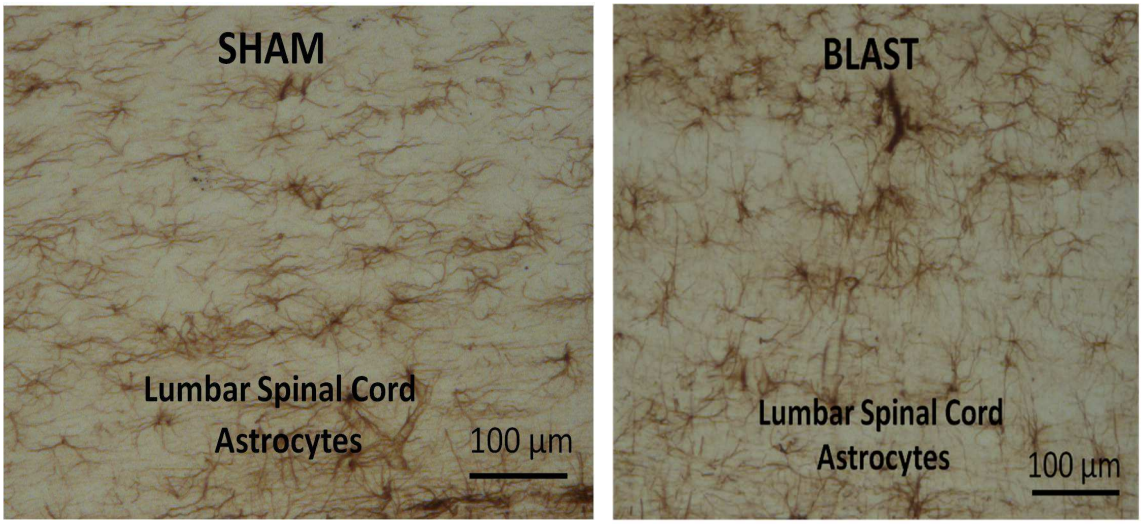

Figure 38: Image showing the expression of astrocytes in the lumbar spinal cord. A: Sham group B. Blast group. Scale Bar: 100 um= 10x magnification.

The grey matter and white matter regions were measured for the expression of astrocytes in the lumbar spinal cord. In both regions, there was significant increase observed in the blast group in comparison to the sham group as shown in figure 39. The gray matter showed higher number of astrocytes compared to the white matter in the lumbar spinal cord.

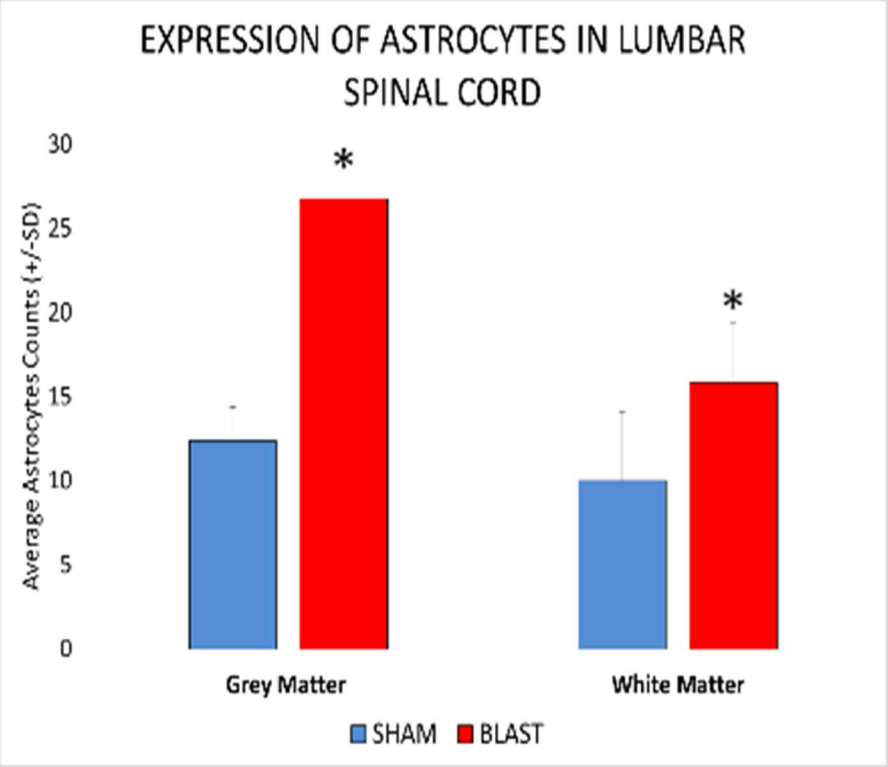

Figure 39: Plot showing alterations in the expression of astrocytes in the grey matter and white matter of lumbar spinal cord.* indicates significant difference ($p<0.05$) in expression of astrocyte in blast group compared to sham.

The extent of astrocyte expression was quantified for grey and white matter regions of the lumbar spinal cord separately to better understand the temporal alterations witnessed at the various survival periods.

Astrocyte proliferation in lumbar spinal cord Grey Matter at various post blast time points

The expression of astrocytes in the grey matter showed significant elevation in the blast group at all survival periods compared to Sham group as shown in figure 40. There was increased expression of astrocytes at 6hours, which reduced at 24hours post exposure. In the 3 days following exposure, the expression increased. The expression of astrocytes reduced at 7days, however it remained higher than the Sham group. The peak

elevation in the expression of astrocytes was observed at 6 hours following blast exposure. The expression of astrocytes was higher in the lumbar spinal cord compared to the other levels of the spinal cord. All the alterations in the blast group were statistically significant for all survival periods. ($p<0.05$).

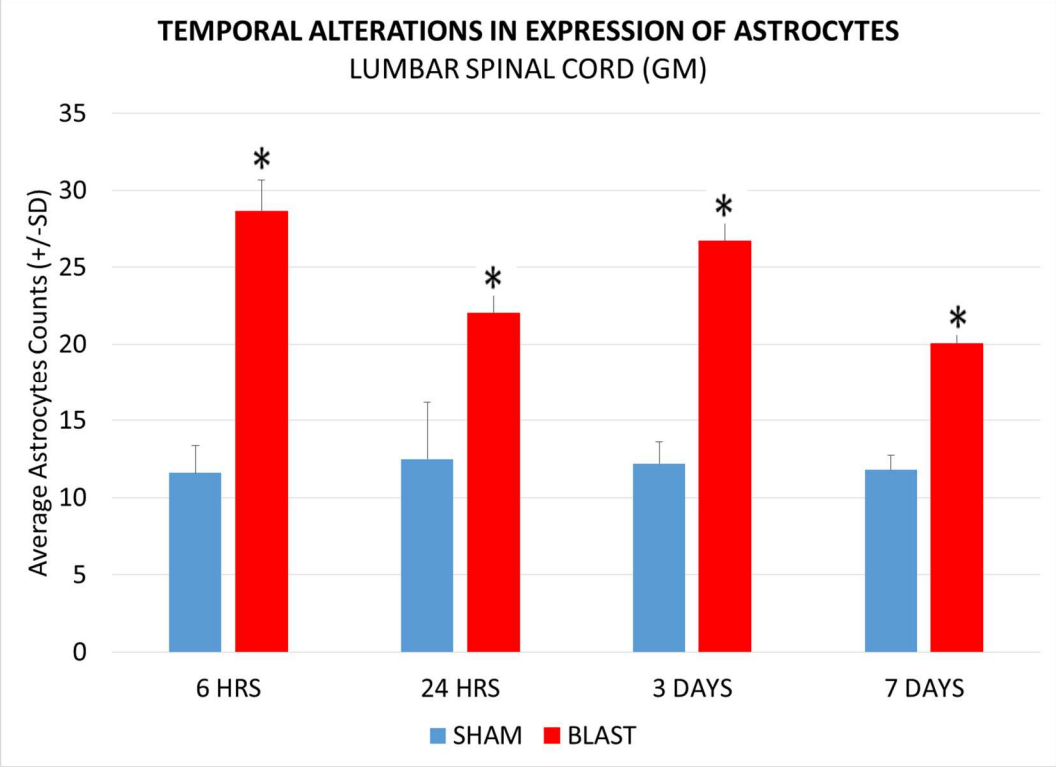

Figure 40: Histogram showing alterations in expression of astrocytes in the grey matter of the lumbar spinal cord at various acute and sub-acute periods (6hours, 24 hours, 3 days and 7 days) following blast overpressure.* indicates significant difference ($p<0.05$) in expression of astrocyte in blast group compared to sham.

Astrocyte proliferation in lumbar spinal cord White Matter at various post blast time points

In the white matter of lumbar spinal cord, the expression of astrocytes showed significant elevation at 6 hours, 3 days and 7 days of the Blast group compared to Sham group as shown in figure 41. Although, the proliferation of astrocytes decreased further at 7days, it stayed significantly elevated compared to sham group.

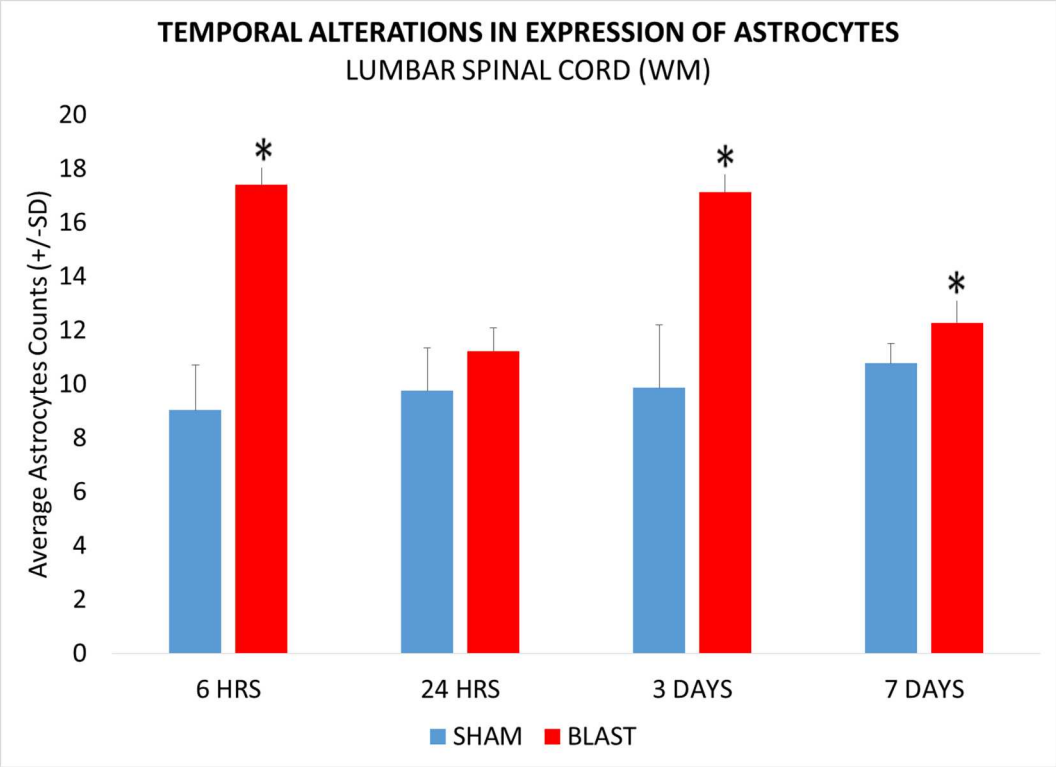

Figure 41: Histogram showing alterations in expression of astrocytes in the white matter of the lumbar spinal cord at various acute and sub-acute periods (6hours, 24 hours, 3 days and 7 days) following blast overpressure.* indicates significant difference ($p<0.05$) in expression of astrocyte in blast group compared to sham.

SPATIAL ALTERATIONS IN THE EXPRESSION OF ASTROCYTES:

Further, we studied the spatial alterations in the expression of astrocytes in the grey matter and white matter at the different levels in the spinal cord The spatial alterations in the grey matter were studied at the cervical, thoracic and lumbar spinal cord as shown in the figure 42. Where as the spatial alterations in the white matter were studied at the cervical, thoracic and lumbar spinal cord as shown in the figure 43. In the grey matter, the lumbar region showed a high number of astrocytes compared to those at thoracic and cervical regions. In the white matter, the number of astrocytes showed no specific pattern with the respect to various regions. Describe what you see in the chart: high lumbar

number at 6 hours with cervical region showing second highets at 6 hours post blast. The counts in thoraci showd a gradual increasing trend with a peak by 3 days compared to the lumabr and cervical counts.

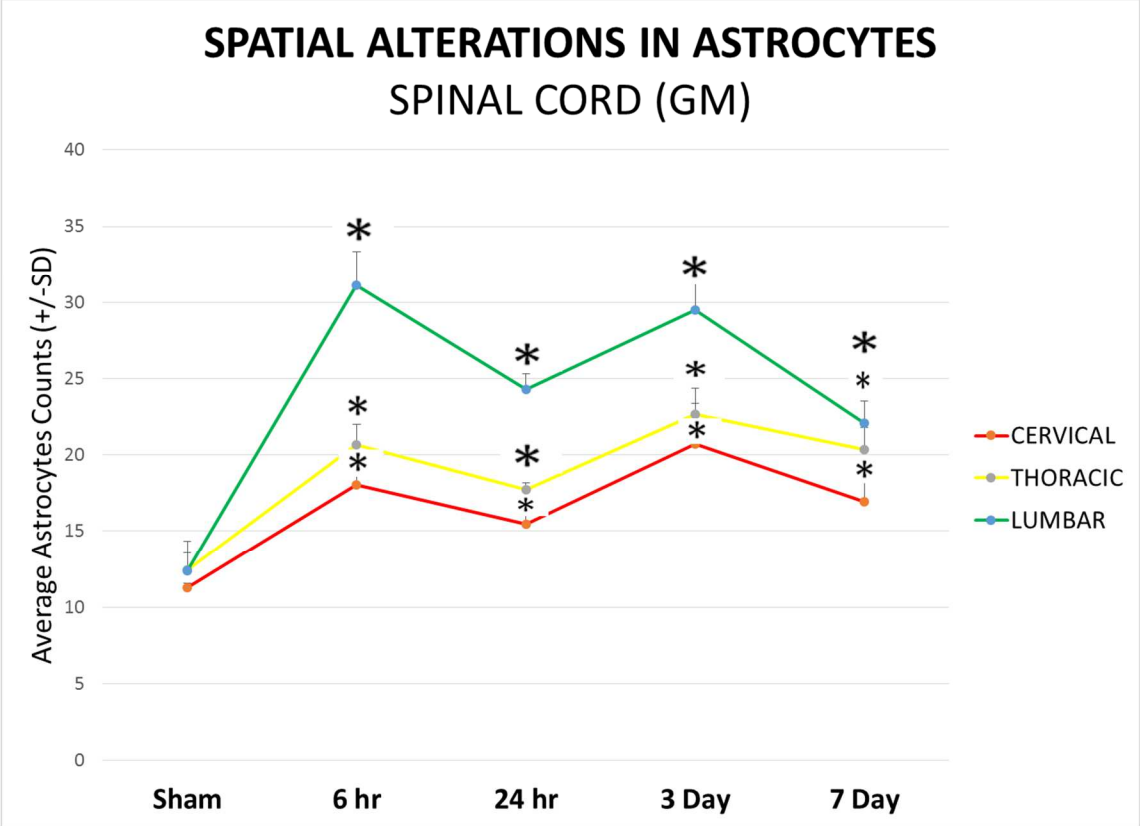

Figure 42: Plot showing the spatial alterations in the expression of astrocytes in the grey matter of cervical, thoracic and lumbar spinal cord in the sham and blast group (6hrs, 24hrs, 3days and 7days). * indicates significant difference ($p<0.05$) in expression of astrocytes in blast group compared to sham.

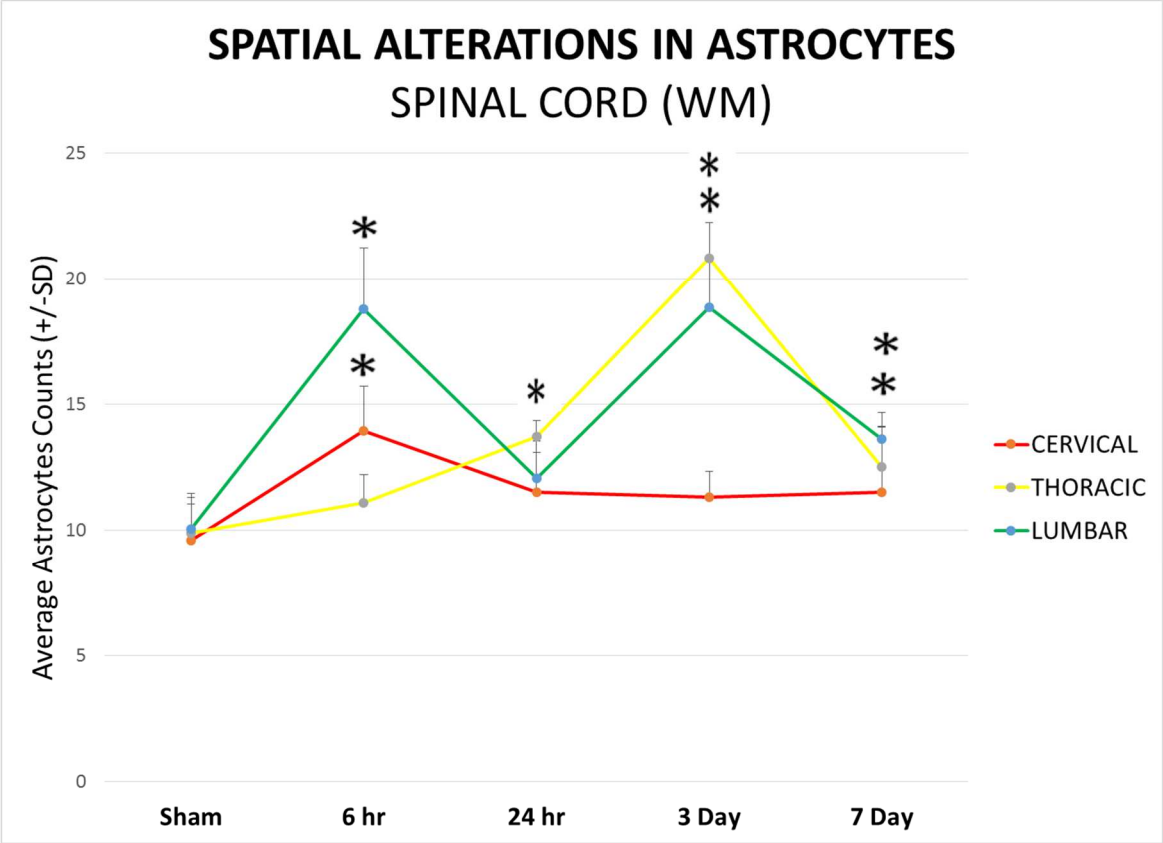

Figure 43: Plot showing the spatial alterations in the expression of astrocytes in the white matter of cervical, thoracic and lumbar spinal cord in the sham and blast group (6hrs, 24hrs, 3days and 7days). * indicates significant difference ($p<0.05$) in expression of astrocytes in blast group compared to sham.

All the regions of the spinal cord showed siginificant proliferation in the expression of astrocytes in the blast group compared to the sham group. Although the expression of astrocytes in the cervical spinal cord showed significant difference at the 6 hours and 24 hours, while the levels decreased at the other survival periods, and closer to the sham group counts. The level of proliferation was highest at the lumbar region at all survival periods (not true at 24 hrs, not true when compared to thoracic at 3 days)

4.3 Alterations in the expression of microglia

The spinal cord sections were stained using Ionized calcium Binding Adaptor molecule-1 (IBA-1) antibody to assess the expression of microglia in blast and sham animals. IBA-1 is considered as an ideal marker for both resting and activated microglia (Ahmed et al., 2007). We were able find morphological differences in the expression of the microglia in the blast group compared to the sham group as shown in figure 44. The microglia in the sham group demonstrated a ramified morphology, while the blast group microglia was amoeboid shape with retracted processes.

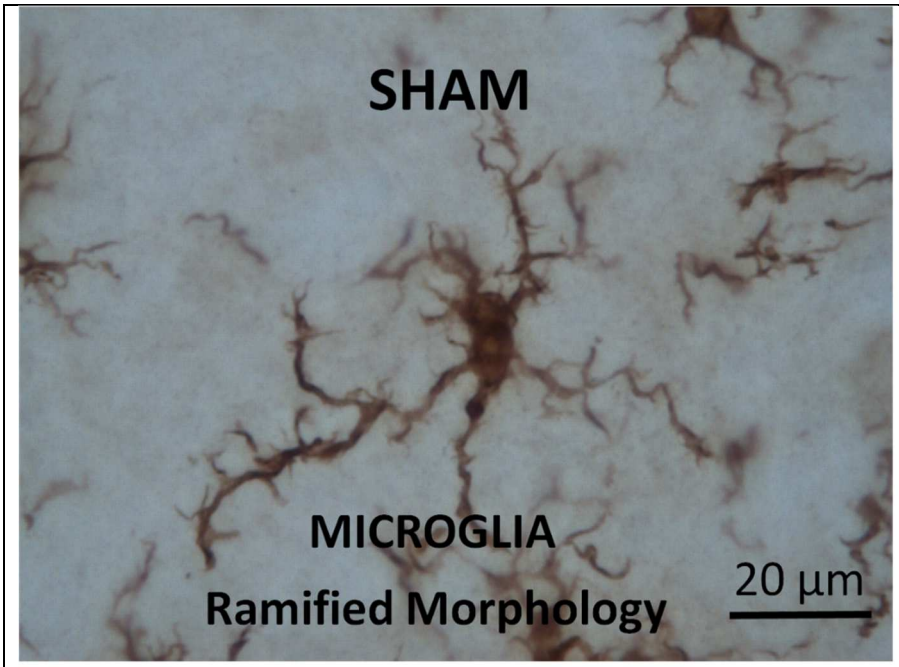

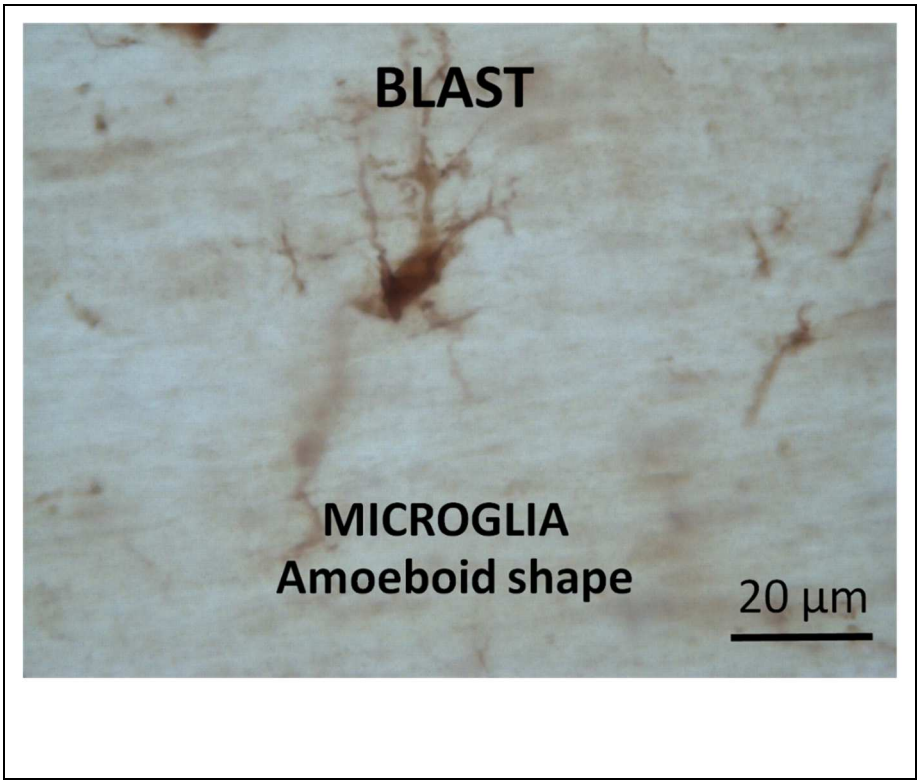

Figure 44: Morphological changes in the expression of microglia in the sham group (A) and blast group (B) at 40x magnification.

We quantified microglia in the different levels of the spinal cord to observe the effects of blast overpressure on their proliferation. The Blast group showed significant proliferation of microglia compared to Sham group. ($p<0.05$) as shown in figure 45.

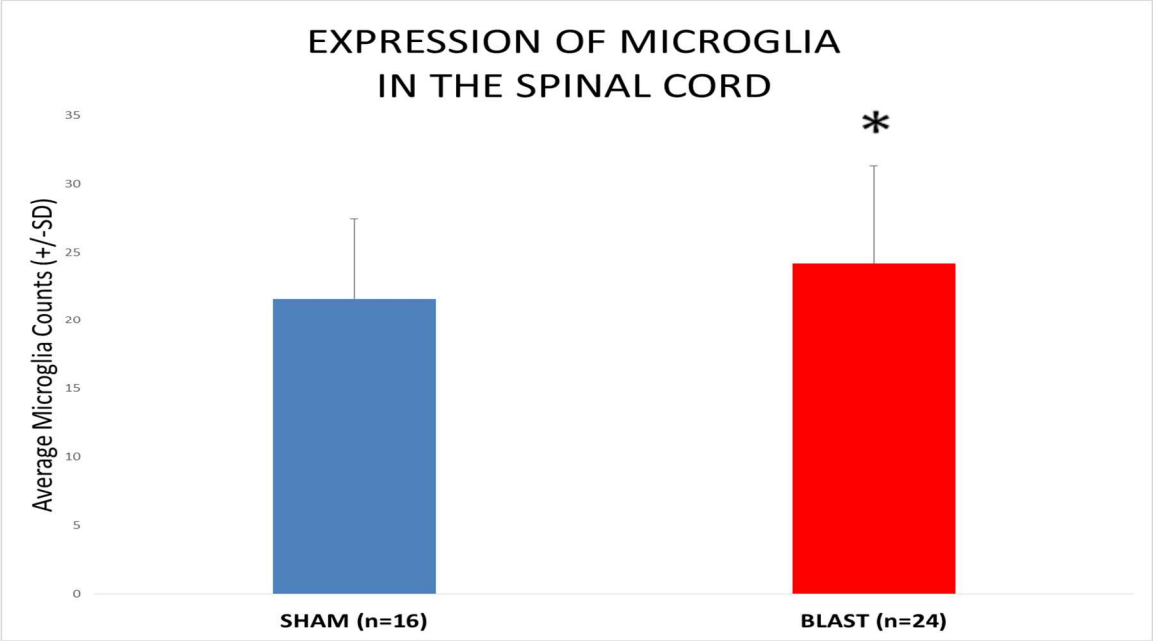

Figure 45: Plot showing alterations in the expression of microglia in the sham and blast group. * indicates significant difference ($p<0.05$) in expression of microglia in blast group compared to sham.

CERVICAL SPINAL CORD- MICROGLIA CHANGES

To study the proliferation changes in the expression of microglia, respective digital images were taken from the sham and blast group as shown in figure 44. Increased number of microglia were observed in the blast group compared to the sham group.

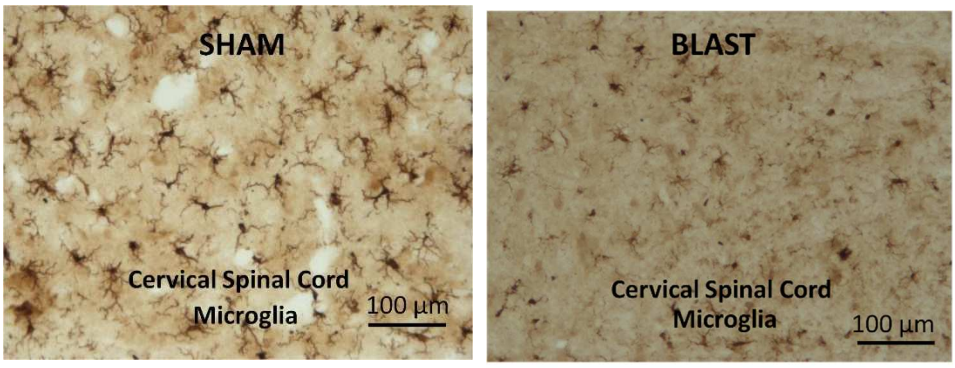

Figure 46: Image showing the expression of microglia in the cervical spinal cord. A: Sham group B. Blast group. Scale Bar: 100 um= 10x magnification.

Futher, we studied the expression of microglia in the grey matter and white matter of the respective cervical, thoracic and lumbar spinal cord. In both the regions, there was significant difference between the blast group and to the sham group as shown in figure 47. However, the microglia in the blast group continued to show a amoeboid appearance compared to the ramified appearance of sham group with their numerous processes.

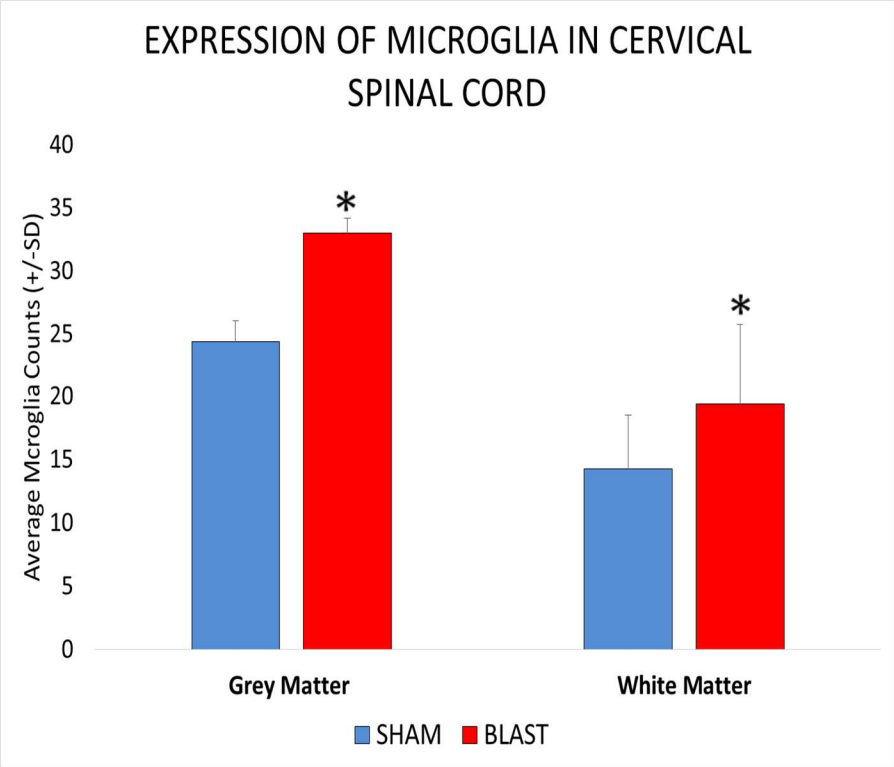

Figure 47: Histogram showing alterations in the expression of microglia in the grey matter and white matter of cervical spinal cord. * indicates significant difference ($p<0.05$) in the expression of microglia in the blast group compared to the sham group.

The expression of microglia were quantified for grey and white matter regions of the cervical spinal cord separately to better understand the temporal alterations witnessed at the various survival periods.

Microglia proliferation in cervical spinal cord Grey Matter at various post blast time points:

In the cervical spinal cord, the expression of microglia showed significant difference at all survival periods of the blast group compared to the corresponding sham group. ($p<0.05$). There was a peak elevation in the number of microglia observed at 6 hour survival period, which reduced at 24 hours and 3 days following blast exposure albeit at significant levels compared to the corresponding sham groups. However, the number of microglia increased by the 7 days survival period, which was closer to the 6 hour survival period.

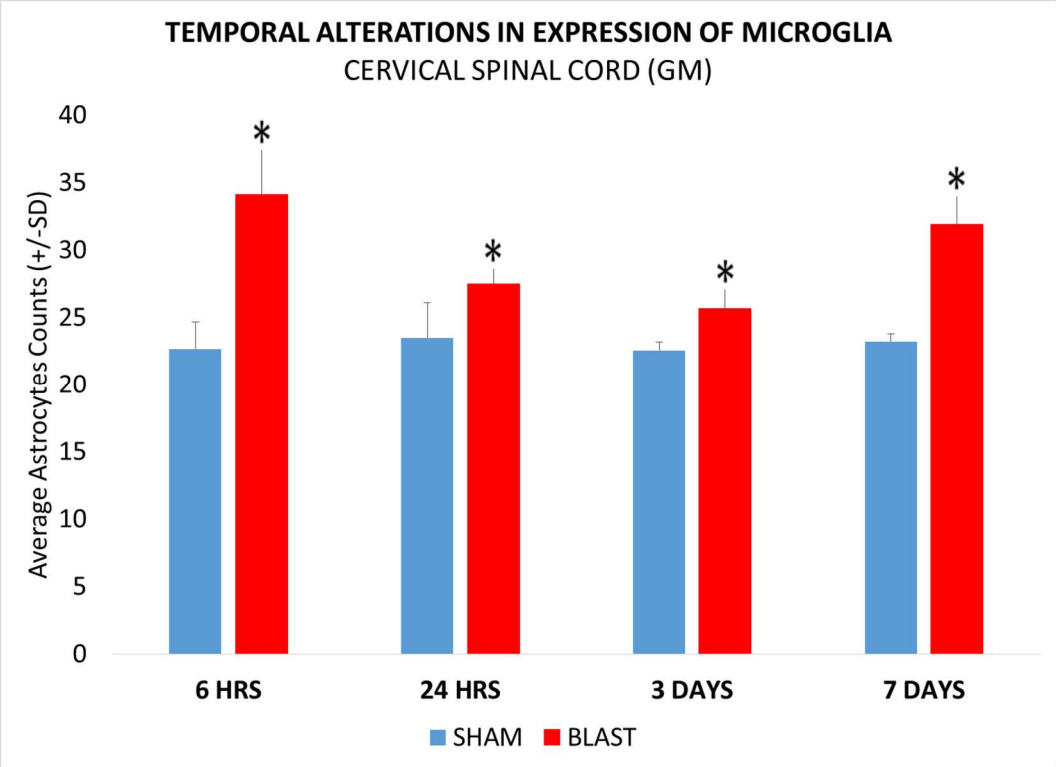

Figure 48: Histogram showing alterations in expression of microglia in the grey matter of the cervical spinal cord in the sham and blast group at various acute and sub-acute periods (6hours, 24 hours, 3 days and 7 days) following blast overpressure.* indicates significant difference ($p<0.05$) in expression of microglia in blast group compared to sham.

Microglia proliferation in cervical spinal cord White Matter at various post blast time points:

The expression of microglia showed significant difference in all survival periods of the Blast group compared to the Sham group. ($p<0.05$). There was a peak expression observed at 6hour survival period, which reduced at 24 hours following blast exposure. A drop was demonstrated in the expression of microglia at the 3 days following blast overpressure which was significantly less compared to the sham group. However, by 7 days post blast, the number of microglia was elevated reaching levels higher than those at 24 hours post blast.

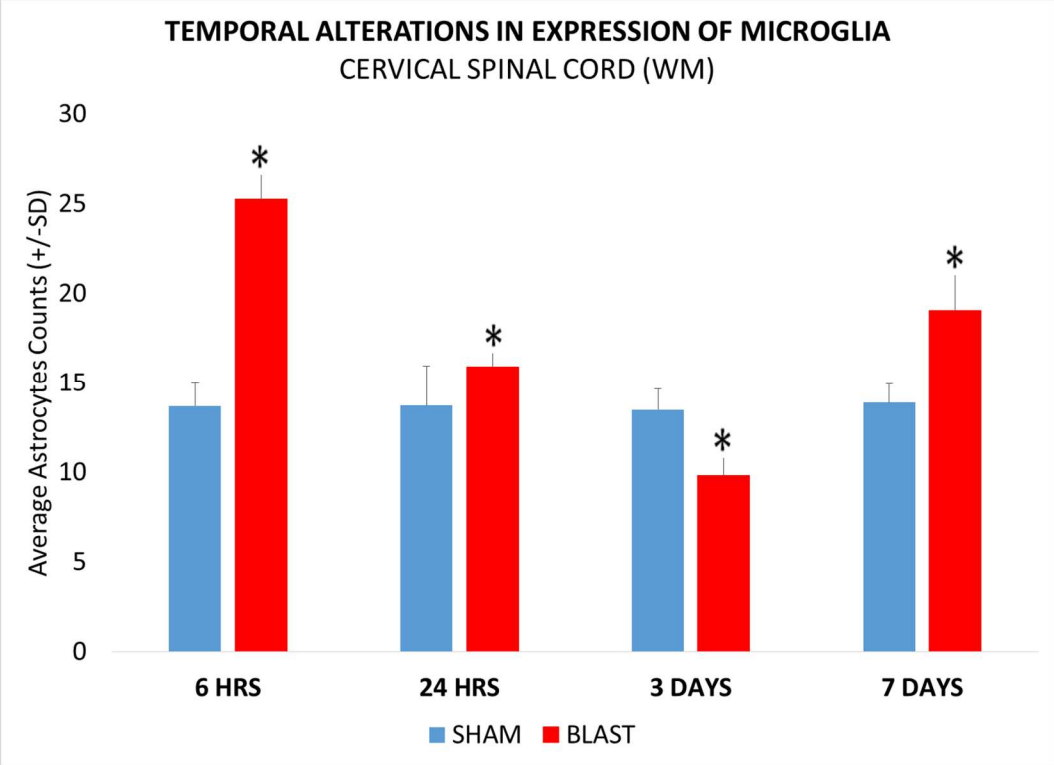

Figure 49: Histogram showing alterations in expression of microglia in the white matter of the cervical spinal cord at various acute and sub-acute periods (6hours, 24 hours, 3 days and 7 days) following blast overpressure.* indicates significant difference ($p<0.05$) in expression of microglia in blast group compared to sham.

THORACIC SPINAL CORD MICROGLIA CHANGES

The images of the sham group and blast group are shown in figure 48. It was observed that the microglia in the sham group demonstrated the ramified morphology, while the blast group demonstrated amoeboid shrunken phenotype with shorter processes similar to those seen in the cervical spinal cord.

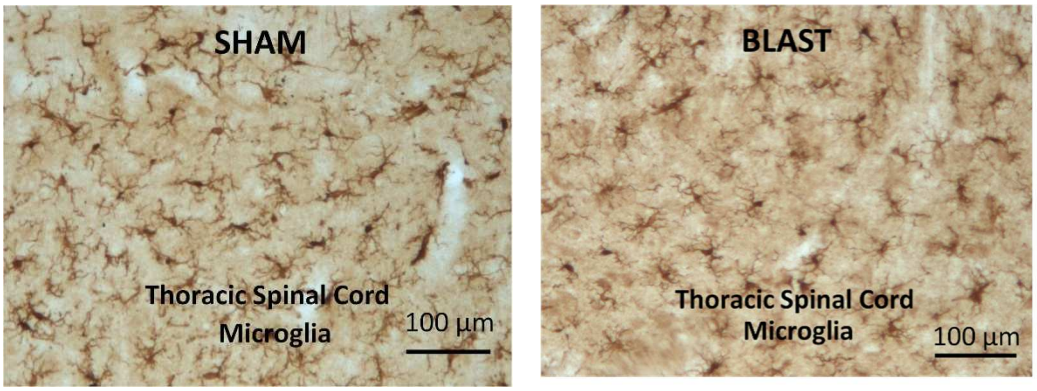

Figure 50: Image showing the expression of microglia in the thoracic spinal cord. A: Sham group B. Blast group. Scale Bar: 100 um= 10x magnification.

The grey matter and white matter regions were measured for the expression of microglia in the lumbar spinal cord. In both regions, there was no significant increase in the blast group in comparison to the sham group as shown in figure 51.

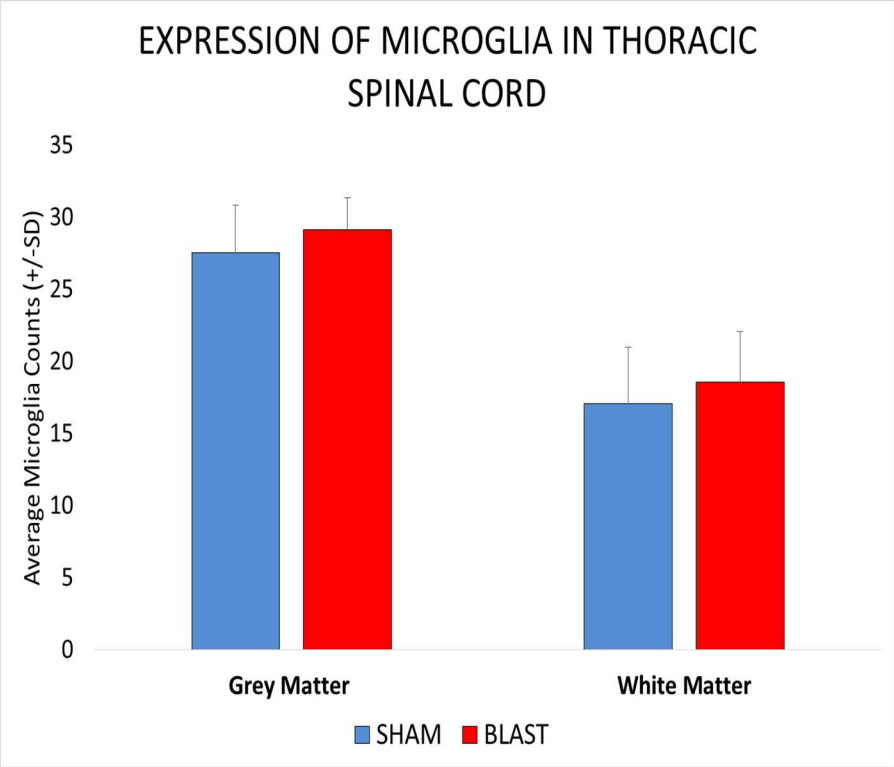

Figure 51: Histogram showing alterations in the expression of microglia in the grey matter and white matter of thoracic spinal cord

The expression of astrocytes were quantified for grey and white matter regions of the thoracic spinal cord separately to better understand study the temporal alterations witnessed at the various survival periods.

Microglia proliferation in thoracic spinal cord Grey Matter at various post blast time points

The expression of microglia in the grey matter of the thoracic spinal cord showed significant elevation only at 6 hours in the Blast group compared to Sham group as shown in figure 52.No significant difference was observed between the sham and blast group at other time periods. Grey matter and white matter microglia counts were not different

between blast and sham group, albeit slightly higher number were observed at 3 and 7 days in the blast group.

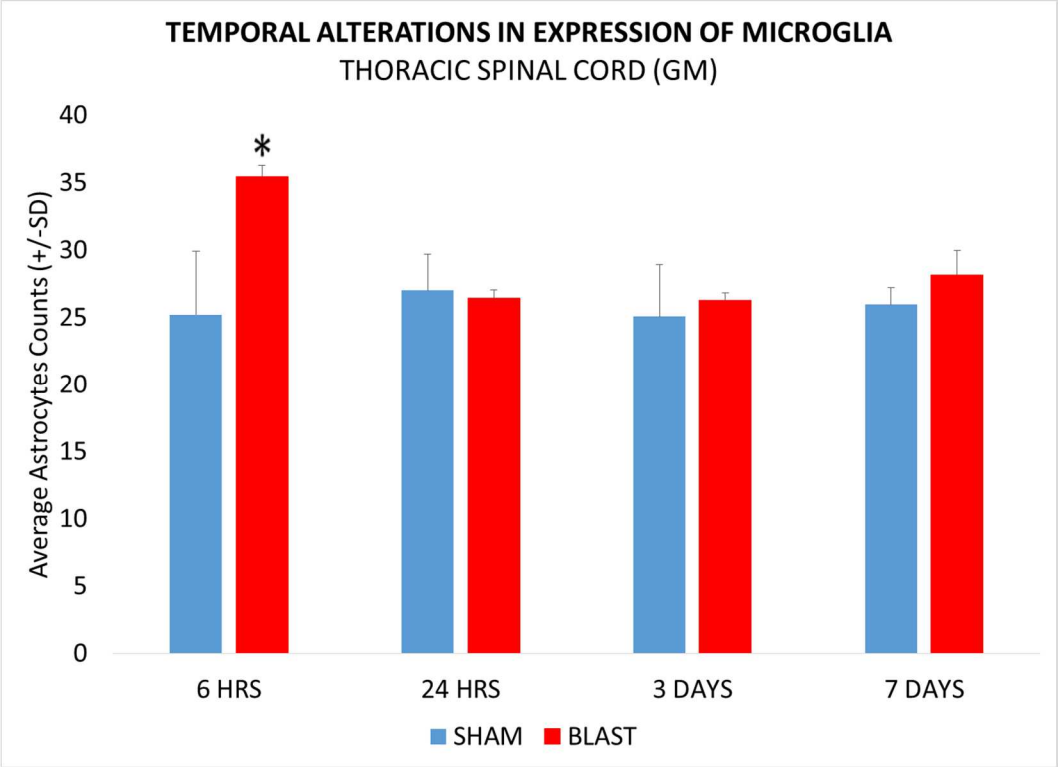

Figure 52: Histogram showing alterations in the expression of microglia in the grey matter of the thoracic spinal cord in the sham and blast group at various acute and sub-acute periods (6hours, 24 hours, 3 days and 7 days) following blast overpressure.* indicates significant difference ($p<0.05$) in expression of microglia in blast group compared to sham.

Microglia proliferation in cervical spinal cord White Matter at various post blast time points

The expression of microglia in the white matter of the thoracic spinal cord showed significant elevated number only at 6 hours in the blast group compared to Sham group as shown in figure 42. However, there were no significant differences observed between the sham and blast group at other time periods.

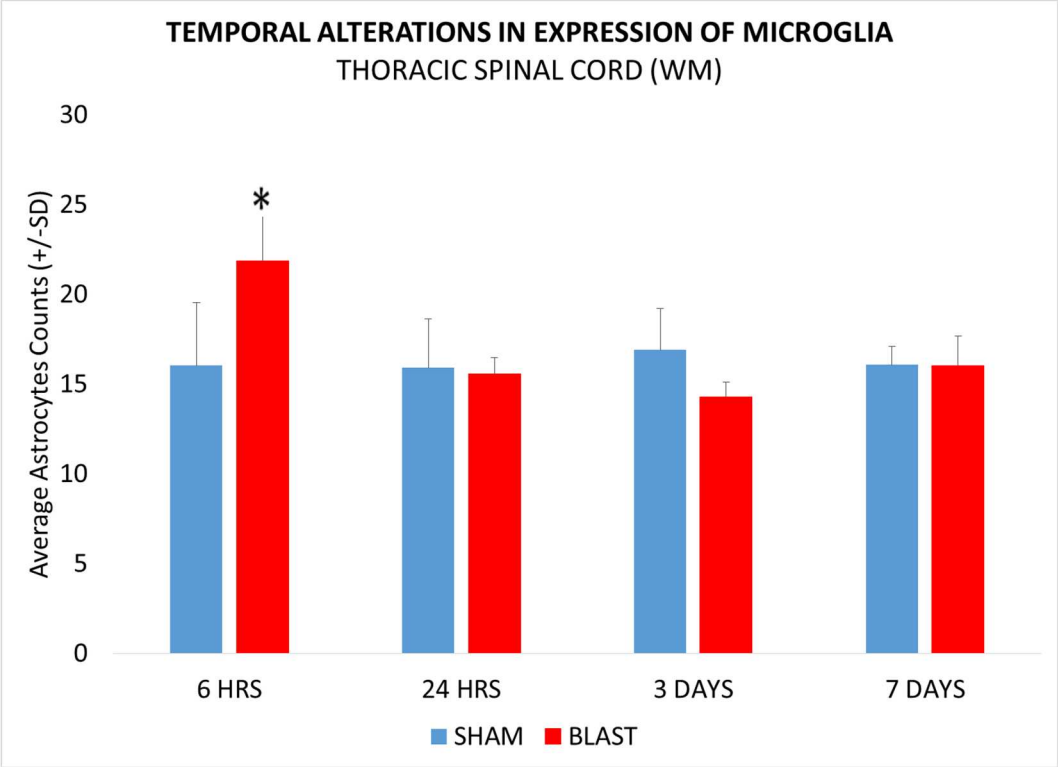

Figure 53: Histogram showing alterations in expression of microglia in the white matter of the thoracic spinal cord at various acute and sub-acute periods (6hours, 24 hours, 3 days and 7 days) following blast overpressure.* indicates significant difference ($p<0.05$) in expression of microglia in blast group compared to sham.

LUMBAR SPINAL CORD MICROGLIA CHANGES

The images of the sham group and blast group are shown in figure 51. It was observed that the microglia in the sham group demonstrated the ramified morphology, while the blast group demonstrated amoeboid shrunken phenotype with shorter processes similar to those seen in cervical and thoracic region.

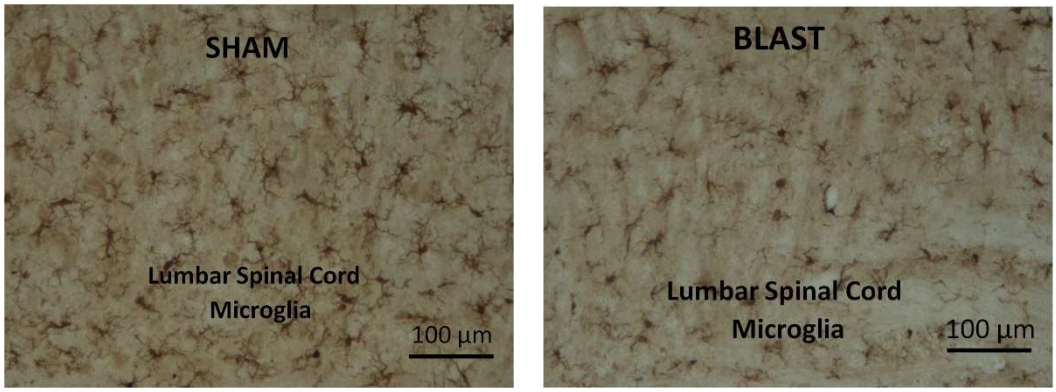

Figure 54: Image showing the expression of microglia in the lumbar spinal cord. A: Sham group B. Blast group. Scale Bar: 100 um= 10x magnification.

There was no siginificant difference observed inthe microglial counts in the grey matter and white matter regions in the blast group compared to the sham group as shown in figure 44.

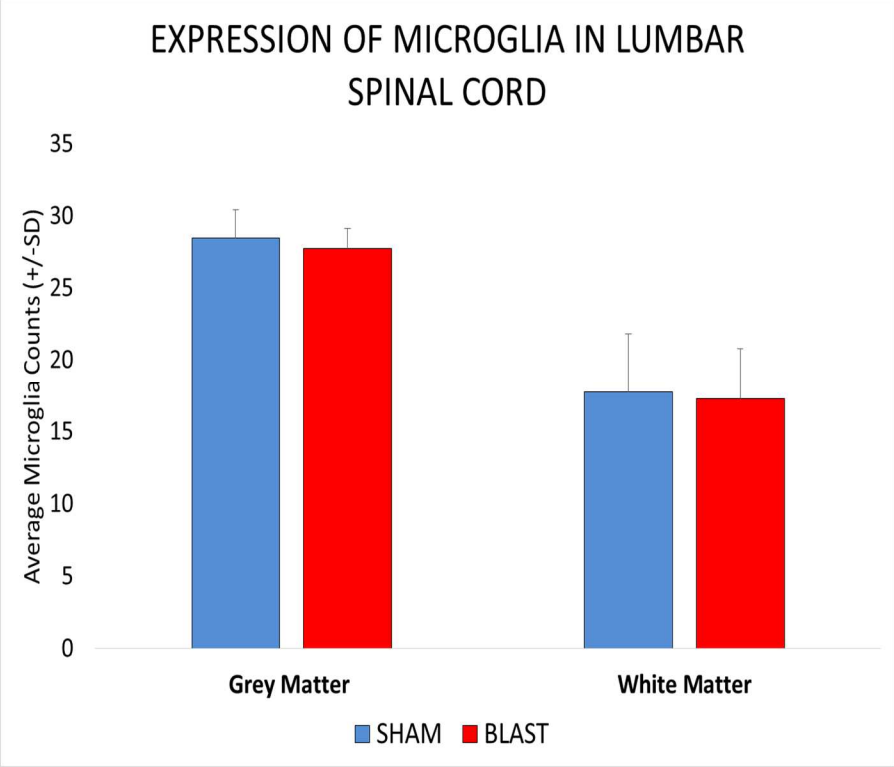

Figure 55: Histogram showing alterations in the expression of microglia in the grey matter and white matter of lumbar spinal cord.

The number of microglia were quantified for grey and white matter regions of the lumbar spinal cord separately to study their temporal alterations

Microglia proliferation in cervical spinal cord Grey Matter at various post blast time points

The expression of microglia in the grey matter of the lumbar spinal cord showed no significant elevated profiles in all survival periods of the blast group compared to sham group as shown in figure 56.

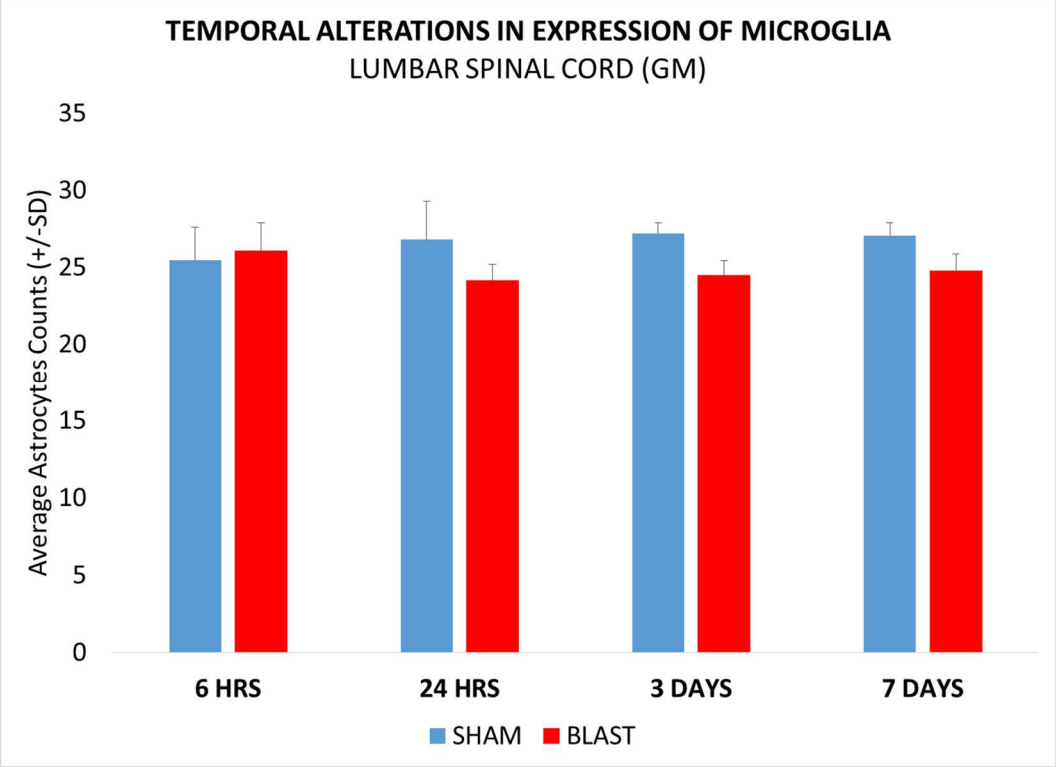

Figure 56: Histogram showing alterations in the expression of microglia in the grey matter of the lumbar spinal cord at various acute and sub-acute periods (6hours, 24 hours, 3 days and 7 days) following blast overpressure.* indicates significant difference ($p<0.05$) in expression of microglia in blast group compared to sham.

Microglia proliferation in cervical spinal cord White Matter at various post blast time points

In the white matter of lumbar spinal cord, the expression of microglia showed no significant elevation at any of the survival period of the blast group compared to Sham group as shown in figure 57.

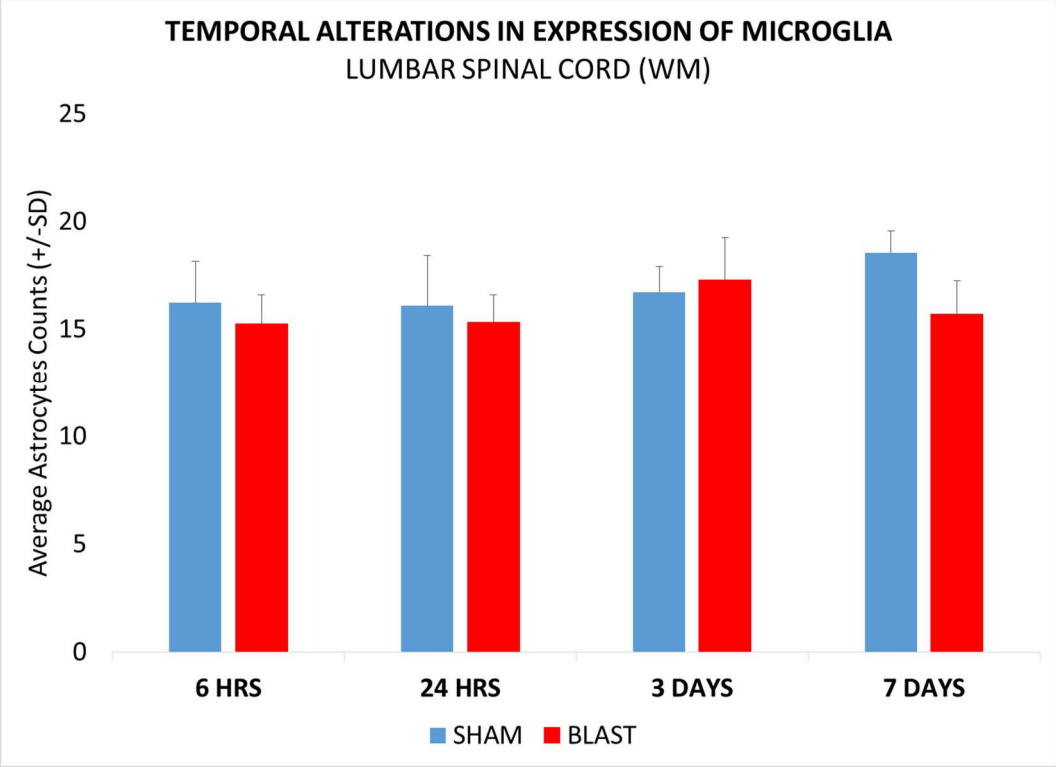

Figure 57: Histogram showing alterations in the expression of microglia in the white matter of the lumbar spinal cord at various acute and sub-acute periods (6hours, 24 hours, 3 days and 7 days) following blast overpressure.* indicates significant difference ($p<0.05$) in expression of microglia in blast group compared to sham.

4.5 SPATIAL ALTERATIONS IN THE EXPRESSION OF MICROGLIA:

Similar to the astrocytes, we also studied the spatial alterations in the expression of microglia in the grey matter and white of the spinal cord. The expression of microglia in the grey matter for the different regions of the spinal cord was studied as shown in figure 58.

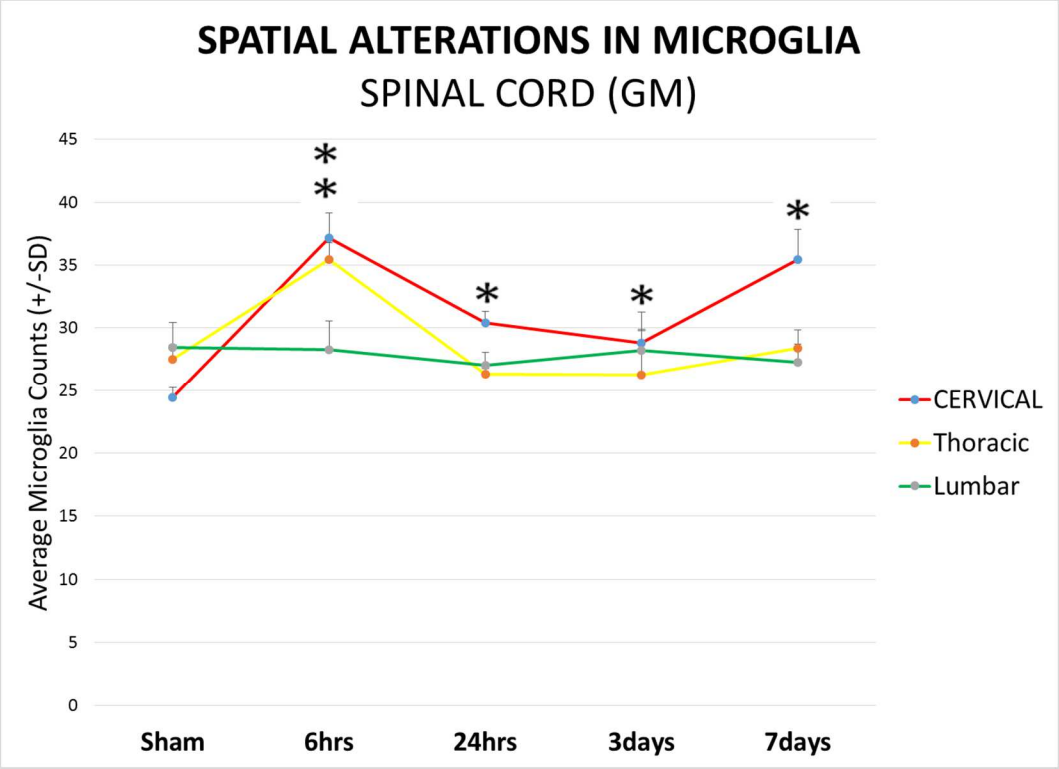

Figure 58: Plot showing the spatial alterations in the expression of microglia in grey matter of cervical, thoracic and lumbar spinal cord in the sham and blast group (6hrs, 24hrs, 3days and 7days). * indicates significant difference ($p<0.05$) in expression of microglia in blast group compared to sham.

From this plot, it was observed that the cervical region had significant elevations in the expression of micrglia at all survival periods, and the thoracic region at 6 hours

following blast overpressure. However, the lumbar region did not show any significant difference to the corresponding sham group.

We also studied the spatial alterations in the expression of microglia in the white matter of the spinal cord was studied as shown in figure 59.

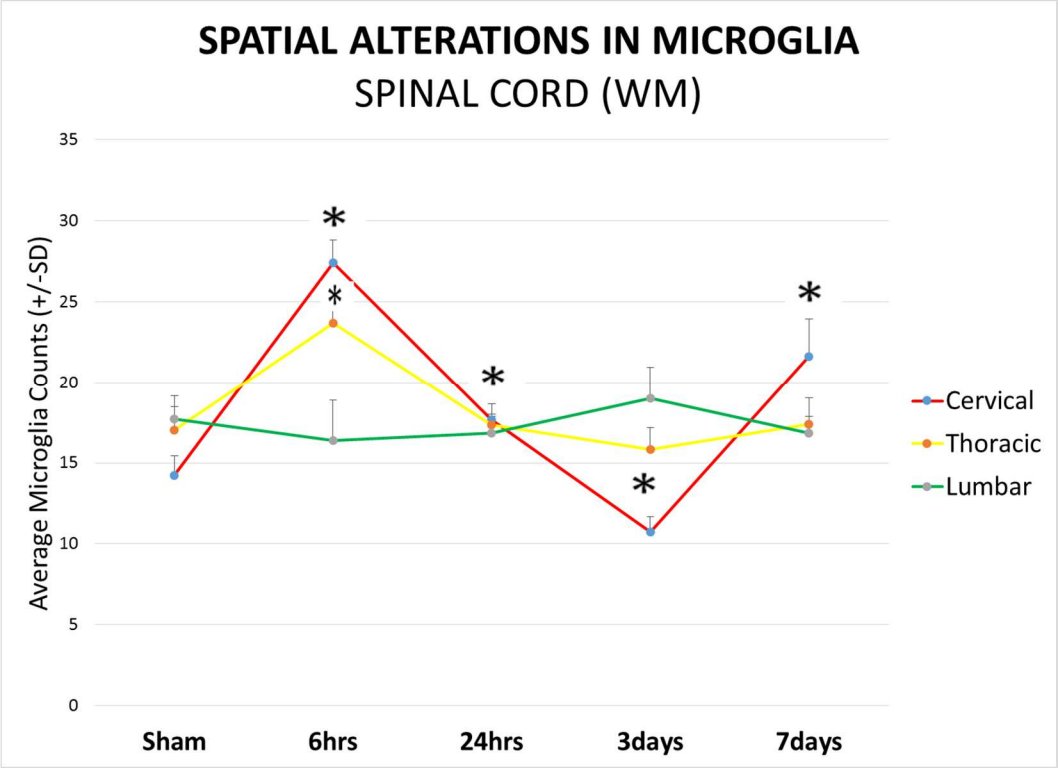

Figure 59: Plot showing the spatial alterations in the expression of microglia in the white of cervical, thoracic and lumbar spinal cord in the sham and blast group (6hrs, 24hrs, 3days and 7days). * indicates significant difference ($p<0.05$) in expression of microglia in blast group compared to sham.

From the plot, it was observed that white matter of the cervical region had significant elevations in the expression of micrglia at all survival periods except at 3 day survvial period. Although the level of expression for thoracic region was significant at the 6 hours following blast overpressure, the other survival periods showed no such

significance. All the survival periods for the cervical spinal cord were statistically significant for the blast group compared to blast group ($p<0.05$).

4.4 Axonal Injury

Immunohistochemistry procedures were used to stain beta-amyloid precursor protein, which is a marker used to study axonal injury(Gentleman et al., 1993). The immune-reactive (IR) zones were counted in the cervical spinal cord from the different acute and sub-acute survival periods. The presence of swollen axons, retraction bulbs and APP accumulation were considered to define the IR regions.

In sham group animals, no prominent presence of IR zones were observed in the cervical spinal cord in the figure 60 (Figure A and B) 6hours and 7days, while the blast group rats demonstrated several immune-reactive zones. Swollen and vacuolated axons could be found as early as 6 hours following blast exposure (22psi) (Figure C and D). Beta-APP reactive IR zones could be seen in several locations of the grey and white matter of the cervical spinal cord of the 24 hours blast group (Figure E and F). At 3 days post blast overpressure, intense staining of beta-APP with axons showing beaded appearance was found as shown in figure (G and H). Also, there were APP deposits seen in the cervical spinal cord at 7 days following blast overpressure as shown in figure (I and J).

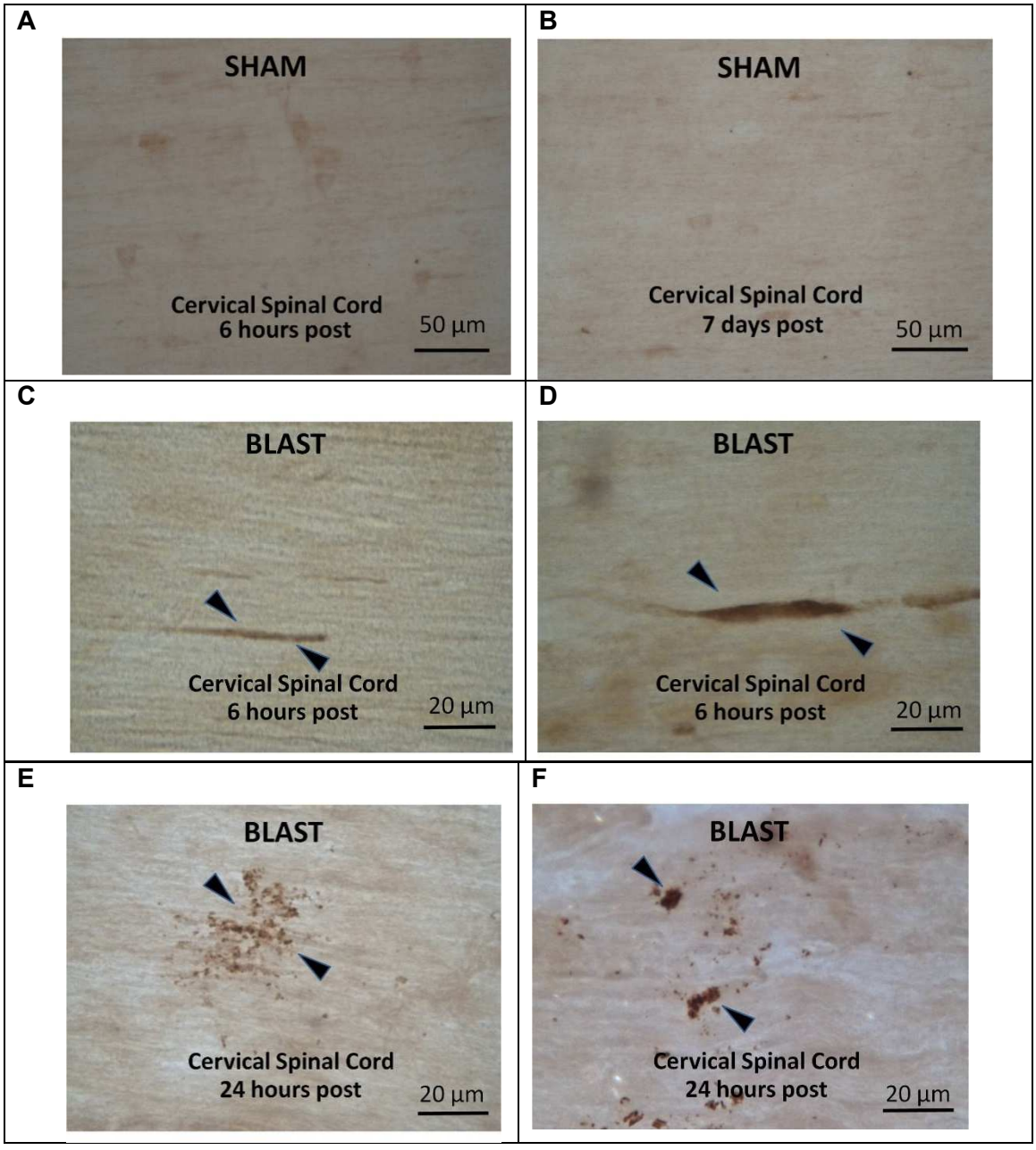
A
SHAM
Cervical Spinal Cord
6 hours post
50 µm
B
SHAM
Cervical Spinal Cord
7 days post
50 µm
C
BLAST
Cervical Spinal Cord
6 hours post
20 µm
D
BLAST
Cervical Spinal Cord
6 hours post
20 µm
E
BLAST
Cervical Spinal Cord
24 hours post
20 µm
F
BLAST
Cervical Spinal Cord
24 hours post
20 µm

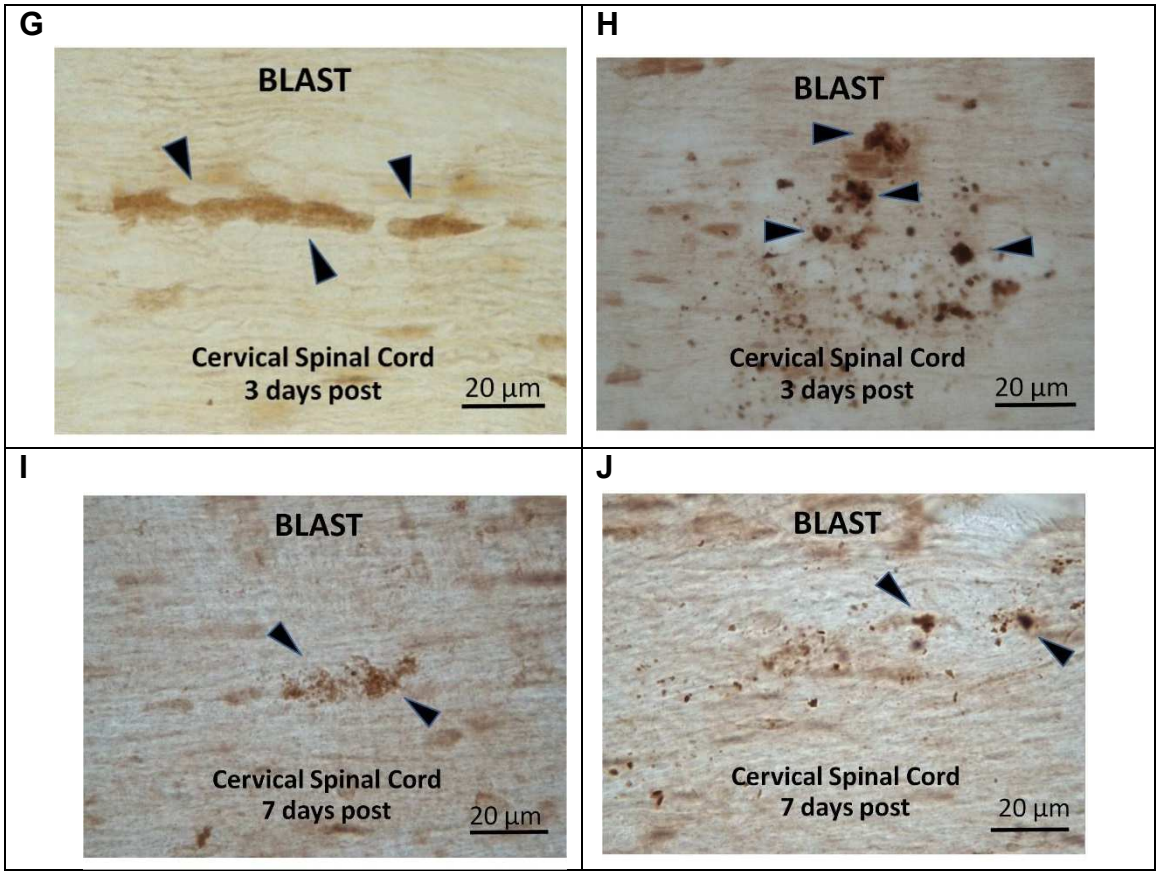

Figure 60: Representative images of immune-reactive (IR) zones in the cervical cord from the respective sham (A and B), 6 hours (C and D), 24 hours (E and F), 3 days (G and H) and 7 days (I and J) groups.

Furthermore, quantitative analysis was done to study the presence of beta-amyloid precursor protein in the cervical spinal cord at the different acute and sub-acute survival periods as shown in figure 61.

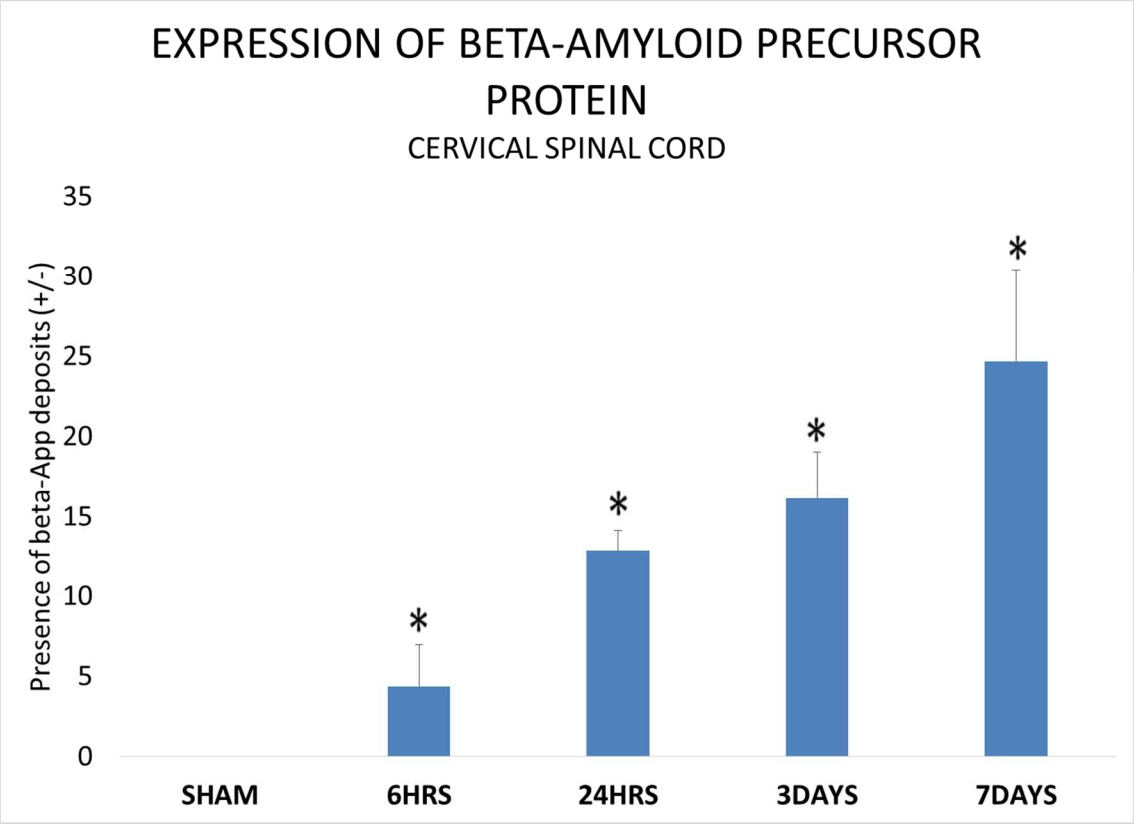

Figure 61: Plot showing the presence of beta-amyloid precursor protein in the sham and blast group at various acute and sub-acute survival periods.

The results indicated greater occurrence of beta-amyloid precursor protein in the blast group in comparison to the sham group ($p<0.05$). Also, there was early presence of beta-APP at 6 hours which gradually increased at other periods. The highest occurrence was observed at 7 days following blast exposure.

CHAPTER 5 - DISCUSSION

Prolonged Surface Rise time

Many studies report that loss of consciousness (LOC) is an indirect indicator for blast injury (Adams, 1986; Li et al., 2011). For that purpose, many researchers monitored SR time as an indirect indicator to study LOC in animal experiments of TBI (Cernak et al., 2011). In this study, it was observed that the blast group animals demonstrated

significantly longer SR time in sham animals compared to the sham group. While both groups were subjected to identical procedures for the induction of anesthesia, the prolonged SR time in blast animals supports their loss of consciousness as a potential consequence of blast injury. In fact, loss of consciousness up to 30 minutes in humans is considered as a sign of mild traumatic brain injury as per the Defense and Veterans Brain Injury Center (DVBIC, 2015).

Alterations in expression of astrocytes:

In the current study, we observed similar morphological changes in the expression of astrocytes in all levels of the spinal cord following blast. The astrocytes demonstrated broader cell body with thicker extended processes suggesting potential morphological changes post blast exposure. Upon injury, the processes get thicker and surround the damaged region. However, in our study there was no blunt injury to the spinal cord, but it can be inferred that the morphological alteration of astrocytes could be a sign of injury to maintain the homeostasis of the nervous system. Previous studies have shown alterations in the morphology and expression of astrocytes following blast induced traumatic brain injury and spinal cord injury as mentioned in the section 1.3.

The vital function of astrocytes is to maintain the homeostasis of the CNS, therefore it is reasonable to suspect that changes observed in the appearance would be response to injury (Ridet et al., 1997; Vernadakis, 1996). Many studies have shown increased levels of GFAP, a sign of reactive astrocytes in the brain in response to the blast overpressure using different animal models (Bauman et al., 2009; Kamnaksh et al., 2011; Miller et al., 2015; Vandevord et al., 2012). Farooque et. al. showed increased expression of reactive astrocytes in the rat spinal cord compression model (Farooque et al., 1995). In a study by Kallakuri and colleagues on rats subjected to similar experimental methods,

showed increased expression of GFAP in the brain following exposure to 22psi overpressure (unpublished data). Our findings from the blast exposed spinal cord supports the observed changes are similar to those in blast exposed brain and spinal cord injury models.

Furthermore, we studied astrocytic alterations in the grey matter and white matter of the spinal cord at the various survival periods. As explained in section 3.1, the grey matter is surrounded by the white matter in the spinal cord unlike the brain. In traumatic brain injury models, white matter region is known to be the most damaged site of injury (Osier et al., 2015). However, the expression of astrocytes in our study were significantly higher in the grey matter of the spinal cord in comparison to the white matter following blast overpressure. This phenomenon needs to be further investigated to better understand the mechanism of these underlying cellular changes.

Moreover, our findings show significant temporal proliferation of astrocytes at all three levels of the spinal cord. The peak proliferation of astrocytes was observed at 3 days following blast overpressure in both grey matter and white matter at all levels. Although, the expression of astrocytes dropped at 7days post exposure, it was still significantly higher in comparison to the corresponding sham group. These results suggest that the astrocytes remained activated in all the three levels of the spinal cord 7 days following blast overpressure.

In a sciatic chronic constriction injury (CCI) study, Garrison et. al. showed the increased expression of astrocytes using GFAP staining in the lumbar spinal cord was related to pain. They used pharmacological treatment to inhibit exaggerated pain, which in turn restrained the activation of astrocytes (Garrison et al., 1991). Various investigators have shown that over activation of astrocytes leads to the release of inflammatory

mediators such as Interleukin-1 (IL-1), Tumor Necrosis Factor-alpha (TNF-α), Substance P (SP), which in turn increase neurotoxicity (Liberto et al., 2004; Rao et al., 2012). These pro-inflammatory mediators are responsible to recruit the immune cells to the site of injury or infection which in turn may result in increased inflammation and cause exaggerated pain in the body.

Thus, it was found that blast induced spatial and temporal alterations at all the levels of the spinal cord. Therefore, it is reasonable to suspect that these alterations may be the result of blast overpressure.

Alterations in expression of microglia:

We were able to show proliferation of microglia using IBA-1 antibody, which is an ideal marker used to stain both resting and activated microglia (Ahmed et al., 2007). Differential expression of microglia was witnessed in the sham group and blast group. While the sham group demonstrated the typical ramified shape of the microglia which indicates that they are in 'resting state', the blast group showed an activated phenotype of microglia i.e. the amoeboid shape. Ravish et. al. defined the distinct phenotypes and activation levels as shown in table 2 below:

		Ways to differentiate stages:	
Grade	**Characteristics**	**Morphology and Markers**	**Cytokines**
Stage 0	Normal-Ramified	Morphology: long ramified processes	
Stage 1	Alert: thicker processes	Less ramified, thicker processes; ⇑OX-42	TGF-β1
Stage 2	Homing, Proliferation	Bushy; Proliferation markers	IL-10
Stage 3a	Clustered phagocytes	Amoeboid; possible ⇑MHCI, ED-1 (CD68)	IL-6, TNF-α
Stage 3b	Bystander activation; Lymphocyte binding	⇑MHCI, Lower ICAM than 3a	IFN-γ

Table 4: Different phenotypes and levels of microglia activation
(Raivich et al., 1999)

Further investigation is needed to better understand the morphology and type of activated microglia i.e. M1 and M2. As mentioned earlier, M1 microglia is responsible for the release inflammatory mediators such as IL-1β, TNFα, which are responsible of fighting injury or infection, while M2 microglia play a vital role in repair, healing and remodeling of neurons by releasing the pro-inflammatory mediators such as IL-10, transforming growth factor beta (TGFβ) (Tanaka et al., 2009). It is difficult to study the phenotypical changes in the microglia and the level of inflammation using a single marker, therefore it is suggested to perform dual labelling immunohistochemical procedures combining cytokines such as IL-1β, TNFα, IL-10 and TGF1β with microglial marker further distinguish the type of microglia. The M1 type microglia is a fully activated state where they appear amoeboid in shape, while the M2 is partially activated with ramified appearance. The presence of M2 microglia is highly recommended since it is beneficial to the repair, remodeling and growth. Also, the cytokines released by M2 microglia are known to block the further microglial activation and neuronal damage (Sharma et al., 2011; Spittau et al., 2013).

The level of expression of microglia demonstrated elevated profiles in the blast group compared to sham group of the spinal cord. On further assessment of the expression of microglia in the grey matter and white matter in the different levels of spinal cord, the proliferation of microglia was only significant in the cervical region. Furthermore, the temporal alterations in the expression of spinal cord at all three levels of the spinal cord was studied. Unlike astrocytes, it was observed that only the cervical spinal cord showed significant temporal alterations in the expression of microglia at all acute and sub-acute survival periods. Although, there were phenotypical changes observed in all the levels of the spinal cord, there was no significant proliferation observed in the thoracic and

lumbar spinal cord. We propose that the shorter distance and greater intensity of the blast wave at the cervical spinal cord level may contribute to the increased levels of microglia. At 6 hours following blast overpressure, although the white and grey matter of the thoracic spinal cord showed significant elevated profiles, there was no significant difference observed at other time points. Overall, the thoracic spinal cord of the blast group showed higher expression of microglia, however no significant difference was detected in both grey matter and white matter. Similarly, there was no significant difference observed in both regions of the lumbar spinal cord compared to their corresponding to their corresponding sham.

Another notable event observed was at 3 days following blast overpressure, there was decreased expression of microglia observed in the white matter of all three levels of blast group in comparison to the sham group. It was significantly lower for the cervical spinal cord. It would be interesting to further identify the reason for the drop in the expression. This expression increased at the 7 days post exposure, and was close to the expression in the 6 hour survival period. An interesting event witnessed in the current findings is the rise in the expression of microglia at 7 days following blast overpressure at the cervical spinal cord. This indicates that microglia continued to remain in activated state even after 7 days post blast exposure. Whether this increased proliferation remains elevated past 7 days remains to be investigated.

As mentioned earlier, activated microglia are responsible for the release of pro-inflammatory and inflammatory mediators. It is apparent that microglia gets activated at a slight change in the environment of the CNS, which may be responsible to harmful effects on the CNS (Kreutzberg, 1996). Our results show the microglia in the spinal cord get activated following blast overpressure, therefore further research is required to better

understand the activated form of microglia. This future research will detect if over activation of microglia is detrimental to the spinal cord.

To summarize, blast induced temporal alterations in the expression of microglia were observed only in the cervical spinal cord with phenotypical alterations being observed at all the levels of the spinal cord.

Axonal Injury

Many investigators reported the presence of axonal injury (AI) in bTBI in the form of increased expression of APP deposits (De Gasperi et al., 2012; Du et al., 2013; Kuehn et al., 2011). All the current research associated with TAI following blast overpressure were focused towards brain, while no such injury changes have been studied in the spinal cord. TAI is characterized by neurofilament compaction (NFC) and impaired axonal transport (IAT). In this study we attempted to assess only IAT in the spinal cord using Beta-Amyloid Precursor Protein (β-APP), a marker used to assess the extent of TAI.

Cervical spinal cord sections were stained using β-APP antibody to investigate the extent of axonal injury. The occurrence of β-APP immune-reactive (IR) zones in the cervical spinal cord in the form of swollen axons with beaded appearance were witnessed as early as 6 hours following blast overpressure (22psi). On further assessment, the level of expression increased at other survival periods with most frequent appearances of retraction bulbs and β-APP deposits at 7days post blast exposure. Koliatsos et. al. have shown evidence of axonal injury in the form of beta amyloid precursor protein swellings and retraction balls in mice corpus callosum at 7 days following blast overpressure (Koliatsos et al., 2011). Our findings support and augment this evidence by showing the highest presence of swollen axons with retraction balls at the 7 days post exposure, suggesting that there was impairment in the axonal transport even in cervical spinal cord

axon. In a rodent model, Czeiter et. al. identified traumatic axonal injury invoked by blunt traumatic brain injury in the white matter tracts of the cervical spinal cord (Czeiter et al., 2008). These results support our results from the spinal cord and suggest that blast induced axonal injury to the cervical spinal cord.

Garman et. al. reported axonal injury in the rat brain following blast overpressure, and it was visible post 2 weeks of exposure with the help of silver staining (Garman et al., 2011). Another study using swine model reported axonal injury as a significant injury witnessed in the brain 2 weeks following blast overpressure (de Lanerolle et al., 2011). These results were shown using immunohistochemistry procedures with β-APP and silver staining. Based on their results, we suggest that further investigation is needed to better assess the extent of axonal injury using immunohistochemistry techniques like neurofilament light and silver staining.

The role of astrocytes in the maintenance of homeostasis in the nervous system is well documented (Buffo et al., 2010). Reactive astrocytes play a vital role in various neurodegenerative diseases such as stroke epilepsy, Alzheimer's disease (AD), Amyloid Lateral Sclerosis (ALS) and Multiple sclerosis (MS) (Pekny et al., 2014). It can be inferred that the presence of activated astrocytes indicated by the proliferation at all the levels of the spinal cord could cause detrimental effects in the spinal cord. We postulate that the differential expression of astrocytes compared to microglia may be related to the severity of injury in the spinal cord. As the shock wave travels rosto-cephalically through the spinal cord, the severe injury may be more pronounced at the cervical spinal cord, as indicated by the increased expression of both astrocytes and microglia. These increased expression of astrocytes and microglia in the cervical spinal cord may also be related to the axonal debris witnessed in the form of βAPP immunoreactive

zones. On the other hand, it is logical that the intensity of the blast wave pressure reduced as it travels through the thoracic and lumbar spinal cord. Albeit, this reduced pressure may be sufficient to trigger a change in local environment of the thoracic and lumbar regions resulting in increased astrogliosis but not enough to activate the microglia to perform phagocytosis. Whether this decreased microglia activation is also supported by decreased βAPP IR in thoracic and lumbar spinal cord regions remains to be investigated.

Many studies have shown strong correlation between the activation of glial cells and pain (Ledeboer et al., 2003; Milligan et al., 2003; Raghavendra et al., 2003). However, it is not proven that activation of glial cells is sufficient for the development of pain. Weissler et. al. suggested that pain is a physiological condition, and is caused due to the cascade of events that lead to the activation of glial cells (Wieseler-Frank et al., 2005). Many studies have shown that the inhibiting the activation of glial cells may block the resulting cascade of events which increase inflammation and cause pain in the body.

Taken together, our results suggest that activated astrocytes and microglia may be responsible for the maintenance of neuropathic pain states. However, this mechanism of glial expression needs further validation. In conclusion, the proposed mechanism for the observed changes in the spinal cord may be due to the propagation of increased inter-cranial pressure (ICP) following blast overpressure. Our study was able to show alterations in the glial cells; astrocytes and microglia. Also, we could find axonal injury in the form of Beta-Amyloid Precursor Protein (Beta-APP) in the cervical spinal cord.

CHAPTER 6: CONCLUSION & FUTURE WORK

The purpose of the current study was to investigate the effects of blast overpressure on rat spinal cord. This thesis offers to be the first step to lay the foundation of the future research on the blast induced spinal cord injury (BISCI). Several previous studies have shown blast overpressure induced changes in the brain. We hypothesized that blast overpressure induces changes not only in the brain but induces changes in the spinal cord also as the blast wave propagates from brain to the most caudal regions of the central nervous system i.e, the spinal cord. Based on this hypothesis, we attempted to study the underlying cellular changes in the form of alterations in the expression of glial cells and axonal injury in the spinal cord following blast overpressure BOP).

Conclusion:

1. Blast overpressure induced morphological, spatial and temporal alterations in the expression of astrocytes at all the levels of the spinal cord.
2. Astrocytes in the blast group appeared to be thicker with longer processes compared to the sham group.
3. Blast exposure induced significant elevation in the number of astrocytes at cervical, thoracic and lumbar regions compared to corresponding sham spinal cord.
4. That the significant elevation in the expression of astrocytes extends to 7 days after blast exposure compared to sham.
5. Lumbar spinal cord has the highest proliferation of astrocytes compared to other spinal cord regions.

6. Blast overpressure exposure induced potential phenotypical alterations (more amoeboid like) in the microglia in the spinal cord (cervical, thoracic and lumbar) of blast group compared to sham group. .
7. Blast exposure induced significant elevation in the number of microglia in the cervical spinal cord extending to 7 days after blast.
8. No such changes were observed in the thoracic and lumbar region of the blast group compared to sham.
9. Our results also showed elevated axonal injury in the cervical spinal cord as evidenced by a significant number of β-APP.immuno-reactive zones (IR zones) comprising APP deposits, swollen axons with retraction balls..

In conclusion, the results of this study support our proposed hypothesis of blast overpressure induced cellular changes in the spinal cord. Furthermore, our findings will encourage the development of future studies associated with similar conditions in humans. It is reasoned that over-activation of the glial cells may release inflammatory mediators such as IL-1, TNF-alpha and SP, that may contribute to altered neuronal function. Lastly, we suggest that attempts should be made to reduce the activation of glial cells in the spinal cord which may reduce the neurotoxicity and enhance axonal regeneration.

Future Work

Our studies have shown evidence of blast overpressure induced spatial and temporal alterations in the glial cells of the rat spinal cord. Also, it has confirmed the presence of beta-APP deposits in the cervical spinal cord, which suggests that exposure to blast results in axonal injury. This research provides the foundation to further investigate the mechanism of glial cell reactivity in the spinal cord following blast overpressure. Based

on our findings, we suggest the following future work to better understand the effects of blast overpressure.

- To investigate the presence of inflammatory mediators such as IL-1beta, TNF-alpha and SP in the spinal cord following blast overpressure.
- To perform dual labelled immunohistochemical procedures with IBA-1 to detect the type of microglia expressed (M1/M2).
- To study to effects of higher blast overpressure (>22psi) and repetitive blast overpressure on rat spinal cord.
- To detect putative behavioral changes.

We suggest the future research may provide more knowledge regarding the effects of blast induced spinal cord injury.

APPENDIX A: Glossary of Acronyms and Abbreviations

ABC – Avidin Biotin Complex

ANOVA - Analysis of variance

Beta-APP – Beta-Amyloid Precursor Protein

BBB - Blood-brain-barrier

BINT – Blast induced Neurotrauma

BISCI – Blast induced spinal cord injury

CNS - Central nervous system

DAI - Diffuse axonal injury

DNA – Deoxyribonucleic acid

GFAP – Glial Fibrillary Acidic Protein

HRS- Hours

IBA-1 – Ionized Calcium Binding Adaptor Molecule 1

IL-1 – Interleukin -1

LOC - Loss of consciousness

Mins – Minutes

NGS – Normal Goat Serum

Rcf - relative centrifugal force

SCI- Spinal Cord Injury

SP – Substance P

SR - Surface righting

STDEV - Standard deviation

TBI – Traumatic Brain Injury

TNF – Tumor Necrosis Factor

APPENDIX B: Surface Rise time for all the animals

Group	Sr. No	Animal Tag	SR Duration (in seconds)	Average
Sham (n=16)	1	Sham#1	78.6	124.875
	2	Sham#2	78	
	3	Sham#3	81.6	
	4	Sham#4	78	
	5	Sham#5	138	
	6	Sham#6	81	
	7	Sham#7	81	
	8	Sham#8	209.4	
	9	Sham#9	258	
	10	Sham#10	72	
	11	Sham#11	24	
	12	Sham#12	207	
	13	Sham#13	258	
	14	Sham#14	87.6	
	15	Sham#15	142.8	
	16	Sham#16	123	
Blast (n=24)	1	6hr#1	250.2	187.80
	2	6hr#2	182.4	
	3	6hr#3	154.8	
	4	6hr#4	267	
	5	6hr#5	84	
	6	6hr#6	256.2	
	7	24Hr#1	324	
	8	24Hr#2	202.8	
	9	24Hr#3	151.8	
	10	24Hr#4	130.8	
	11	24Hr#5	246.6	
	12	24Hr#6	68.4	
	13	3Day#1	140.4	
	14	3Day#2	144	
	15	3Day#3	140.4	
	16	3Day#4	213	
	17	3Day#5	183.6	
	18	3Day#6	70.2	
	19	7Day#1	138	
	20	7Day#2	132	
	21	7Day#3	380.4	
	22	7Day#4	253.2	
	23	7Day#5	198	
	24	7Day#6	195	

REFERENCES

1. Adams, J., 1986. Methods in Behavioral Teratology, in: Riley, E., Vorhees, C. (Eds.), Handbook of Behavioral Teratology. Springer US, pp. 67-97.
2. Aguzzi, A., Barres, B.A., Bennett, M.L., 2013. Microglia: scapegoat, saboteur, or something else? Science 339, 156-161.
3. Ahmed, Z., Shaw, G., Sharma, V.P., Yang, C., McGowan, E., Dickson, D.W., 2007. Actin-binding proteins coronin-1a and IBA-1 are effective microglial markers for immunohistochemistry. J Histochem Cytochem 55, 687-700.
4. Albert-Weissenberger, C., Varrallyay, C., Raslan, F., Kleinschnitz, C., Siren, A.L., 2012. An experimental protocol for mimicking pathomechanisms of traumatic brain injury in mice. Exp Transl Stroke Med 4, 1.
5. Alkire, M.T., McReynolds, J.R., Hahn, E.L., Trivedi, A.N., 2007. Thalamic microinjection of nicotine reverses sevoflurane-induced loss of righting reflex in the rat. Anesthesiology 107, 264-272.
6. Armstead, W.M., 2001. Vasopressin-induced protein kinase C-dependent superoxide generation contributes to atp-sensitive potassium channel but not calcium-sensitive potassium channel function impairment after brain injury. Stroke 32, 1408-1414.
7. Bauman, R.A., Ling, G., Tong, L., Januszkiewicz, A., Agoston, D., Delanerolle, N., Kim, Y., Ritzel, D., Bell, R., Ecklund, J., Armonda, R., Bandak, F., Parks, S., 2009. An introductory characterization of a combat-casualty-care relevant swine model of closed head injury resulting from exposure to explosive blast. Journal of neurotrauma 26, 841-860.

8. Bhattacharjee, Y., 2008. Neuroscience. Shell shock revisited: solving the puzzle of blast trauma. Science 319, 406-408.

9. Bignall, K.E., 1974. Ontogeny of levels of neural organization: the righting reflex as a model. Experimental neurology 42, 566-573.

10. Bolander, R., 2012. A MULTI-SPECIES ANALYSIS OF BIOMECHANICAL RESPONSES OF THE HEAD TO A SHOCK WAVE. Wayne State University, Detroit, MI.

11. Bolander, R., Mathie, B., Bir, C., Ritzel, D., VandeVord, P., 2011. Skull flexure as a contributing factor in the mechanism of injury in the rat when exposed to a shock wave. Annals of biomedical engineering 39, 2550-2559.

12. Buffo, A., Rolando, C., Ceruti, S., 2010. Astrocytes in the damaged brain: molecular and cellular insights into their reactive response and healing potential. Biochemical pharmacology 79, 77-89.

13. Bush, T.G., Puvanachandra, N., Horner, C.H., Polito, A., Ostenfeld, T., Svendsen, C.N., Mucke, L., Johnson, M.H., Sofroniew, M.V., 1999. Leukocyte infiltration, neuronal degeneration, and neurite outgrowth after ablation of scar-forming, reactive astrocytes in adult transgenic mice. Neuron 23, 297-308.

14. Carbonell, W.S., Maris, D.O., McCall, T., Grady, M.S., 1998. Adaptation of the fluid percussion injury model to the mouse. Journal of neurotrauma 15, 217-229.

15. Celic, T., Spanjol, J., Bobinac, M., Tovmasyan, A., Vukelic, I., Reboucas, J.S., Batinic-Haberle, I., Bobinac, D., 2014. Mn porphyrin-based SOD mimic, MnTnHex-2-PyP(5+), and non-SOD mimic, MnTBAP(3-), suppressed rat spinal cord ischemia/reperfusion injury via NF-kappaB pathways. Free Radic Res 48, 1426-1442.

16. Cernak, I., Merkle, A.C., Koliatsos, V.E., Bilik, J.M., Luong, Q.T., Mahota, T.M., Xu, L., Slack, N., Windle, D., Ahmed, F.A., 2011. The pathobiology of blast injuries and blast-induced neurotrauma as identified using a new experimental model of injury in mice. Neurobiology of disease 41, 538-551.

17. Cernak, I., Noble-Haeusslein, L.J., 2010. Traumatic brain injury: an overview of pathobiology with emphasis on military populations. Journal of cerebral blood flow and metabolism : official journal of the International Society of Cerebral Blood Flow and Metabolism 30, 255-266.

18. Cernak, I., Savic, J., Ignjatovic, D., Jevtic, M., 1999. Blast injury from explosive munitions. The Journal of trauma 47, 96-103; discussion 103-104.

19. Cernak, I., Wang, Z., Jiang, J., Bian, X., Savic, J., 2001. Ultrastructural and functional characteristics of blast injury-induced neurotrauma. The Journal of trauma 50, 695-706.

20. Chavko, M., Koller, W.A., Prusaczyk, W.K., McCarron, R.M., 2007. Measurement of blast wave by a miniature fiber optic pressure transducer in the rat brain. Journal of neuroscience methods 159, 277-281.

21. Chen, Y., Constantini, S., Trembovler, V., Weinstock, M., Shohami, E., 1996. An experimental model of closed head injury in mice: pathophysiology, histopathology, and cognitive deficits. Journal of neurotrauma 13, 557-568.

22. Cheng, M.K., Robertson, C., Grossman, R.G., Foltz, R., Williams, V., 1984. Neurological outcome correlated with spinal evoked potentials in a spinal cord ischemia model. J Neurosurg 60, 786-795.

23. Cherry, J.D., Olschowka, J.A., O'Banion, M.K., 2014. Neuroinflammation and M2 microglia: the good, the bad, and the inflamed. J Neuroinflammation 11, 98.

24. Cho, H.J., Sajja, V.S., Vandevord, P.J., Lee, Y.W., 2013. Blast induces oxidative stress, inflammation, neuronal loss and subsequent short-term memory impairment in rats. Neuroscience 253, 9-20.

25. Cifu, D.X., Taylor, B.C., Carne, W.F., Bidelspach, D., Sayer, N.A., Scholten, J., Campbell, E.H., 2013. Traumatic brain injury, posttraumatic stress disorder, and pain diagnoses in OIF/OEF/OND Veterans. Journal of rehabilitation research and development 50, 1169-1176.

26. Clemedson, C.J., 1956. Shock wave transmission to the central nervous system. Acta Physiol Scand 37, 204-214.

27. Colton, C.A., 2009. Heterogeneity of microglial activation in the innate immune response in the brain. Journal of neuroimmune pharmacology : the official journal of the Society on NeuroImmune Pharmacology 4, 399-418.

28. Cornish, R., Blumbergs, P.C., Manavis, J., Scott, G., Jones, N.R., Reilly, P.L., 2000. Topography and severity of axonal injury in human spinal cord trauma using amyloid precursor protein as a marker of axonal injury. Spine (Phila Pa 1976) 25, 1227-1233.

29. Czeiter, E., Pal, J., Kovesdi, E., Bukovics, P., Luckl, J., Doczi, T., Buki, A., 2008. Traumatic axonal injury in the spinal cord evoked by traumatic brain injury. Journal of neurotrauma 25, 205-213.

30. David, S., Kroner, A., 2011. Repertoire of microglial and macrophage responses after spinal cord injury. Nature reviews. Neuroscience 12, 388-399.

31. De Gasperi, R., Gama Sosa, M.A., Kim, S.H., Steele, J.W., Shaughness, M.C., Maudlin-Jeronimo, E., Hall, A.A., Dekosky, S.T., McCarron, R.M., Nambiar, M.P., Gandy, S., Ahlers,

S.T., Elder, G.A., 2012. Acute blast injury reduces brain abeta in two rodent species. Frontiers in neurology 3, 177.

32. de Lanerolle, N.C., Bandak, F., Kang, D., Li, A.Y., Du, F., Swauger, P., Parks, S., Ling, G., Kim, J.H., 2011. Characteristics of an explosive blast-induced brain injury in an experimental model. Journal of neuropathology and experimental neurology 70, 1046-1057.

33. Donnelly, D.J., Popovich, P.G., 2008. Inflammation and its role in neuroprotection, axonal regeneration and functional recovery after spinal cord injury. Experimental neurology 209, 378-388.

34. Drake, R.L., Vogl, W., Mitchell, A.W.M., Gray, H., 2015. Gray's Anatomy for students.

35. Du, X., Ewert, D.L., Cheng, W., West, M.B., Lu, J., Li, W., Floyd, R.A., Kopke, R.D., 2013. Effects of antioxidant treatment on blast-induced brain injury. PLoS One 8, e80138.

36. DVBIC, 2015. DoD Worldwide Numbers for TBI. Defense and veterans brain injury center.

37. Eric P. Widmaier, H.R., Kevin T. Strang, 2006. Vander's Human Physiology: The Mechanisms of Body Function.

38. Farooque, M., Badonic, T., Olsson, Y., Holtz, A., 1995. Astrocytic reaction after graded spinal cord compression in rats: immunohistochemical studies on glial fibrillary acidic protein and vimentin. Journal of neurotrauma 12, 41-52.

39. Feeney, D.M., Boyeson, M.G., Linn, R.T., Murray, H.M., Dail, W.G., 1981. Responses to cortical injury: I. Methodology and local effects of contusions in the rat. Brain Res 211, 67-77.

40. Fitch, M.T., Doller, C., Combs, C.K., Landreth, G.E., Silver, J., 1999. Cellular and molecular mechanisms of glial scarring and progressive cavitation: in vivo and in vitro analysis of

inflammation-induced secondary injury after CNS trauma. The Journal of neuroscience : the official journal of the Society for Neuroscience 19, 8182-8198.

41. Garman, R.H., Jenkins, L.W., Switzer, R.C., 3rd, Bauman, R.A., Tong, L.C., Swauger, P.V., Parks, S.A., Ritzel, D.V., Dixon, C.E., Clark, R.S., Bayir, H., Kagan, V., Jackson, E.K., Kochanek, P.M., 2011. Blast exposure in rats with body shielding is characterized primarily by diffuse axonal injury. Journal of neurotrauma 28, 947-959.

42. Garrison, C.J., Dougherty, P.M., Kajander, K.C., Carlton, S.M., 1991. Staining of glial fibrillary acidic protein (GFAP) in lumbar spinal cord increases following a sciatic nerve constriction injury. Brain Res 565, 1-7.

43. Gentleman, S.M., Nash, M.J., Sweeting, C.J., Graham, D.I., Roberts, G.W., 1993. Beta-amyloid precursor protein (beta APP) as a marker for axonal injury after head injury. Neurosci Lett 160, 139-144.

44. Gerber, A.M., Olson, W.L., Harris, J.H., 1980. Effect of phenytoin on functional recovery after experimental spinal cord injury in dogs. Neurosurgery 7, 472-476.

45. Ghasemlou, N., Lopez-Vales, R., Lachance, C., Thuraisingam, T., Gaestel, M., Radzioch, D., David, S., 2010. Mitogen-activated protein kinase-activated protein kinase 2 (MK2) contributes to secondary damage after spinal cord injury. The Journal of neuroscience : the official journal of the Society for Neuroscience 30, 13750-13759.

46. Gironda, R.J., Clark, M.E., Massengale, J.P., Walker, R.L., 2006. Pain among veterans of Operations Enduring Freedom and Iraqi Freedom. Pain Med 7, 339-343.

47. Goldmann, T., Prinz, M., 2013. Role of microglia in CNS autoimmunity. Clinical & developmental immunology 2013, 208093.

48. Goldstein, L.E., Fisher, A.M., Tagge, C.A., Zhang, X.L., Velisek, L., Sullivan, J.A., Upreti, C., Kracht, J.M., Ericsson, M., Wojnarowicz, M.W., Goletiani, C.J., Maglakelidze, G.M., Casey, N., Moncaster, J.A., Minaeva, O., Moir, R.D., Nowinski, C.J., Stern, R.A., Cantu, R.C., Geiling, J., Blusztajn, J.K., Wolozin, B.L., Ikezu, T., Stein, T.D., Budson, A.E., Kowall, N.W., Chargin, D., Sharon, A., Saman, S., Hall, G.F., Moss, W.C., Cleveland, R.O., Tanzi, R.E., Stanton, P.K., McKee, A.C., 2012. Chronic traumatic encephalopathy in blast-exposed military veterans and a blast neurotrauma mouse model. Sci Transl Med 4, 134ra160.

49. Gurdjian, E.S., Lissner, H.R., Hodgson, V.R., Patrick, L.M., 1964. Mechanism of head injury. Clinical neurosurgery 12, 112-128.

50. Hanani, M., 2005. Satellite glial cells in sensory ganglia: from form to function. Brain research. Brain research reviews 48, 457-476.

51. Hartl, R., Medary, M., Ruge, M., Arfors, K.E., Ghajar, J., 1997. Blood-brain barrier breakdown occurs early after traumatic brain injury and is not related to white blood cell adherence. Acta Neurochir Suppl 70, 240-242.

52. Hashizume, K., Ueda, T., Shimizu, H., Mori, A., Yozu, R., 2005. Effect of the free radical scavenger MCI-186 on spinal cord reperfusion after transient ischemia in the rabbit. Jpn J Thorac Cardiovasc Surg 53, 426-433.

53. Hayes, R.L., Stalhammar, D., Povlishock, J.T., Allen, A.M., Galinat, B.J., Becker, D.P., Stonnington, H.H., 1987. A new model of concussive brain injury in the cat produced by extradural fluid volume loading: II. Physiological and neuropathological observations. Brain Inj 1, 93-112.

54. Hicks, R.R., Fertig, S.J., Desrocher, R.E., Koroshetz, W.J., Pancrazio, J.J., 2010. Neurological effects of blast injury. The Journal of trauma 68, 1257-1263.

55. Hooshmand, M.J., Galvan, M.D., Partida, E., Anderson, A.J., 2014. Characterization of recovery, repair, and inflammatory processes following contusion spinal cord injury in old female rats: is age a limitation? Immun Ageing 11, 15.

56. Huber, B.R., Meabon, J.S., Martin, T.J., Mourad, P.D., Bennett, R., Kraemer, B.C., Cernak, I., Petrie, E.C., Emery, M.J., Swenson, E.R., Mayer, C., Mehic, E., Peskind, E.R., Cook, D.G., 2013. Blast exposure causes early and persistent aberrant phospho- and cleaved-tau expression in a murine model of mild blast-induced traumatic brain injury. Journal of Alzheimer's disease : JAD 37, 309-323.

57. Kamnaksh, A., Kovesdi, E., Kwon, S.K., Wingo, D., Ahmed, F., Grunberg, N.E., Long, J., Agoston, D.V., 2011. Factors affecting blast traumatic brain injury. Journal of neurotrauma 28, 2145-2153.

58. Kaur, C., Singh, J., Lim, M.K., Ng, B.L., Yap, E.P.H., Ling, E.A., 1995. The response of neurons and microglia to blast injury in the rat brain. Neuropathology and Applied Neurobiology 21, 369-377.

59. Kerns, R.D., Philip, E.J., Lee, A.W., Rosenberger, P.H., 2011. Implementation of the veterans health administration national pain management strategy. Translational behavioral medicine 1, 635-643.

60. Koliatsos, V.E., Cernak, I., Xu, L., Song, Y., Savonenko, A., Crain, B.J., Eberhart, C.G., Frangakis, C.E., Melnikova, T., Kim, H., Lee, D., 2011. A mouse model of blast injury to brain: initial pathological, neuropathological, and behavioral characterization. Journal of neuropathology and experimental neurology 70, 399-416.

61. Kreutzberg, G.W., 1996. Microglia: a sensor for pathological events in the CNS. Trends in neurosciences 19, 312-318.

62. Kroenke, K., Koslowe, P., Roy, M., 1998. Symptoms in 18,495 Persian Gulf War veterans. Latency of onset and lack of association with self-reported exposures. Journal of occupational and environmental medicine / American College of Occupational and Environmental Medicine 40, 520-528.

63. Kuehn, R., Simard, P.F., Driscoll, I., Keledjian, K., Ivanova, S., Tosun, C., Williams, A., Bochicchio, G., Gerzanich, V., Simard, J.M., 2011. Rodent model of direct cranial blast injury. Journal of neurotrauma 28, 2155-2169.

64. Kyrkanides, S., Olschowka, J.A., Williams, J.P., Hansen, J.T., O'Banion, M.K., 1999. TNF alpha and IL-1beta mediate intercellular adhesion molecule-1 induction via microglia-astrocyte interaction in CNS radiation injury. Journal of neuroimmunology 95, 95-106.

65. Larry R. Squire, D.B., Floyd Bloom 2008. Fundamental Neuroscience.

66. Ledeboer, A., Wierinckx, A., Bol, J.G., Floris, S., Renardel de Lavalette, C., De Vries, H.E., van den Berg, T.K., Dijkstra, C.D., Tilders, F.J., van dam, A.M., 2003. Regional and temporal expression patterns of interleukin-10, interleukin-10 receptor and adhesion molecules in the rat spinal cord during chronic relapsing EAE. Journal of neuroimmunology 136, 94-103.

67. Lee, J.H., Jones, C.F., Okon, E.B., Anderson, L., Tigchelaar, S., Kooner, P., Godbey, T., Chua, B., Gray, G., Hildebrandt, R., Cripton, P., Tetzlaff, W., Kwon, B.K., 2013. A novel porcine model of traumatic thoracic spinal cord injury. Journal of neurotrauma 30, 142-159.

68. Lee, Y.L., Shih, K., Bao, P., Ghirnikar, R.S., Eng, L.F., 2000. Cytokine chemokine expression in contused rat spinal cord. Neurochemistry international 36, 417-425.

69. Leonardi, A.D., Bir, C.A., Ritzel, D.V., VandeVord, P.J., 2011. Intracranial pressure increases during exposure to a shock wave. Journal of neurotrauma 28, 85-94.

70. Lew, H.L., Otis, J.D., Tun, C., Kerns, R.D., Clark, M.E., Cifu, D.X., 2009. Prevalence of chronic pain, posttraumatic stress disorder, and persistent postconcussive symptoms in OIF/OEF veterans: polytrauma clinical triad. J Rehabil Res Dev 46, 697-702.

71. Li, Y., Zhang, L., Kallakuri, S., Zhou, R., Cavanaugh, J.M., 2011. Injury predictors for traumatic axonal injury in a rodent head impact acceleration model. Stapp Car Crash J 55, 25-47.

72. Li, Z., Hogan, E.L., Banik, N.L., 1995. Role of calpain in spinal cord injury: increased mcalpain immunoreactivity in spinal cord after compression injury in the rat. Neurochemistry international 27, 425-432.

73. Liberto, C.M., Albrecht, P.J., Herx, L.M., Yong, V.W., Levison, S.W., 2004. Pro-regenerative properties of cytokine-activated astrocytes. Journal of neurochemistry 89, 1092-1100.

74. Ling, G., Bandak, F., Armonda, R., Grant, G., Ecklund, J., 2009. Explosive blast neurotrauma. Journal of neurotrauma 26, 815-825.

75. Liu, Y., Zhou, J., 2013. Oligodendrocytes in neurodegenerative diseases. Front. Biol. 8, 127-133.

76. Liuzzi, F.J., Lasek, R.J., 1987. Astrocytes block axonal regeneration in mammals by activating the physiological stop pathway. Science 237, 642-645.

77. Lu, J., Ng, K.C., Ling, G., Wu, J., Poon, D.J., Kan, E.M., Tan, M.H., Wu, Y.J., Li, P., Moochhala, S., Yap, E., Lee, L.K., Teo, M., Yeh, I.B., Sergio, D.M., Chua, F., Kumar, S.D., Ling, E.A., 2012. Effect of blast exposure on the brain structure and cognition in Macaca fascicularis. Journal of neurotrauma 29, 1434-1454.

78. Luo, J., Li, N., Robinson, J.P., Shi, R., 2002. The increase of reactive oxygen species and their inhibition in an isolated guinea pig spinal cord compression model. Spinal Cord 40, 656-665.

79. Marmarou, A., Foda, M.A., van den Brink, W., Campbell, J., Kita, H., Demetriadou, K., 1994. A new model of diffuse brain injury in rats. Part I: Pathophysiology and biomechanics. J Neurosurg 80, 291-300.

80. Martin, E.M., Lu, W.C., Helmick, K., French, L., Warden, D.L., 2008. Traumatic brain injuries sustained in the Afghanistan and Iraq wars. Journal of trauma nursing : the official journal of the Society of Trauma Nurses 15, 94-99; quiz 100-101.

81. Mayorga, M.A., 1997. The pathology of primary blast overpressure injury. Toxicology 121, 17-28.

82. McIntosh, T.K., Noble, L., Andrews, B., Faden, A.I., 1987. Traumatic brain injury in the rat: characterization of a midline fluid-percussion model. Cent Nerv Syst Trauma 4, 119-134.

83. McIntosh, T.K., Vink, R., Noble, L., Yamakami, I., Fernyak, S., Soares, H., Faden, A.L., 1989. Traumatic brain injury in the rat: characterization of a lateral fluid-percussion model. Neuroscience 28, 233-244.

84. Mellor, S.G., 1988. The pathogenesis of blast injury and its management. British journal of hospital medicine 39, 536-539.

85. Miller, A.P., Shah, A.S., Aperi, B.V., Budde, M.D., Pintar, F.A., Tarima, S., Kurpad, S.N., Stemper, B.D., Glavaski-Joksimovic, A., 2015. Effects of blast overpressure on neurons and glial cells in rat organotypic hippocampal slice cultures. Frontiers in neurology 6, 20.

86. Milligan, E.D., Twining, C., Chacur, M., Biedenkapp, J., O'Connor, K., Poole, S., Tracey, K., Martin, D., Maier, S.F., Watkins, L.R., 2003. Spinal glia and proinflammatory cytokines

mediate mirror-image neuropathic pain in rats. The Journal of neuroscience : the official journal of the Society for Neuroscience 23, 1026-1040.

87. Morioka, T., Kalehua, A.N., Streit, W.J., 1991. The microglial reaction in the rat dorsal hippocampus following transient forebrain ischemia. Journal of cerebral blood flow and metabolism : official journal of the International Society of Cerebral Blood Flow and Metabolism 11, 966-973.

88. Nimmerjahn, A., Kirchhoff, F., Helmchen, F., 2005. Resting microglial cells are highly dynamic surveillants of brain parenchyma in vivo. Science 308, 1314-1318.

89. Noble, L.J., Wrathall, J.R., 1989. Correlative analyses of lesion development and functional status after graded spinal cord contusive injuries in the rat. Experimental neurology 103, 34-40.

90. Osier, N.D., Carlson, S.W., DeSana, A., Dixon, C.E., 2015. Chronic Histopathological and Behavioral Outcomes of Experimental Traumatic Brain Injury in Adult Male Animals. Journal of neurotrauma.

91. Parekkadan, B., Tilles, A.W., Yarmush, M.L., 2008. Bone marrow-derived mesenchymal stem cells ameliorate autoimmune enteropathy independently of regulatory T cells. Stem cells 26, 1913-1919.

92. Pegg, C.C., He, C., Stroink, A.R., Kattner, K.A., Wang, C.X., 2010. Technique for collection of cerebrospinal fluid from the cisterna magna in rat. Journal of neuroscience methods 187, 8-12.

93. Pekny, M., Wilhelmsson, U., Pekna, M., 2014. The dual role of astrocyte activation and reactive gliosis. Neurosci Lett 565, 30-38.

94. Persu, C., Caun, V., Dragomiriteanu, I., Geavlete, P., 2009. Urological management of the patient with traumatic spinal cord injury. J Med Life 2, 296-302.

95. Pfenninger, E.G., Reith, A., Breitig, D., Grunert, A., Ahnefeld, F.W., 1989. Early changes of intracranial pressure, perfusion pressure, and blood flow after acute head injury. Part 1: An experimental study of the underlying pathophysiology. J Neurosurg 70, 774-779.

96. Pode, D., Landau, E.L., Lijovetzky, G., Shapiro, A., 1989. Isolated pulmonary blast injury in rats--a new model using the extracorporeal shock-wave lithotriptor. Military medicine 154, 288-293.

97. Prevention., C.f.D.C.a., 2006. Emergency preparedness and response. Explosions and blast injuries: a primer for clinicians, in: Atlanta, G.C.D.C.P. (Ed.), http://emergency.cdc.gov/masscasualties/explosions.asp.

98. Rafaels, K.A., Bass, C.R., Panzer, M.B., Salzar, R.S., Woods, W.A., Feldman, S.H., Walilko, T., Kent, R.W., Capehart, B.P., Foster, J.B., Derkunt, B., Toman, A., 2012. Brain injury risk from primary blast. The journal of trauma and acute care surgery 73, 895-901.

99. Raghavendra, V., Tanga, F., DeLeo, J.A., 2003. Inhibition of microglial activation attenuates the development but not existing hypersensitivity in a rat model of neuropathy. J Pharmacol Exp Ther 306, 624-630.

100. Raivich, G., Bohatschek, M., Kloss, C.U., Werner, A., Jones, L.L., Kreutzberg, G.W., 1999. Neuroglial activation repertoire in the injured brain: graded response, molecular mechanisms and cues to physiological function. Brain research. Brain research reviews 30, 77-105.

101. Ransohoff, R.M., Perry, V.H., 2009. Microglial physiology: unique stimuli, specialized responses. Annual review of immunology 27, 119-145.

102. Ransom, B.R., 1991. Vertebrate glial classification, lineage, and heterogeneity. Ann N Y Acad Sci 633, 19-26.

103. Rao, J.S., Kellom, M., Kim, H.W., Rapoport, S.I., Reese, E.A., 2012. Neuroinflammation and synaptic loss. Neurochemical research 37, 903-910.

104. Readnower, R.D., Chavko, M., Adeeb, S., Conroy, M.D., Pauly, J.R., McCarron, R.M., Sullivan, P.G., 2010. Increase in blood-brain barrier permeability, oxidative stress, and activated microglia in a rat model of blast-induced traumatic brain injury. J Neurosci Res 88, 3530-3539.

105. Ren, K., 2010. Emerging role of astroglia in pain hypersensitivity. The Japanese dental science review 46, 86.

106. Ridet, J.L., Malhotra, S.K., Privat, A., Gage, F.H., 1997. Reactive astrocytes: cellular and molecular cues to biological function. Trends in neurosciences 20, 570-577.

107. Rintala, D.H., Holmes, S.A., Fiess, R.N., Courtade, D., Loubser, P.G., 2005. Prevalence and characteristics of chronic pain in veterans with spinal cord injury. Journal of rehabilitation research and development 42, 573-584.

108. Ruff, R.L., Ruff, S.S., Wang, X.F., 2008. Headaches among Operation Iraqi Freedom/Operation Enduring Freedom veterans with mild traumatic brain injury associated with exposures to explosions. Journal of rehabilitation research and development 45, 941-952.

109. Saijo, K., Glass, C.K., 2011. Microglial cell origin and phenotypes in health and disease. Nature reviews. Immunology 11, 775-787.

110. Saljo, A., Bao, F., Hamberger, A., Haglid, K.G., Hansson, H.A., 2001. Exposure to short-lasting impulse noise causes microglial and astroglial cell activation in the adult rat brain. Pathophysiology : the official journal of the International Society for Pathophysiology / ISP 8, 105-111.

111. Sharma, S., Yang, B., Xi, X., Grotta, J.C., Aronowski, J., Savitz, S.I., 2011. IL-10 directly protects cortical neurons by activating PI-3 kinase and STAT-3 pathways. Brain Res 1373, 189-194.

112. Shohami, E., Shapira, Y., Cotev, S., 1988. Experimental closed head injury in rats: prostaglandin production in a noninjured zone. Neurosurgery 22, 859-863.

113. Simon, F., Scheuerle, A., Groger, M., Vcelar, B., McCook, O., Moller, P., Georgieff, M., Calzia, E., Radermacher, P., Schelzig, H., 2011. Comparison of carbamylated erythropoietin-FC fusion protein and recombinant human erythropoietin during porcine aortic balloon occlusion-induced spinal cord ischemia/reperfusion injury. Intensive Care Med 37, 1525-1533.

114. Sjovold, S.G., Mattucci, S.F., Choo, A.M., Liu, J., Dvorak, M.F., Kwon, B.K., Tetzlaff, W., Oxland, T.R., 2013. Histological effects of residual compression sustained for 60 minutes at different depths in a novel rat spinal cord injury contusion model. Journal of neurotrauma 30, 1374-1384.

115. Smith, C., 2013. Review: the long-term consequences of microglial activation following acute traumatic brain injury. Neuropathol Appl Neurobiol 39, 35-44.

116. Somjen, G.G., 1988. Nervenkitt: notes on the history of the concept of neuroglia. Glia 1, 2-9.

117. Spittau, B., Wullkopf, L., Zhou, X., Rilka, J., Pfeifer, D., Krieglstein, K., 2013. Endogenous transforming growth factor-beta promotes quiescence of primary microglia in vitro. Glia 61, 287-300.

118. Stone, D.H., Conrad, M.F., Albadawi, H., Entabi, F., Stoner, M.C., Cambria, R.P., Watkins, M.T., 2009. Effect of PJ34 on spinal cord tissue viability and gene expression in a murine model of thoracic aortic reperfusion injury. Vasc Endovascular Surg 43, 444-451.

119. Sundaramurthy, A., Chandra, N., 2014. A parametric approach to shape field-relevant blast wave profiles in compressed-gas-driven shock tube. Frontiers in neurology 5, 253.

120. Svetlov, S.I., Prima, V., Kirk, D.R., Gutierrez, H., Curley, K.C., Hayes, R.L., Wang, K.K., 2010. Morphologic and biochemical characterization of brain injury in a model of controlled blast overpressure exposure. The Journal of trauma 69, 795-804.

121. Tanaka, T., Ueno, M., Yamashita, T., 2009. Engulfment of axon debris by microglia requires p38 MAPK activity. The Journal of biological chemistry 284, 21626-21636.

122. Tikka, T., Fiebich, B.L., Goldsteins, G., Keinanen, R., Koistinaho, J., 2001. Minocycline, a tetracycline derivative, is neuroprotective against excitotoxicity by inhibiting activation and proliferation of microglia. The Journal of neuroscience : the official journal of the Society for Neuroscience 21, 2580-2588.

123. van Hedel, H.J., Dietz, V., 2010. Rehabilitation of locomotion after spinal cord injury. Restor Neurol Neurosci 28, 123-134.

124. Vandevord, P.J., Bolander, R., Sajja, V.S., Hay, K., Bir, C.A., 2012. Mild neurotrauma indicates a range-specific pressure response to low level shock wave exposure. Annals of biomedical engineering 40, 227-236.

125. Vernadakis, A., 1996. Glia-neuron intercommunications and synaptic plasticity. Progress in neurobiology 49, 185-214.

126. Warden, D.L., French, L., 2005. Traumatic brain injury in the war zone. N Engl J Med 353, 633-634.

127. Warden, D.L., French, L.M., Shupenko, L., Fargus, J., Riedy, G., Erickson, M.E., Jaffee, M.S., Moore, D.F., 2009. Case report of a soldier with primary blast brain injury. NeuroImage 47 Suppl 2, T152-153.

128. Watson, B.D., Prado, R., Dietrich, W.D., Ginsberg, M.D., Green, B.A., 1986. Photochemically induced spinal cord injury in the rat. Brain Res 367, 296-300.

129. Watson, J.L., Hala, T.J., Putatunda, R., Sannie, D., Lepore, A.C., 2014. Persistent at-level thermal hyperalgesia and tactile allodynia accompany chronic neuronal and astrocyte activation in superficial dorsal horn following mouse cervical contusion spinal cord injury. PLoS One 9, e109099.

130. Wieseler-Frank, J., Maier, S.F., Watkins, L.R., 2005. Central proinflammatory cytokines and pain enhancement. Neuro-Signals 14, 166-174.

131. Wollaars, M.M., Post, M.W., van Asbeck, F.W., Brand, N., 2007. Spinal cord injury pain: the influence of psychologic factors and impact on quality of life. The Clinical journal of pain 23, 383-391.

132. Xiong, Y., Mahmood, A., Chopp, M., 2013. Animal models of traumatic brain injury. Nature reviews. Neuroscience 14, 128-142.

133. Yang, C.H., Lee, B.B., Jung, H.S., Shim, I., Roh, P.U., Golden, G.T., 2002. Effect of electroacupuncture on response to immobilization stress. Pharmacology, biochemistry, and behavior 72, 847-855.

134. Yezierski, R.P., 2000. Pain following spinal cord injury: pathophysiology and central mechanisms. Prog Brain Res 129, 429-449.

ABSTRACT

ASSESSMENT OF TEMPORAL AND SPATIAL ALTERATIONS IN SPINAL GLIAL REACTIVITYAND THE EXTENT OF CERVICAL SPINAL DIFFUSE AXONAL INJURY IN THE RAT AFTER BLAST OVERPRESSURE EXPOSURE.

by

HEENA SULTAN PURKAIT

MAY 2015

Advisor: Dr. Srinivasu Kallakuri

Major: Biomedical Engineering

Degree: Master of Science

Blast induced neurotrauma (BINT) is the signature wound of veterans returning from various military operations. A substantial percentage of Operations Enduring Freedom (OEF) and Iraqi Freedom (OIF) veterans have reported to experience ongoing or new pain following their military service. Head (58%) and back (55%) have been the high prevailing locations of pain in these returning OIF and OEF veterans and the underlying pathomechanism of these conditions is yet to be understood. In the context of blast overpressure induced pathological changes, the fundamental question that still needs to be addressed is whether there are any underlying cellular injury changes the spinal cord following blast. If proven, it is postulated that cellular injury changes in the form of glial activation may contribute to neuronal sensitization and altered sensation through the release of various inflammatory mediators. Much of the previous and ongoing research studies have been directed at understanding blast induced changes in the brain alone with changes in the spinal cord still remaining an enigma. Accordingly, as a first step, we attempted to investigate spatial and temporal alterations in glial activation in the spinal

cord following blast exposure. In addition, we also attempted to study the presence of axonal injury in the cervical spinal cord following blast overpressure.

As part of this investigation, anaesthetized male Sprague Dawley rats were subjected to a single insult of blast overpressure (22psi)using a helium driven shock tube. The rats were divided into two groups; Sham and Blast with acute and sub-acute survival periods; 6hrs, 24hrs, 3days and 7days respectively. Glial activation was assessed by GFAP (Glial Fibrillary Acidic Protein) and IBA1 (Ionized Calcium Binding Molecule 1) immunohistochemistry. GFAP and Iba1 are routinely used to investigate astrocytic and microglial activation in the brain and spinal cord. Axonal injury in the cervical spinal cord was assessed by β-APP (Beta Amyloid Precursor Protein) immunohistochemistry. βAPP is a commonly used marker to detect the presence of diffuse axonal injury in the brain.

Behaviorally, blast exposed rats exhibited significantly increased surface righting duration compared to sham rats. Our immunohistochemistry results indicate differential activation of astrocytes and microglia in various spinal cord regions in blast exposed group compared to sham. Rats subjected to blast overpressure showed increased expression of astrocytes and microglia at acute and sub-acute periods. Evidence of diffuse axonal injury also observed in the cervical spinal cord following the blast overpressure. Taken together, our results suggest that blast exposure in a craniocephalic orientation in rats resulted an enhanced spinal glial reactivity as well as cervical spinal axonal injury. We postulate that injury changes in the form of activation of astrocytes and microglia with diffuse axonal injury may contribute to the release of various inflammatory mediators which may in turn be related to the ensuing sensory changes. These results lay foundation to further studies on blast related injury changes in the spinal cord.

AUTOBIOGRAPHICAL STATEMENT

HEENA PURKAIT

EDUCATION:

Master of Science, Biomedical Engineering; Wayne State University, USA (2015)

Bachelor of Engineering, Biomedical Engineering; Mumbai University, India (2010)

EXPERIENCE:

Graduate Research Assistant	Wayne State University, MI, USA	2013-2015
Clinical Engineering Intern	William Beaumont Hospital, MI, USA	2014
Sales & Service Engineer	Allwin Lifecare, Mumbai, India	2010-2011
Biomedical Engineer Trainee	S. L. Raheja Hospital , Mumbai, India	2009

AWARDS:

Graduate Professional Scholarship	Wayne State University, MI, USA	2014-2015
Best Poster Award	Master's Showcase, Wayne State University, MI, USA	2015
Best Poster Award	Tech Arete, MGM's College of Engineering & Technology	2010